Investigation of Point Particle Effective Field Theory for the Inverse Square Model

By

DANIEL RUIZ

Department of Physics & Astronomy
MCMASTER UNIVERSITY

A dissertation submitted to McMaster University in accordance with the requirements of the degree of MASTER OF SCIENCE in the Faculty of Science.

APRIL 2020

Information and Declaration

McMaster University MASTER OF SCIENCE (2020)
Hamilton, Ontario, Canada
Department of Physics

TITLE: Investigation of Point Particle Effective Field Theory for the Inverse Square Model
AUTHOR: Daniel Ruiz, B.Sc.
SUPERVISOR: Professor Cliff P. Burgess
NUMBER OF PAGES: xv, 90

I, the author hereby certify that the work in this dissertation is, unless otherwise acknowledged through citation, original and has not been otherwise submitted for any academic degree or qualification. Any ideas, techniques or other materials belonging to others are explicitly referenced in the texts. Any views expressed in the dissertation are those of the author.

Abstract

In this thesis, we study non-relativistic scalar fields in (3+1) space-time subjected to an inverse-square potential. We use a point-particle effective field theory (PPEFT) framework to describe the scalar fields coupling to a point-particle in different cases of interest. In Chapter 3, we encode particle conversion for both Schrodinger and Klein-Gordon fields in a two-species toy model and find that the point-particle couplings all must be renormalized with respect to the radial cut-off near the origin. In addition to this, we find that cross sections have an interesting dependence on the ratio $k_{\text{out}}/k_{\text{in}}$ of outgoing and incoming momenta. In certain regimes at low energies, we found inelastic behaviour $\sigma_S^{(in)} \sim \mathcal{O}(1)$ and $\sigma_{KG}^{(in)} \sim 1/k_{in}$ for Schrodinger and Klein-Gordon fields respectively. In Chapter 4, we study the case of a single-particle non-self-adjoint PPEFT whose formulation is taken to next-to-leading order. We find that the point-particle couplings continue to require renormalization and present a series of relevant computations such as field equations, boundary conditions and renormalization runnings, concluding with an exposition of bound state energies, scattering lengths and cross sections. Similar to what was found in Chapter 3, a $1/k_{\text{in}}$ enhancement is observed in a particular regime of the PPEFT in Chapter 4. In addition, we find that the observables computed therein are modified from what was found in other papers [3, 13], where only the leading PPEFT term was kept. These results may provide relevance for future calculations in more complex reactions such as baryon number violation and monopole catalysis.

Acknowledgements

I would like to express my thanks to Dr. Cliff Burgess for overseeing this project and helping me navigate through the research avenues that ended up culminating in this thesis. To Ryan Plestid and the guys of the McMaster Particle Research Group: Laszlo Zalavari, Peter Hayman, Joshua Hainge, Gregory Kaplanek and Markus Rummel; thank you for the many useful discussions that we've had within and outside our group meetings. In addition, Hank "topology enthusiast" Chen has my regards for further instilling an admiration for mathematical physics and providing many useful insights into pertinent research questions. To the faculty and staff at both McMaster and the Perimeter Institute, you have my gratitude for providing an excellent experience during my Master's. Lastly, a great appreciation to my family, friends and teachers in helping me grow through the last 26 years.

DEDICATION

While having considered Physics to be my home over the past 6 years, the next chapters of my life will likely lie in industries that are external to it. In that spirit, I would like to dedicate this thesis to any student that is undergoing the process of *finding themselves* or homing in on the domains of life that provide the most meaning to them.

List of Abbreviations

QFT: **Q**uantum **F**ield **T**heory
EFT: **E**ffective **F**ield **T**heory
PPEFT: **P**oint **P**article **E**ffective **F**ield **T**heory
HET: **H**igh **E**nergy **T**heory
LET: **L**ow **E**nergy **T**heory
RG: **R**enormalization **G**roup
KG: **K**lein-**G**ordon
UV: **U**ltra**v**iolet
IR: **I**nfra**r**ed
BF: **B**ackground **F**ield
NRQED: **N**on-**R**elativistic **Q**uantum **E**lectro**d**ynamics
NR: **N**on-**R**elativistic
BEC: **B**ose **E**instein **C**ondensate
LO: **L**eading **O**rder
NLO: **N**ext to **L**eading **O**rder

Notation

Within the contents of this thesis, I will sometimes make use of convenient notation for a variety of objects and relations. When this comes up, I will make clear what the notation corresponds to. However, for more standard notation, I will generally assume that the reader is familiar but will now provide a brief overview for the pieces of notation that are more frequently encountered in this thesis:

z^*: Let $z \in \mathbb{C}$, we use the star operand, $*$ to denote complex conjugation.
$|z|$: Let $z \in \mathbb{C}$, then we define $|z|$ as the absolute complex magnitude $|z| = \sqrt{z^* z}$.
Re[z]: Let $z \in \mathbb{C}$, then Re[z] denotes the real component of z, defined by Re[z]:=$\frac{z+z^*}{2}$.
Im[z]: Let $z \in \mathbb{C}$, then Im[z] denotes the imaginary component of z, defined by Im[z]:=$\frac{z-z^*}{2i}$.
$\sim$: Asymptotic Notation. We say that $f(x) \sim g(x)$ as x $\to a$ iff $\lim_{x \to a} \frac{f(x)}{g(x)} = 1$.
$\propto$: Proportionality. We say that $f(x) \propto h(x)$ iff $\frac{f(x)}{h(x)} = c$ for some non-zero constant, $c \in \mathbb{C} \setminus \{0\}$.
(a, b): Interval on the Real line. This is a set defined as $(a, b) = \{x \in \mathbb{R} |\ a < x < b\}$.

TABLE OF CONTENTS

List of Figures

Figure **Page**

CHAPTER 1

INTRODUCTION

"The story so far: In the beginning the Universe was created. This has made a lot of people very angry and been widely regarded as a bad move."

– Douglas Adams, *The Restaurant at the End of the Universe*

In every domain of the theoretical sciences, we are tasked with codifying a physical phenomena of interest. In doing so, we generally avoid the inclusion of unnecessary degrees of freedom and instead seek out an *effective* description of the problem at hand. This simplification, though not capturing the full picture, still provides valuable insight and can be modified to accommodate the desire for greater precision in the theory's predictions. This *effective theory* paradigm has seen great application in non-relativistic particle physics [3–5, 9], emphasized through the formalism known as *effective field theories* (EFTs)[1].

In this thesis, we study the quantum mechanics of non-relativistic scalar fields interacting with a point-source through an inverse-square potential. One can consider the point-particle description an effective one, for which we formally encode by a point-particle EFT (PPEFT). In essence, our PPEFT model is a useful description of the physical problem at a particular set of scales. To clarify this, suppose that the length scale associated with the size of the source is denoted by R, contrasted with a physical scale of interest a.[2] The physical relevance of these scales would depend upon the context of the problem. For instance, applied to atoms could mean that R denotes the size of a nucleus sourcing the potential and a could represent the atomic electron orbital [3]. The interest of this thesis lies in the $R << a$ regime, which allows us to benefit from an EFT formalism. Since EFTs can efficiently exploit a hierarchy of scales, we are able to truncate many of the terms appearing in the point-particle action. In essence, given that

[1] EFTs are applicable across many domains of physics. They also see usage in condensed matter systems as well.
[2] One can take this to signify a macroscopic probe being applied at this scale.

$R/a << 1$, we can largely be ignorant about the details of the source's underlying structure [3]. Furthermore, a full fledged quantum field theory is overkill for such non-relativistic systems and so this has the conceptual benefit of systematically shaving off higher-order terms that contribute marginally. How this precisely plays out will be explored in the proceeding chapter and then utilized in §3 and §4.

The inverse-square problem has been extensively studied, belonging to a class of potentials referred to as singular potentials. They are known to give rise to an arbitrary choice in what the boundary condition should be at $\mathbf{r} = 0$. Specifying this boundary condition requires knowing further details about the source and since this would encode observable quantities, the presence of a source action is obligatory as the lone inverse-square would not fully specify the physical problem. Some common techniques to deal with the lone inverse-square Hamiltonian's non-self-adjointness include the construction of self-adjoint extensions. One of the goals is to therefore establish what this boundary condition is, which for our case turns out to be directly cast in terms of the PPEFT coupling parameters. This procedure has been utilized in other papers [3] and we similarly argue that this is the most *'natural'* choice for the B.C, and further demonstrates the efficacy of the EFT in removing the guesswork out of the problem.

I would now like to provide an overview of the thesis' contents so that one can reach a good bird's eye view on the lay of the land. This thesis is divided into two main research inquiries, each of which has its own devoted chapter, seen by §3 and §4. To have a more solid foundation when venturing into these sections, I provided a cursory overview of some of the gadgets and techniques utilized in this thesis, described in §2: *Preliminaries*. In essence, §2 aims to provide the background material on the precise inverse-square model, renormalization, EFTs, background fields, and a multiple species formalism. The details provided therein are not entirely self-contained and so we reference material that the reader would find more comprehensive. It should be noted that the model described thus far has already been explored in several papers [3–5, 13]. We will therefore now comment on how the contents of this thesis are distinguished from the research performed in these articles.

In the pursuit of providing a clearer picture, I'll provide a preview of the point-particle action, S_b:

$$S_b = \int \mathrm{d}^4x \, [h_2|\Psi|^2 + h_4|\Psi|^4 + ...] \, \delta^3(x), \tag{1.1}$$

where h_2, h_4 are the effective couplings and Ψ represents the Schrodinger field of interest. Equation (1.1) forms the underlying point-particle model upon which the inquiries of §3 and §4 rest. The details of this point-particle action will be further explored in §2, but in the interest of helpfully describing these chapters, it's useful to outline the details of how this source action are modified. In §3, we explore the phenomena of particle catalysis and how a point-particle described by an action like (1.1) can induce this process. We truncate the expression in (1.1) by only keeping the quadratic term, $h_2|\Psi|^2$ within the action, a procedure that has likewise been used in other papers [3–5, 13]. More precisely, we want to show a low energy enhancement of

scattering cross sections (σ), demonstrating that in certain regimes they can go as $\sigma \sim 1/k_{\text{in}}$ with k_{in} denoting incident momenta. Our interest lies in the two-particle sector for both Schrodinger and Klein-Gordon Fields. To consider this research inquiry, we accordingly modify S_b for a two species toy model for both Schrodinger and Klein-Gordon fields. The work in §3 was heavily collaborated with Peter Hayman, to which he extended upon in a paper titled *Point-Particle Catalysis* [9]. We also recognize his work being referenced numerous times throughout §3, with §3.1.3 being a brief exposition of results that he had computed himself and therefore credit to him.

Section §4 comprises the bulk of the author's work. We extend the leading order formulation of the single-particle PPEFT by keeping both the quadratic and quartic terms in (1.1). In essence, we consider a next-to-leading order description of the point-particle model with the extra property of allowing effective couplings h_2, h_4 to be complex-valued. This non-self-adjoint PPEFT allows us to model absorptive processes since complex couplings generically encode non-unitary boundary conditions, a condition of theoretical interest that has been explored in other papers [13]. We use a background field method to aid in the simplification of computing observables such as scattering lengths and elastic, and inelastic cross sections. The focus is to therefore record how observables are modified in this next-to-leading order formulation. We also motivate a renormalization argument in the running of the couplings h_2, h_4 and comment on the bound state energies of the model.

In the next chapter, we present an overview of some of the techniques, and concepts mentioned here and try to motivate their utility.

CHAPTER 2

PRELIMINARIES

"[Quantum Mechanics] describes nature as absurd from the point of view of common sense. And it fully agrees with experiment. So I hope you can accept nature as She is - absurd."
– Richard Feynman, *QED: The Strange Theory of Light and Matter*

Effective theories extend into every domain of Physics. The focus of this thesis lies in the very small, for which the degrees of freedom associated with the investigated systems are generally of order $\mathcal{O}(1)$-$\mathcal{O}(10)$. This research was therefore an inquiry into the dynamics between objects such as atoms and particles for which the underpinning theory is suitably described by quantum mechanics. However, our discussion often makes use of interactions and an effective theory paradigm for which the language of field theory best encodes. It is therefore the goal of this section to provide an overview of the main model and necessary background material to provide a firm footing of the context and investigated applications. One of the focal efforts here will be to introduce and motivate the machinery of the point-particle effective field theory (PPEFT) framework. In addition, I provide a cursory review on techniques such as background field methods and renormalization.

2.1 The Bulk Model in $(d+1)$-Spacetime

The primary model of consideration is a Schrodinger field in $(d+1)$-dimensional Euclidean space, for which we adopt spherical coordinates to have the canonical metric $ds^2 = dr^2 + r^2 \hat{g}_{mn} d\theta^m d\theta^n$. We note here that r is the radial coordinate and the θ^i coordinates $\{\theta^1, \theta^2, .., \theta^{d-1}\}$, parameterizes the $(d-1)$-sphere with $\hat{g}_{mn}$ denoting the standard metric on the $(d-1)$-sphere. The action, which will come to be known as the *bulk action*, S_B is given below by

$$S_B = \int \mathrm{d}t\ \mathrm{d}^d x\ \frac{i}{2}\Big\{\Psi^\dagger(\partial_t\Psi) - (\partial_t\Psi^\dagger)\Psi\Big\} - \Big[\frac{1}{2m}|\nabla\Psi|^2 - \frac{g}{r^2}\Psi^\dagger\Psi\Big], \tag{2.1}$$

where we have chosen natural units ($\hbar = c = 1$). We note here that Ψ are second quantized *spin-0* Schrodinger fields. The model of interest in this thesis is the inverse-square system, for which we have taken the potential to be $V(r) = -\frac{g}{r^2}$. One of the interesting aspects of this model is the necessity of using renormalization arguments. This will be made more explicit down the road, particularly emphasizing a Point-Particle Effective Field Theory (PPEFT) approach.

We first recall that for a generic metric, g on some Riemannian Manifold (M, g), the Laplacian is defined by

$$\nabla^2\psi = \frac{1}{\sqrt{g}}\partial_i\big(\sqrt{g}\,g^{ij}\partial_j\psi\big), \tag{2.2}$$

where g denotes the determinant of the metric and g^{ij} is the inverse metric, satisfying as usual $\sum_k g^{ik}g_{kj} = \delta_{ij}$. Since our metric is diagonal, we have that $g^{ij} = \frac{1}{g_{ij}}\ \forall\ 1 \le i,j \le d$. We note that $\sqrt{g} = r^{d-1}\sqrt{\hat{g}}$ with $\hat{g}$ denoting the metric determinant on the $(d-1)$-sphere. We now expand into radial and angular pieces so as to establish

$$\begin{aligned}\nabla^2\psi &= \frac{1}{r^{d-1}}\frac{\partial}{\partial r}\Big(r^{d-1}\frac{\partial\psi}{\partial r}\Big) + \frac{1}{r^2}\frac{1}{\sqrt{g}}\frac{\partial}{\partial\theta^i}\Big(\sqrt{\hat{g}}\,\hat{g}^{ij}\frac{\partial\psi}{\partial\theta^j}\Big)\\ &= \frac{1}{r^{d-1}}\frac{\partial}{\partial r}\Big(r^{d-1}\frac{\partial\psi}{\partial r}\Big) + \frac{1}{r^{d-1}}\Delta_{S^{d-1}}\psi,\end{aligned} \tag{2.3}$$

where we have defined $\Delta_{S^{d-1}}$ [1] to be the Laplacian on the $(d-1)$-sphere. Extremizing the action (2.1) determines the field equations, which are given below by

$$0 = \frac{\delta S_B}{\delta\Psi^\dagger} \to \nabla^2\Psi + \frac{2mg}{r^2}\Psi = \kappa^2\Psi, \tag{2.4}$$

where we have defined $\kappa^2 = -2mE$. Given that we have a spherically symmetric potential, standard techniques provide us with a clean product of the fields into radial and angular components so that a general solution can be expressed below by

$$\Psi(r,\theta^1,...,\theta^{d-1}) = \sum_\omega \psi_\omega(r)Y_\omega(\theta^1,\theta^2,..,\theta^{d-1}). \tag{2.5}$$

Here, ω defines a collection of parameters associated with the d-dimensional spherical harmonics Y_ω (ex. in $d=3$, a suitable choice of parameters is $\{l,m\}$ with $l(l+1)$ denoting the total angular momentum eigenvalue and m being the projection onto the z-axis). We note that Y_ω are eigenstates of the $\Delta_{S^{d-1}}$ Laplacian with defined eigenvalue $-\bar{\omega}_d$. This eigenvalue depends on the dimension of the space, taking for instance in $d=2$ the value $\bar{\omega}_2 = l$ whereas in $d=3$ the familiar $\bar{\omega}_3 = l(l+1)$. For brevity, we'll express the eigenvalue as just this: $\Delta_{S^{d-1}}Y_\omega = -\bar{\omega}_d Y_\omega$. Doing so, we obtain the radial equation

$$\frac{d^2\psi}{dr^2} + \frac{(d-1)}{r}\frac{d\psi}{dr} - \Big[\frac{\bar{\omega}_d - \alpha}{r^2}\Big]\psi = \kappa^2\psi, \tag{2.6}$$

[1] The notation S^{d-1} is the standard mathematical convention for the collection of points on the surface of the d-sphere: $S^{d-1} = \{\mathbf{x}\in\mathbb{R}^d \,\big|\, |\mathbf{x}| = 1\}$.

where we have defined $\alpha := 2mg$ and dropped the l-subscript for compactness (It should be noted that ψ depends on l). One suitable choice of basis for the radial solutions to (2.6) are given by confluent hypergeometrics. We write down $\{\psi_-, \psi_+\}$ to denote the two linearly independent solutions supplied with associated constants $\{C_-, C_+\}$ so that the general form can be expressed by

$$\psi(r) = C_-\psi_-(r) + C_+\psi_+(r), \tag{2.7}$$

where each of these has the radial profile given below by

$$\psi_\pm(r) = (2\kappa r)^{\frac{1}{2}(2-d\pm\zeta)} e^{-\kappa r} \mathscr{M}\big[\frac{1}{2}(1\pm\zeta), 1\pm\zeta; 2\kappa r\big], \tag{2.8}$$

where we have defined $\zeta := \sqrt{(d-2)^2 + 4(\bar{\omega}_d - \alpha)}$ and note that $\mathscr{M}[a,b;z]$ are the standard confluent hypergeometrics. This radial function will frequently be host to asymptotic analysis as we'll be interested in the *small r* and *large r* limits.

For a particular class of $\bar{\omega}_d, \alpha$ values, the inverse-square system exhibits interesting qualitative behaviour near the origin. This detail will be explored in the following section of §2.2 but we make note of this asymptotic behaviour below by

$$\psi_\pm(r) \sim (2\kappa r)^{\frac{1}{2}(2-d\pm\zeta)}\big[1 + \mathscr{O}\big(r^2\big)\big] \text{ as } r \to 0. \tag{2.9}$$

This depicts a power law for the *small r* asymptotics, going as $\psi_\pm \propto r^{s_\pm}$ where $s_\pm = \frac{1}{2}(2-d\pm\zeta)$. The utility here being the ability to see the field's behaviour near the origin.

2.2 Point Particle Effective Field Theory

Suppose that we're interested in investigating a system that happens to exhibit a singular nature in its solutions space. From the physics vantage point, whenever we run into divergences, it is signalling some failure of the theory or the validity of the techniques utilized therein. Our experimental observables, whatever they may be should always yield finite values.

Consider for instance, the problem of solutions that diverge at the origin. Typically, when one encounters this, one prescription is to set the associated constants of the linearly independent solutions to a particular value so as to eliminate the part that is causing the divergence. However, consider the model of §2.1 in the case where $\alpha > \bar{\omega}_d$. Notice that for $d \geq 3$, both of s_+ and s_- possess a negative sign and so dictate that each linearly independent solution diverges at the origin. If we were to arm ourselves with the same prescription as has just been discussed, this would require setting both C_-, C_+ to zero, resulting in the lone solution of $\Psi = 0$. Such a trivial result is a signal of failure as this prescription necessarily can remove a broad class of states that may have been of interest. Therefore, the chosen methodology isn't the correct systematic approach to this problem.

The non-uniqueness of these regularization methods are made more clear in the literature,

as one can witness a whole host of arguments for regularizing solutions. For instance, many have observed that the Schrodinger Hamiltonian can fail to be self-adjoint, depending on the boundary conditions that hold at the origin. Selecting a choice of boundary condition to fix its self-adjointness is not a unique construction; the process of doing so being referred to as constructing its self-adjoint extension. In essence, given some physical situation, *which method is the right or best one?* The answer to this question is the remaining goal of this section and my hope is that this will provide a clearer picture on a more systematic approach to setting up the boundary condition story.

2.2.1 Effective Field Theories

Interesting physics exists at all scales, but portions of the underlying *full theory* can be neglected if they play a negligible role at the energy scales of interest. It becomes difficult to compute quantities if *everything* is taken into account. We want the simplest framework that captures all the essential physics, but in a manner that can be corrected to arbitrary precision. In essence, we want to be able to somehow *expand* the QFT. The fruits of this collection of techniques are known as Effective Field Theories (EFT's) [15].

The general procedure to describe a physical system at some desired scale is captured below:

1. Determine the relevant degrees of freedom → *What Fields?*
2. Determine the symmetries. → *What Interactions?*
3. Expansion parameters, leading order description. → *What power counting?*

Once you take these three in aggregate and figure out the leading order description, you have created an effective field theory. One of the key principles to note here is that if you are interested in describing physics at some scale m^2, you don't need to know the detailed dynamics of what is going on at $\Lambda^2 >> m^2$. In this example, one may perform an expansion in powers of m^2/Λ^2.

For instance, computing hydrogen energy levels are a standard exercise in an undergraduate quantum mechanics course but the performed calculations don't take into account the heavier quarks of the standard model. Yet, our predictions match the experimental data quite well. In essence, one need not know about bottom quarks to describe non-relativistic hydrogen, but first order treatment in NRQED [15] can give the ground state energy solution below by

$$E_0 = \frac{1}{2} m_e \alpha^2 \Big(1 + \mathcal{O}\Big[\frac{m_e^2}{m_b^2}\Big]\Big). \tag{2.10}$$

Equation (2.10) takes into account the first set of corrections, a ratio m_e^2/m_b^2 that is of order $\sim 10^{-8}$. While the quantity is negligible in the NR regime, it can play a deep role if the interest

is in hydrogen spectrum precision measurements as to see if accounting for relativistic fields matches the data.

In general, EFT's are used in two distinct ways.

The Top-Down Approach
In this case, the High Energy Theory (HET) is well understood in the sense that we can write down a Lagrangian for it. However, it is useful to have a simpler theory at low energies. The process of turning the HET into a Low Energy Theory (LET) means that we *integrate out* (remove) the heavier particles and match onto a LET. This matching procedure means finding new operators and low-energy constants.

Schematically, this is depicted by an expansion in decreasing relevance:

$$\mathscr{L}_{\text{High}} = \sum_n \mathscr{L}^{(n)}_{\text{Low}} \tag{2.11}$$

Hence, $\mathscr{L}_{\text{High}}$ and $\mathscr{L}_{\text{Low}}$ would agree in the infrared (IR) but generically differ in the ultraviolet (UV). The desired precision tells us when to stop this expansion (i.e up to which n we go until).

The Bottom-Up Approach
This technique is utilized when the underlying theory is unknown *or* the matching program is too difficult to carry out (e.g non-perturbative). You may need to know information about the HET, such as if it's Lorentz invariant, exhibits certain gauge symmetries, etc.

One constructs $\sum_n \mathscr{L}^{(n)}_{\text{Low}}$ by writing down the most general possible operators / interactions that are consistent with all symmetries. While the couplings are unknown, they can be fit to experiment.

The subject of Effective Field theories is both a rich and deep topic and the prior paragraphs serve to provide a cursory overview of its punchlines. For an improved and further review of the topic, I would advise checking [2][15]. If there is a prime lesson to be taken away from here, it is this: For all intents and purposes, sometimes the cow really is a sphere.

2.2.2 PPEFT and Brane Cosmology

Point Particle EFT (PPEFT) is a specialization of the EFT story to the case where *something* is being treated as a point particle. Point particles should present familiarity as you have likely sharpened this tool in your arsenal in the past. If not, then consider the following example: suppose that one aimed to compute the trajectories of a planet around a star. Planets are quite massive objects, comprised of an astronomical amount of atomic species. However, this fact can be neglected by expressing a model for celestial motion that treats their entire mass distribution to be localized at a point (i.e a point particle). Depending on the precision of interest, we can yield

answers that model reality quite well. We can establish corrections by including varying degrees of planet substructure as well as unequipping Newtonian gravitation for General Relativity for our main hammer. In the language of QFT, each succession will furnish higher-dimensional operators in our Lagrangian expansion, thereby generating corrections that may be desirable, it all depends on the scales of interest.

Def 2.1. : **Bulk and Branes**
In string theory as well as related fields in brane cosmology, it's common to consider the possibility that the universe is embedded in a higher-dimensional space, containing more than the 3 spatial dimensions that we experience. In this picture, the *true* higher-dimensional space is referred to as the *bulk*. Within the bulk, a subspace of codimension ≥ 1 can generally be referred to as a *brane* [14], a sort of generalization of point particles to higher dimensions as the space can be viewed to be fixed to some subset of the bulk dimensions. Hence, there is a lot of theoretical interest in considering the universe being confined to a brane. Formally, the bulk can be formulated as a Riemannian Manifold and the branes being viewed as a sub-Riemannian manifold of some codimension ≥ 1.

When the internal structure of an object can be neglected, allowing us to instead focus on its centre-of-mass motion is the regime in which the point-particle approximation is brought into the fold. However, the efficacy of PPEFT is typically best understood in the low energy limit. Suppose that we were interested in scattering between two particles, with the chosen frame being the centre of mass of the heavier object. It's mass, M is taken to be much larger than that of the light particle, m ($M >> m$) and localizing it to a point provides a convenient description. However, the higher the energy of the incident particle, the greater its ability to interact with the physics of the source, or if no potential barrier is present we obtain a scenario referred to as a *fall to the centre*. If this is the case, then we necessarily have to write down an improved description for the physics going on near the origin which will invariably mean including higher-dimensional interactions.

It's common to write down an effective field theory action of the form $S = S_B + S_b$. We refer to the pieces of this action as the *bulk* and *brane* respectively. The motivation here being that we can cleanly split the fields among those confined to the brane and those that exist in the bulk, coupling to one another on the brane in a particular way [See [6] for a review of this procedure]. Our goal is to generate a point-particle action, S_b which in the language of brane cosmology is considered the brane action[2] as it would encode information about a field localized to a point.

2.2.3 Schrodinger Brane

We now aim to construct the Schrodinger brane action that forms the model of interest within the contents of this thesis. We consider ordinary quantum mechanics in d spatial dimensions. In

[2]In the chapters that follow, I will often use brane action, source action and point particle action interchangeably as the underpinning context is typically motivated from these angles.

§2.1, we introduced the bulk action which was precisely described by S_B in (2.1). The microscopic physics of the source at the origin is considered to be described by the brane action S_b.

Def 2.2. Worldline:
The worldline of an object is the path that becomes traced out in space-time. It is the set of points on space-time that the object's coordinate passes through.

We consider a point-particle where the time coordinate, t parameterizes the worldline, γ of the object and have it situated at the spatial origin, $\gamma^\mu = \{t, 0, .., 0\}$. We're interested in how this point-particle couples to the fields of the bulk, Ψ and so we therefore write down a generic point-particle action expressed below by

$$S_b = \int \mathrm{d}t\ \mathscr{L}_b\big[\Psi(\mathbf{r}=0), \Psi^*(\mathbf{r}=0)\big] = \int \mathrm{d}t\ \mathrm{d}^d x\ \mathscr{L}_b(\Psi, \Psi^*)\ \delta^{(d)}(\mathbf{r}). \tag{2.12}$$

Writing down the action with the full *(d+1)*-spacetime measure can be formulated through the introduction of a d-dimensional delta function, $\delta^d(\mathbf{r})$. We construct $\mathscr{L}_b$ so as to respect the symmetries of the bulk action. In the bulk action of interest, we consider two main pieces of information that dictate $\mathscr{L}_b$'s form. The first being the $U(1)$ gauge symmetry under the transformation

$$\Psi \mapsto e^{i\theta}\Psi \qquad \mathscr{L}_B \to \mathscr{L}_B. \tag{2.13}$$

The second is that our system possesses rotational symmetry, which can be seen by the action of $SO(3)$ on the spatial variable $\mathbf{x}$ leaving the Lagrangian invariant. With these properties in mind, one can construct a point-particle action to exhibit the following form:

$$S_b = \int \mathrm{d}t \sqrt{-g_{\mu\nu}\dot{\gamma}^\mu\dot{\gamma}^\nu}\big[-M + h|\Psi|^2 + ...\big] \tag{2.14}$$

Where γ continues to denote the world-line of the source, $\dot{\gamma}^\mu = \frac{d\gamma^\mu}{dt}$ and $g_{\mu\nu} = diag(+1, +1, +1, +1)$ is the Euclidean metric. The first term $-\sqrt{g_{\mu\nu}\dot{\gamma}^\mu\dot{\gamma}^\nu}M$ is recognized as the point particle Lagrangian for the source with mass M. In the low energy limit, its dynamics can be best approximated by regular quantum mechanics. We define a characteristic length scale, R of the source itself (ex. R can serve as a proxy for the size of the source) and a as the scale at which we would probe the system where $a >> R$. One is therefore able to generate an EFT in a R/a like expansion since we are interested in the physics occurring at the scale a and are able to ignore the physics of the characteristic length scale, R. The lowest dimensional coupling to particles of the bulk occurs via the second term $h|\Psi|^2$.

We want to present the couplings to the bulk in a series of decreasing relevance. We introduce a delta function to reproduce the $d+1$-dimensional measure of the brane action. To make it more explicit, our brane action will be given by

$$S_b = -\int \mathrm{d}t\ \mathrm{d}^d x\ \big[h_2|\Psi|^2 + h_4|\Psi|^4 + ...\big]\delta^d(\mathbf{r}). \tag{2.15}$$

We note that the ellipsis denotes higher-dimensional interactions that also respect the $U(1)$ and rotational symmetry of the problem, thereby including derivatives of the field and greater powers of the field[3].

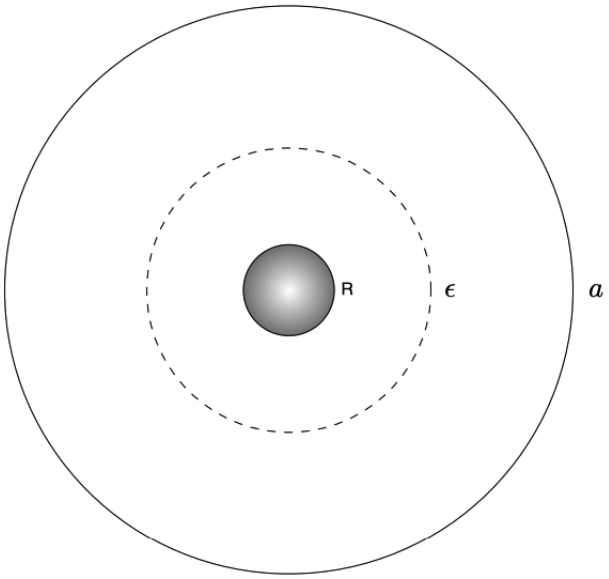

Figure 2.1: The hierarchy of scales in the problem, with a source of size R probed at scales a [3].

To provide a visual aid to accompany the introduced scales, we refer to Fig 2.1. The hierarchy of scales presents an intermediate scale we have labeled ϵ. The aim is to simplify the problem so that we only keep the most relevant terms. To contextualize the discussion, we consider some macroscopic probe at a scale a that doesn't consider the size of the source as relevant to the problem. Our domain of interest will be a Gaussian pillbox of spherical size ϵ satisfying $R << \epsilon << a$. We introduce ϵ by regularizing the point-particle action through extending the radial coordinate from the origin to some scale $\epsilon > 0$, thereby generating a closely related *boundary action* of codimension 1, fixed at the position of a $(d-1)$-sphere of radius ϵ [See dashed line in Fig 2.1]. The hierarchy of scales allows us to write the point-particle action through an expansion in powers of R/ϵ, thereby suppressing higher-dimensional interactions. The relative scale $\epsilon << a$ is used to truncate the action to its lowest-dimensional terms, so that probe at a isn't sensitive to the boundary action. We will often continue to employ the $\delta^3(r)$ notation in the action but it

[3]Through the lens of field theory, one can garner a good interpretation of this point-particle action. Consider two fields χ and Ψ in regular space-time, coupling to one another through a ϕ^4-like interaction:

$$S_{int}[\chi,\Psi] = h\int \mathrm{d}^4x\ \chi^\dagger\chi\Psi^\dagger\Psi, \tag{2.16}$$

where h denotes the coupling. Then if χ is sufficiently compact relative to Ψ, one can argue that its probability distribution is localized to a point: $\chi^\dagger\chi \sim \delta^3(r)$. Technically, through the EFT paradigm, the heavy field χ would be integrated out via the splitting of light and heavy fields in the path-integral generating functional.

should be noted that we are using a regularized delta-function at $r = \epsilon$. The near source boundary condition in §2.2.4 will make this more clear.

2.2.4 Near Source Boundary Condition

In this section, we discuss the details of how the boundary condition near the origin is derived. With the setup enlisted, the field equations of the total action $S = S_B + S_b$ have delta-function contributions from the brane. The natural choice for establishing the boundary condition is now presented here. We want to perform an integration over some infinitesimal sphere, $0 \leq \mathbf{r} \leq \epsilon$. One can see that doing so casts the boundary condition directly in terms of the source action. For some potential, $V(r)$ in $d = 3$ dimensions, provided that it satisfies $|V(r)| \geq \mathcal{O}\left[\frac{1}{r^2}\right]$ near the origin, we can safely ignore its contribution to the performed integral. The field equation of the Schrodinger action reproduces Schrodinger's equation with a new term contributed from the brane. This is depicted by

$$\nabla^2\Psi + [k^2 - 2mV(r)]\Psi = -2m\frac{\delta S_b}{\delta \Psi}. \tag{2.17}$$

For compactness, we let $Y_\omega(\xi)$ denote the spherical harmonic of degree d, indexed by a collection of parameters, ω and function of a collection of angular variables $\xi = \{\theta^1, \theta^2, .., \theta^{d-1}\}$. We make note of the orthogonality property over the surface of the d-sphere:

$$\int_{S^{d-1}} Y_\omega(\xi) Y_\mu(\xi) d\Omega = \delta_{\omega\mu} \tag{2.18}$$

where $\delta_{\omega\mu}$ is a product of Kronecker deltas to match each labeling index. This orthogonality can be exploited for the integral of interest as we first construct a superposition of states via an expansion given by

$$\Psi = \sum_\omega \phi_\omega(r) Y_\omega(\xi). \tag{2.19}$$

We then proceed to multiply both sides by a spherical harmonic, $Y_l(\xi)$ indexed by the state of interest for our boundary condition[4]. We compute the kinetic term integration below:

$$\begin{aligned}
\int \mathrm{d}^d x \, \left[\nabla^2\Psi\right] Y_l(\xi) &= \int \mathrm{d}^d x \, \left[\nabla^2 \sum_\omega \phi_\omega(r) Y_\omega(\xi)\right] Y_l(\xi) \\
&= \sum_\omega \int \mathrm{d}^d x \, \left[\frac{1}{r^{d-1}}\frac{\partial}{\partial r}\left(r^{d-1}\frac{\partial \phi_\omega}{\partial r}\right) Y_\omega + \phi_\omega \frac{\Delta_{S^{d-1}}}{r^{d-1}} Y_\omega\right] Y_l \\
&= \sum_\omega \int \mathrm{d}r \, d\Omega_{d-1} \, \left[\frac{\partial}{\partial r}\left(r^{d-1}\frac{\partial \phi_\omega}{\partial r}\right) Y_\omega - \bar{\omega}_d \phi_\omega Y_\omega\right] Y_l \\
&= \sum_\omega \int_0^\epsilon \mathrm{d}r \, \left[\frac{\partial}{\partial r}\left(r^{d-1}\frac{\partial \phi_\omega}{\partial r}\right) - \bar{\omega}_d \phi_\omega\right] \int_{S^{d-1}} d\Omega_{d-1} Y_\omega Y_l \\
&= \epsilon^{d-1}\frac{\partial \phi_l}{\partial r}\Big|_{r=\epsilon}
\end{aligned} \tag{2.20}$$

[4]One can use Stoke's theorem to arrive at the $l = 0$ boundary condition but this more complicated exercise is demonstrated because we want to obtain the boundary condition for any desirable index.

In addition, we consider the rate of convergence of the integral for the second term in (2.17). The efficacy of this boundary condition story lies in having $\int \mathrm{d}^d x\, [k^2 - 2mV(r)]\Psi \to 0$ as $\epsilon \to 0$. This procedure works out here as $|V(r)| \geq \mathcal{O}\left[1/r^2\right]$. Hence, we ignore the $\left[k^2 - 2mV(r)\right]\Psi$ contribution to the boundary condition.

For the source action contribution to the integral, we first express the d-dimensional spherical delta function at the origin as given below:

$$\delta^d(\mathbf{r}) = \frac{1}{\Omega_{d-1} r^{d-1}} \delta(r) \tag{2.21}$$

Then multiplying the right hand side of (2.17) by $Y_l(\xi)$, we follow the same procedure of integration over an ϵ-ball. If we suppose that our Lagrangian, $\mathscr{L}_b$ is strictly in terms of Ψ (i.e no derivatives), then we can express this integration below by

$$\int \mathrm{d}^d x\, \frac{\delta S_b}{\delta \Psi} Y_l(\xi) = \int \mathrm{d}^d x\, \frac{\partial \mathscr{L}_b}{\partial \Psi}\, \delta^d(\mathbf{r}) Y_l(\xi) = \frac{1}{\Omega_{d-1}} \int \frac{\partial \mathscr{L}_b}{\partial \Psi}\, \delta(r) Y_l(\xi)\, \mathrm{d}r\, \mathrm{d}\Omega_{d-1}. \tag{2.22}$$

The generic boundary condition is therefore given by

$$\epsilon^{d-1} \frac{\partial \phi_l}{\partial r}\Big|_{r=\epsilon} = \frac{1}{\Omega_{d-1}} \int \frac{\partial \mathscr{L}_b}{\partial \Psi}\, \delta(r) Y_l(\xi)\, \mathrm{d}r\, \mathrm{d}\Omega_{d-1}. \tag{2.23}$$

Quadratic Coupling Case

For simplicity, consider the point-particle action $S_b = -\int \mathrm{d}^d x\, h|\Psi|^2\, \delta^d(\mathbf{r})$. Then multiplying the right hand side of (2.17) by $Y_l(\xi)$ and following the same procedure of integration over an ϵ-ball leads to the following:

$$\int \mathrm{d}^d x\, \frac{\delta S_b}{\delta \Psi} Y_l(\xi) = -h \int \mathrm{d}^d x\, \Psi\, \delta^d(\mathbf{r}) Y_l(\xi) = -\frac{h}{\Omega_{d-1}} \phi_l(\epsilon) \tag{2.24}$$

Hence, for this quadratic source action, we can therefore establish the following boundary condition:

$$\Omega_{d-1} \epsilon^{d-1} \frac{\partial \phi_l}{\partial r}\Big|_{r=\epsilon} = 2mh\, \phi_l(\epsilon). \tag{2.25}$$

This boundary condition story and result (2.25) has also been explored in several papers for the inverse-square system [3][4][5].

2.3 Renormalization Group

In this section, I provide a brief overview of concepts from renormalization that are made use of in this thesis. Renormalization Group (RG) is a mathematical tool that allows us to systematically determine how a theory changes under scale transformations. For instance, I can consider a theory on large-distance scales and compare it with its small distance behaviour or high energy vs low energy [12].

In QFT, one common tool in the renormalization arsenal is to introduce a cutoff parameter, Λ

that enters into the integration limits of the problem. One of its primary motivations was as a means to counter the UV divergences of the perturbative expansion of the QFT. Depending on the problem of interest, one can view this parameter as a calculational crutch aimed at taming the divergences that emerge. In essence, Λ isn't physically relevant to the problem of interest and must therefore drop out of the problem entirely. How this must drop out can be found in the couplings of the Lagrangian. One can argue that some of these couplings would necessarily *run* with Λ as to make any computed observables Λ-independent [12].

When solving for the equations of motion, we will typically have to solve second-order differential equations. We can generically express the solutions, Ψ by

$$\Psi = C_- \Psi_- + C_+ \Psi_+, \tag{2.26}$$

where Ψ_-, Ψ_+ are linearly independent functions of the coordinates and C_-, C_+ are the associated constants. When we use the ϵ boundary condition of (2.23), we are able to isolate for quantities that are relevant to observables such as cross sections. In particular, this generally means establishing what C_-/C_+ must be[5]. Since (2.23) is being evaluated at $r = \epsilon$, one would necessarily find that C_-/C_+ holds an apparent ϵ dependence once isolated for. However, this presents a problem as C_-/C_+ should be an ϵ-independent quantity as ϵ is not in itself related to the physics of the problem. Hence, we require for it to drop out and recognize that the most suitable parameters to vary with ϵ are the couplings. In the case of interest, we have two classes of couplings: those that are internal to the bulk and the source-bulk couplings of the brane action. The divergences that appear are localized at the source and so we argue that it is the source-bulk couplings themselves that are the ones that renormalize these divergences [3]. Hence, our inverse-square coupling g is handed to us by the physical problem of interest whereas the brane action is constructed through the EFT machine and so the associated couplings of the source action are *effective*, applied at the chosen ϵ scale. In the quadratic source action explored earlier, we have that h in (2.25) necessarily *runs* with ϵ.

Def 2.3. : **Beta Function and Fixed Points**
In theoretical physics, the beta function encodes the information of a coupling parameter, g and how they run with the scales, μ of a physical process. Typically, the scale μ is an energy scale but in the problem of interest, we'll have a length scale ϵ that is the flowing parameter. The beta function is defined by

$$\beta(g) = \mu \frac{\partial g}{\partial \mu}. \tag{2.27}$$

We say that g_f is a *fixed point* of (2.27) if it satisfies $\beta(g_f) = 0$.

Def 2.4. : **RG Invariant**
I first want to better formalize what I mean by an RG invariant, as they are useful concepts

[5] We can usually cast cross sections in terms of the ratio C_-/C_+.

that are made use of in this thesis. Each beta function is formalized as a first-order differential equation. Its solutions space is a one-parameter family where the integration constant varying over $\mathbb{R}$ generates every possible *flow*. Typically, our RG flows exhibit certain properties that are common to some set of sub-classes to the problem (For instance, for any chosen RG flow, if it is strictly positive for all ϵ, we can consider this property to be an RG invariant). Suppose that we find our running equation to be $\beta(g) = f(\mu, g)$, then we define its solutions space by $X_\beta = \{g_c \in C^1 \big| \beta(g_c) = f(\mu, g_c)\}$ where g_c is uniquely determined by the function g with integration constant c satisfying the beta equation. In essence, one can consider this space to be parameterized by g_c. Then, let $S_\beta \subset X_\beta$ be a subspace. If $\forall\ h \in S_\beta\ \exists\ \epsilon_* \in \mathbb{R}$ such that $h(\epsilon_*) = z$ where $z \in \mathbb{R}$ is fixed, we then say that ϵ_* is an *RG invariant* of the subclass of flows S_β. It should be emphasized that ϵ_* will generically vary, we simply want there to be some scale where g exhibits a particular behaviour (For instance, perhaps every function g that satisfies the beta equation exhibits a singularity at some point). If g is allowed to be complex, then we'll generally have two RG invariants, with z being related to the second one.

2.4 Background Field Method

In this section, I provide a brief overview of background fields. Background field methods provide great utility in acquiring an effective action for our theory. The procedure begins with a semi-classical perturbative approach by splitting the field $\hat{\phi}(x)$ into a *classical background* component, $\psi_c(x)$ and a quantum fluctuation $\hat{\eta}(x)$ [12].

$$\hat{\phi}(x) = \psi_c(x) + \hat{\eta}(x) \tag{2.28}$$

Def 2.5. : **Background Fields**
The background fields provide most utility in instances where the norms of the quantum fluctuations are much less than that of the classical background (i.e. $|\hat{\eta}| << |\psi_c|$). They typically satisfy the regular equations of motion:

$$\frac{\delta S}{\delta \phi}\Big|_{\phi=\psi_c} = 0 \qquad \frac{\delta S}{\delta \phi}\Big|_{\phi=\psi_c} + J = 0 \tag{2.29}$$

In the latter equation of (2.29), we supposed that some source J was present and so the classical field equations are correspondingly homogeneous. In the procedure used in §4, we precisely seek out the configurations that minimize the energy functional, H. Hence, we require that ψ_c is a minimizing extremum of H. In addition, we obtain a unique background configuration by demanding that it satisfy the relevant boundary conditions of the problem. The first is obtained by demanding for $H[\psi_c]$ to be finite and the second by demanding for the field equations to satisfy the canonical boundary condition as determined from the brane action.

2.5 Multiple Species Formalism

In this section, I want to develop the general action and formalism that we can use for a multiple species framework. This formalism will be used in §3 for the case of 1 and 2 particle species. Our aim is to include multiple particles in our model as to observe the behaviour of generic flavour changing processes such as particle A decaying into particle B. The main interest is observing how we can induce catalytic processes through absorptive decay channels. We first consider the bulk action of N second quantized Schrodinger fields in the presence of a potential $\hat{V}(r)$, which is simply the sum over each particle index of the regular single-particle Schrodinger action given below by

$$S_B = \sum_{a=1}^{N} \int \mathrm{d}^4x \left[\frac{i}{2} \left\{ \Psi_a^\dagger (\partial_t \Psi_a) - (\partial_t \Psi_a^\dagger) \Psi_a \right\} - \left(\frac{1}{2m_a} |\nabla_a \Psi_a|^2 + \Psi_a^\dagger(\vec{r},t) \hat{V}(\vec{r}) \Psi_a(\vec{r},t) \right) \right], \tag{2.30}$$

where Ψ_a and m_a denotes the field and mass for particle species a respectively. We can observe that this bulk action doesn't contain any interaction terms between the species. Since we are interested in having our source serve as a catalyst for decay processes, we instead encode all the interaction terms in the brane action itself.

Hence, the next step is to build our brane action. Our model is constructed by having all interactions located at the source itself and we therefore require a suitable brane action to encode all of these mixing terms. We use (2.15) as the basis for our model. In §3, we keep terms up to quadratic order in the fields as they are the most dominant contributions to the action. In addition, we extend this point-particle action to include mixing terms between the species. For a system of N distinct species, the resulting point-particle action is then given below by

$$S_b = -\sum_{a=1}^{N} \sum_{b=1}^{N} \int \mathrm{d}^4x \, M_{ab} \Psi_a^\dagger \Psi_b \, \delta^3(\mathbf{r}), \tag{2.31}$$

where M_{ab} denote the coupling strengths of the respective interactions at the source.

Our aim is to establish the field equations of the system and so we do this for each particle species a. We note that the field equations are as usual given below by

$$0 = \frac{\delta S_B}{\delta \Psi_a^\dagger} + \frac{\delta S_b}{\delta \Psi_a^\dagger}. \tag{2.32}$$

We begin by establishing the expected variation of the bulk action, leaving $\hat{H}_a$ present for compactness, denoting the induced bulk Hamiltonian operator for particle species a. To be explicit, it is defined below by

$$\hat{H}_a = -\frac{\nabla_a^2}{2m_a} + \hat{V}(r). \tag{2.33}$$

We compute the variation of the bulk action, given below by

$$\frac{\delta S_B}{\delta \Psi_a^\dagger} = i\partial_t \Psi_a - \hat{H}_a \Psi_a. \tag{2.34}$$

Similarly, the variation of the point-particle action is

$$\frac{\delta S_b}{\delta \Psi_a^\dagger} = -\sum_{b=1}^{N} M_{ab}\Psi_b \; \delta^3(r). \tag{2.35}$$

Observe that it is precisely the point-particle action that gives rise to a set of coupled equations between all the fields. This coupling is necessary if we are interested in flavour changes $a \rightarrowtail b$ as the corresponding cross sections will be proportional to the strength of M_{ab}. Substituting (2.34) and (2.35) into (2.32) establishes our equations of motion:

$$H_a\Psi_a + \sum_{b=1}^{N} M_{ab}\Psi_b \; \delta^3(r) = i\partial_t \psi_a. \tag{2.36}$$

When the species index is the same ($a = b$), the point-particle variation contributes a Dirac-delta potential. For the $a \neq b$ fields, the Dirac-delta doesn't act as a potential in the usual sense. This set of coupled equations can be viewed linearly, choosing $\{\Psi_a\}$ as a canonical choice of basis. They can be compactly represented by the linear transformation given by

$$\begin{bmatrix} H_1 + M_{11}\delta^3(r) & M_{12}\delta^3(r) & .. & M_{1N}\delta^3(r) \\ M_{21}\delta^3(r) & H_2 + M_{22}\delta^3(r) & .. & M_{2N}\delta^3(r) \\ .. & .. & .. & .. \\ .. & .. & .. & .. \\ .. & .. & .. & .. \\ M_{N1}\delta^3(r) & .. & .. & H_N + M_{NN}\delta^3(r) \end{bmatrix} \begin{bmatrix} \Psi_1 \\ .. \\ .. \\ .. \\ .. \\ \Psi_N \end{bmatrix} = E \begin{bmatrix} \Psi_1 \\ .. \\ .. \\ .. \\ .. \\ \Psi_N \end{bmatrix}. \tag{2.37}$$

Denoting $\tilde{H}$ as the N × N matrix represented above, we can adopt the notation $|\Psi\rangle$ to denote the Ψ vector above, thereby expressing (2.37) by

$$\tilde{H}\,|\Psi\rangle = E\,|\Psi\rangle\,. \tag{2.38}$$

In the standard basis $\{|i\rangle : i \in \mathbb{Z}_N\}$[6], the matrix elements of this formulation are given by

$$\langle i|\tilde{H}\,|j\rangle = H_i\delta_{ij} + M_{ij}\delta^3(r), \tag{2.39}$$

where δ_{ij} denotes the Kronecker-delta. It's natural to split this matrix into components as establishing the boundary condition follows from some key portions. We first define $\mathbf{m}$ as the $N \times N$ mass matrix, $\mathbf{m} = diag(m_1, m_2, .., m_N)$ and $\mathbf{m}^{-1}$ as its inverse[7]. In addition, we take $\mathbf{M}$ to

[6] Where $|i\rangle$ indicates a 1 × N basis vector with zeroes everywhere except for a 1 on the i^{th} entry.

[7] The inverse mass matrix exists if and only if none of our particle species are massless.

be the $N \times N$ coupling matrix, whose matrix elements are given by M_{ij}. With these definitions in mind, one can write the Hamiltonian matrix, $\tilde{H}$ as

$$\tilde{H} = -\frac{1}{2}\mathbf{m}^{-1}\nabla^2 + V(r) + \mathbf{M}\,\delta^3(r). \tag{2.40}$$

We observe that the bulk profile to each species is precisely the same as for the case of a single particle:

$$\Psi_a = \sum_{\omega} e^{-iE_\omega t}\psi_{a,\omega}(r)Y_\omega(\theta,\phi), \tag{2.41}$$

where ω in $d = 3$ are the collection of parameters $\{l, m\}$ corresponding to the angular quantum numbers, just as in §2.2.4. We can therefore express our N-particle state vector via

$$|\Psi\rangle = \sum_{j=1}^{N}\sum_{\omega_j} e^{-iE_{\omega_j}t}\psi_{j,\omega_j}Y_{j,\omega_j}\,|j\rangle\,. \tag{2.42}$$

Just as in §2.2.4, we compute an analogous boundary condition using the argument that the potential and energy terms do not contribute to the integral performed over an ϵ-ball. This procedure gives rise to a new boundary condition given by

$$\lim_{\epsilon\to 0}\, 4\pi\epsilon^2\frac{\partial}{\partial r}|\psi_l\rangle\Big|_{r=\epsilon} = \lim_{\epsilon\to 0}\, 2\mathbf{m}\mathbf{M}|\psi_l\rangle\Big|_{r=\epsilon}, \tag{2.43}$$

where we have defined $|\psi_l\rangle$ as the $1 \times N$ vector with i$^{\text{th}}$ entry given by the radial component of the i$^{\text{th}}$ species $\psi_{i,l}(r)$[8], indexed by the angular momentum state of interest l.

[8]To be explicit, this is how the notation transfers over: $\psi_{i,l} := \langle i|\psi_l\rangle$.

CHAPTER 3

FLAVOUR CATALYSIS IN QUADRATIC CONTACT POTENTIALS

In this section, our focus will be on non-relativistic scalar fields interacting with a compact object through an inverse-square potential. The inverse-square is host to a variety of prescribed methodologies aimed at tackling the issue of Hamiltonian self-adjointness. In addition, it gives rise to non-trivial behaviour within the context of PPEFT as demonstrated in [3][4]. The compact object setting is employed as it's an effective description that makes contact with numerous scattering scenarios between light and heavy fields. Through the PPEFT framework, we construct a point-particle action and derive observable quantities of interest (such as cross sections). A natural choice for the boundary conditions of the light field(s) near the origin emerges as a consequence of the PPEFT framework, as seen in §2.2.3. This removes the guesswork of fixing adjointness as motivated in §2.2.

One of the primary relations of interest is on how cross sections depend on the incoming and outgoing momenta k_{in} and k_{out}. We will observe that there are enhancements in certain regimes where cross sections are proportional to $1/k$ at low energies, thereby describing an enhanced catalytic process. The investigation was split into the consideration of both Schrodinger and Klein-Gordon fields, each being equipped with two species of particles.

3.1 Schrodinger Fields

We begin by considering scalar Schrodinger fields, Ψ interacting with a potential sourced by a compact object at the origin. One way to contextualize this discussion is through an interaction between a heavy nucleus and a Schrodinger particle. Our aim is to encode a flavour changing process by examining whether such a compact object can induce catalysis. We will make ample use of the multiple species formalism in §2.5.

3.1.1 Point Particle EFT for Single Schrodinger Species

Our aim is to now demonstrate a few key features of the observables that emerge from this single particle action. For a single species of scalar Schrodinger fields, Ψ we write down the inverse-square bulk action below by

$$S_B = \int \mathrm{d}^4x \; \frac{i}{2}\Big\{\Psi^\dagger(\partial_t\Psi) - (\partial_t\Psi^\dagger)\Psi\Big\} - \Big[\frac{1}{2m}|\nabla\Psi|^2 - \frac{g}{r^2}\Psi^\dagger(\vec{r},t)\Psi(\vec{r},t)\Big], \tag{3.1}$$

which is precisely that of (2.1) in §2.1 (specialized to $d = 3$ dimensions).

We also bring in the introduction of our point-particle action, describing the coupling of the source to the bulk fields. As motivated in §2.2 and §3.1.1, we only keep the dominant quadratic term on the effective brane action. This is given by

$$S_b = -h\int \mathrm{d}^4x|\Psi|^2\;\delta^3(x), \tag{3.2}$$

where h is the associated coupling strength of this interaction. As has been discussed in §2.2.3, we regularize (3.2) by extending the δ-function's radial argument to some $r = \epsilon$ scale.

We compute the relevant field equation for Ψ, given by

$$0 = \frac{\delta S}{\delta\Psi^\dagger} = i\partial_t\Psi + \Big[\frac{1}{2m}\nabla^2\Psi + \frac{g}{r^2}\Psi\Big] - h\Psi\delta^3(x). \tag{3.3}$$

As has already been demonstrated in §2.1, the spherical symmetry of the problem allows us to construct a clean product of radial and angular components, $\Psi(\mathbf{r}) = e^{-iEt}\psi_l(r)Y_l^m(\theta,\phi)$ where Y_l^m are the standard spherical harmonics in $d = 3$ dimensions [See Appendix A]. The radial equation for the inverse-square system in the bulk is therefore given by

$$\frac{d^2\psi_l(r)}{dr^2} + \frac{2}{r}\frac{d\psi_l(r)}{dr} + \frac{2mg - l(l+1)}{r^2}\psi_l(r) = \kappa^2\psi_l(r), \tag{3.4}$$

where we have defined $\kappa = \sqrt{-2mE}$. The linearly independent solutions to the radial equations, $\{\psi_-,\psi_+\}$ are precisely those in §2.1. Hence, provided that $\zeta \neq 0$, we express the full radial solution as

$$\psi(r) = C_+\psi_+(r) + C_-\psi_-(r), \tag{3.5}$$

where we have chosen the eigenbasis of these radial profiles to be described by confluent hypergeometrics $\mathscr{M}[a,b;z]$. These are given by

$$\psi_\pm(r) = (2\kappa r)^{\frac{1}{2}(-1\pm\zeta)}e^{-\kappa r}\mathscr{M}\Big[\frac{1}{2}(1\pm\zeta), 1\pm\zeta; 2\kappa r\Big], \tag{3.6}$$

where we have defined $\zeta := \sqrt{(2l+1)^2 - 8mg}$. The boundary condition for the single species was already shown earlier in §2.2 [See equation (2.25)] and likewise in §2.5. Specializing to $N = 1$, we present it below:

$$\lim_{\epsilon\to 0} 4\pi\epsilon^2\partial_r\Psi\big|_{r=\epsilon} = \lim_{\epsilon\to 0} 2mh\Psi\big|_{r=\epsilon}. \tag{3.7}$$

Depending on whether we are interested in scattering or bound states, this boundary condition encodes the central piece of information necessary to establish the observables of interest. Hence, substituting (3.5) and (3.6) into the above boundary condition (3.7) defines the ratio C_-/C_+ and therefore allows us to directly compute cross sections. To begin we note that we are interested in the near-source asymptotic form of the radial equation. This is given by

$$\psi_{l\pm} \sim (2ikr)^{\frac{-1\pm\zeta}{2}} \text{ as } r \to 0. \tag{3.8}$$

We now aim to compute the ratio C_-/C_+ by substituting the above expression into the boundary condition (3.7). Once the dust settles, we obtain

$$\frac{C_-}{C_+} = (2ik\epsilon)^{\zeta}\frac{\zeta-\hat{\lambda}}{\zeta+\hat{\lambda}}, \tag{3.9}$$

where we have made a convenient redefinition $\hat{\lambda} := mh/\pi\epsilon + 1$.

Renormalization

While C_-/C_+ is key to establishing cross sections, it currently holds an apparent ϵ dependence. To circumvent this, we introduce a renormalization argument. Since ϵ is a parameter used to regularize the problem, it does not hold any physical relevance. Hence, it is argued that observables should be independent of it. Given that cross sections are directly cast in terms of C_-/C_+ requires that the ratio is ϵ-independent. By (3.9), one can observe that this necessarily requires an ϵ dependence hidden within the brane-bulk couplings $\hat{\lambda}$. The beta / running equation for $\hat{\lambda}$ can be found by differentiating (3.9), to which we obtain

$$\epsilon\frac{d}{d\epsilon}\Big(\frac{\hat{\lambda}}{\zeta}\Big) = \frac{\zeta}{2}\Big[1-\Big(\frac{\hat{\lambda}}{\zeta}\Big)^2\Big]. \tag{3.10}$$

We note that (3.10) was also found in [3], where the system was precisely that of the single particle action.

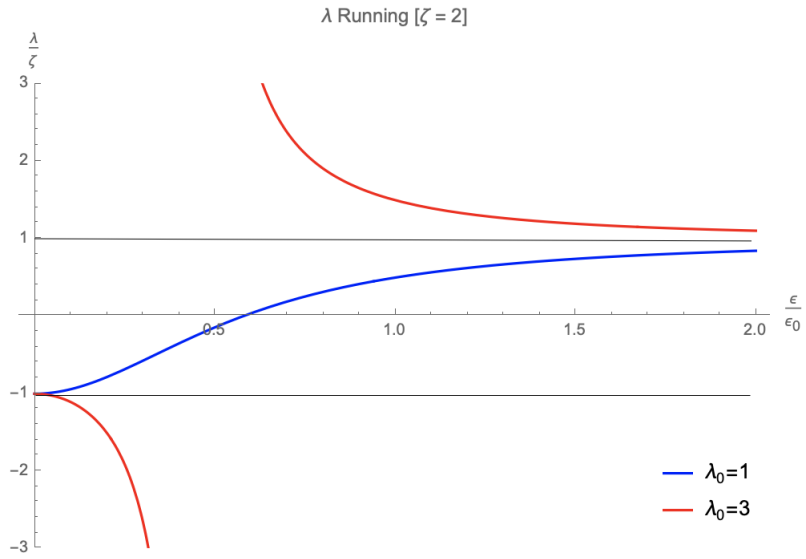

Figure 3.1: The running of $\hat{\lambda}$ for the $\zeta = 2$ case for two different initial values of λ_0. We have chosen a representative flow for each of the two RG-invariant classes. Each horizontal asymptote corresponds to the UV and IR fixed points. In correspondence to the original coupling h, this running informs us that a delta-function is obligatory given that h is non-zero for all ϵ and all flows. It is the IR asymptote at $\lambda = 1$ that is in one-to-one correspondence with $h = 0$. In addition, one can see that the flows select out a special scale that breaks the continuous scale invariance, where $\lambda = 0$ or $\lambda \to +\infty$.

Hence, one can observe that there are two fixed points of this beta equation, precisely lying at $\hat{\lambda} = \pm\zeta$. Defining $\hat{\lambda}(\epsilon_0) := \lambda_0$ for our integration constant, the solution to (3.10) is given by

$$\frac{\hat{\lambda}(\epsilon)}{\zeta} = \frac{(\epsilon/\epsilon_0)^{\zeta}\left[\frac{\lambda_0}{\zeta}+1\right]+\left[\frac{\lambda_0}{\zeta}-1\right]}{(\epsilon/\epsilon_0)^{\zeta}\left[\frac{\lambda_0}{\zeta}+1\right]-\left[\frac{\lambda_0}{\zeta}-1\right]}. \tag{3.11}$$

3.1.2 Point Particle EFT for Two Schrodinger Species

Since the focus of this chapter is on flavour changing from one species to another via $A \to B$ interactions, we need only focus our discussion onto a model that includes two distinct Schrodinger species that we will label 1 and 2. In essence, we set $N = 2$ for the multiple species formalism explored in §2.5. We note that our discussion is limited to single particle states, therefore taking our Hilbert space to be $\mathscr{H} = \mathscr{H}_1 \oplus \mathscr{H}_2$ where $\mathscr{H}_i$ denotes the single particle Hilbert space of species i. We therefore begin by expressing the relevant bulk action for the system by

$$S_B = \sum_{a=1}^{2}\int \mathrm{d}^4x\left[\frac{i}{2}\left\{\Psi_a^*(\partial_t\Psi_a)-(\partial_t\Psi_a^*)\Psi_a\right\}-\left(\frac{1}{2m_a}|\nabla_a\Psi_a|^2-\frac{g}{r^2}|\Psi_a|^2\right)\right]. \tag{3.12}$$

In addition, we write out the brane action as motivated in §3.1.1 (specialized to $N = 2$) as

$$S_b = -\sum_{a=1}^{2}\sum_{b=1}^{2}\int \mathrm{d}^4x\ \Psi_a^* M_{ab}\Psi_b\delta^3(x), \tag{3.13}$$

where M_{ab} denote the associated coupling strengths. Therefore, our field equations are given below by

$$\begin{aligned}\big[H_1 - i\partial_t + M_{11}\delta^3(r)\big]\Psi_1 + M_{12}\delta^3(r)\Psi_2 = 0\\ \big[H_2 - i\partial_t + M_{22}\delta^3(r)\big]\Psi_2 + M_{21}\delta^3(r)\Psi_1 = 0.\end{aligned} \tag{3.14}$$

We can choose to also represent this in the matrix formalism for a two-species Fock space as seen in §3.1.1:

$$\begin{bmatrix} H_1 + M_{11}\delta^3(r) & M_{12}\delta^3(r) \\ M_{21}\delta^3(r) & H_2 + M_{22}\delta^3(r)\end{bmatrix}\begin{bmatrix}\Psi_1\\ \Psi_2\end{bmatrix} = E\begin{bmatrix}\Psi_1\\ \Psi_2\end{bmatrix}. \tag{3.15}$$

The bulk solutions to both species exhibits the same form as for the single case, with the modification being an emphasis on the parameters contained therein. To make this concrete, we write the bulk solutions for the i$^{\text{th}}$ species below in (3.16).

$$\Psi_i(\mathbf{r},t) = e^{-iEt}\big(C_{i-}\psi_{i-} + C_{i+}\psi_{i+}\big)Y_l^m(\theta,\phi) \tag{3.16}$$

With each of the radial profiles given by

$$\psi_{i\pm}(r) = (2\kappa_i r)^{\frac{1}{2}(-1\pm\zeta_i)}e^{-\kappa_i r}\mathscr{M}\Big[\frac{1}{2}(1\pm\zeta_i), 1\pm\zeta_i; 2\kappa_i r\Big], \tag{3.17}$$

where we have defined $\zeta_i := \sqrt{(2l+1)^2 - 8m_i g}$ and $\kappa_i^2 := -2m_i E$. In essence, the species mass m_i is the main parameter that distinguishes them.

The boundary conditions are what will inform us about key ratios such as C_{1-}/C_{1+} and C_{2-}/C_{1+}. As motivated by §2.5, specializing to $N = 2$ furnishes the PPEFT boundary condition, compactly presented below by

$$\lim_{\epsilon\to 0} 2\pi\epsilon^2\partial_r|\psi\rangle\big|_{r=\epsilon} = \lim_{\epsilon\to 0}\mathbf{m}\mathbf{M}\ |\psi\rangle\big|_{r=\epsilon}, \tag{3.18}$$

where we have defined

$$|\psi\rangle = \begin{bmatrix}\psi_1\\ \psi_2\end{bmatrix}, \qquad \mathbf{m} = \begin{bmatrix} m_1 & 0\\ 0 & m_2\end{bmatrix}, \qquad \mathbf{M} = \begin{bmatrix} M_{11} & M_{12}\\ M_{21} & M_{22}\end{bmatrix}. \tag{3.19}$$

(3.18) relates the fields and their radial derivatives at ϵ to one another. This can alternatively be expressed below by

$$\begin{aligned} 2\pi\epsilon^2\frac{\partial\psi_1}{\partial r}\Big|_{r=\epsilon} &= m_1\big(M_{11}\psi_1(\epsilon) + M_{12}\psi_2(\epsilon)\big),\\ 2\pi\epsilon^2\frac{\partial\psi_2}{\partial r}\Big|_{r=\epsilon} &= m_2\big(M_{21}\psi_1(\epsilon) + M_{22}\psi_2(\epsilon)\big).\end{aligned} \tag{3.20}$$

We will make use of the above relations in the proceeding section.

3.1.3 Renormalization

In this section, our aim is to provide the renormalized running of the brane-bulk couplings. We credit Peter Hayman for having derived these quantities and associated figures. These can be found in the paper *Point Particle Catalysis* [9].

We first begin by making convenient re-definitions of our couplings [9]:

$$\lambda_{11} := \frac{1}{\zeta_1}\Big(\frac{m_1 M_{11}}{\pi\epsilon}+1\Big), \qquad \lambda_{22} = \frac{1}{\zeta_2}\Big(\frac{m_2 M_{22}}{\pi\epsilon}+1\Big), \tag{3.21}$$

$$\lambda_{12} = \frac{M_{12}\sqrt{m_1 m_2}}{2\pi\epsilon\sqrt{\zeta_1\zeta_2}}, \qquad \lambda_{21} = \frac{M_{21}\sqrt{m_1 m_2}}{2\pi\epsilon\sqrt{\zeta_1\zeta_2}}. \tag{3.22}$$

In addition, we employ the notation $C_{ij} := \frac{C_{i-}}{C_{j+}}$ for convenience. We now define the RG-invariant length scales ϵ_1, ϵ_2 and ϵ_3 by the following relations to the C-ratios [9]:

$$C_{11} = -y_1(2ik_1\epsilon_1)^{\zeta_1}, \qquad C_{22} = -y_2(2ik_2\epsilon_2)^{\zeta_2}, \tag{3.23}$$

$$C_{12} = \frac{m_2 k_2 \zeta_1}{m_1 k_1 \zeta_2}, \qquad C_{21} = y_3\sqrt{\frac{m_2 k_2 \zeta_1}{m_1 k_1 \zeta_2}}(2ik_1\epsilon_3)^{\zeta_1/2}(2ik_2\epsilon_3)^{\zeta_2/2}, \tag{3.24}$$

where $y_i = \pm 1$ characterize a particular class of flows. We can therefore express our running equations in terms of these scales [9]:

$$\lambda_{11} = \frac{\big(1+y_1(\epsilon/\epsilon_1)^{-\zeta_1}\big)\big(1-y_2(\epsilon/\epsilon_2)^{-\zeta_2}\big)+(\epsilon/\epsilon_3)^{-(\zeta_1+\zeta_2)}}{\big(1-y_1(\epsilon/\epsilon_1)^{-\zeta_1}\big)\big(1-y_2(\epsilon/\epsilon_2)^{-\zeta_2}\big)-(\epsilon/\epsilon_3)^{-(\zeta_1+\zeta_2)}}, \tag{3.25}$$

$$\lambda_{12} = \lambda_{21} = \frac{y_3(\epsilon/\epsilon_3)^{-(\zeta_1+\zeta_2)/2}}{\big(1-y_1(\epsilon/\epsilon_1)^{-\zeta_1}\big)\big(1-y_2(\epsilon/\epsilon_2)^{-\zeta_2}\big)-(\epsilon/\epsilon_3)^{-(\zeta_1+\zeta_2)}}, \tag{3.26}$$

$$\lambda_{22} = \frac{\big(1-y_1(\epsilon/\epsilon_1)^{-\zeta_1}\big)\big(1+y_2(\epsilon/\epsilon_2)^{-\zeta_2}\big)+(\epsilon/\epsilon_3)^{-(\zeta_1+\zeta_2)}}{\big(1-y_1(\epsilon/\epsilon_1)^{-\zeta_1}\big)\big(1-y_2(\epsilon/\epsilon_2)^{-\zeta_2}\big)-(\epsilon/\epsilon_3)^{-(\zeta_1+\zeta_2)}}. \tag{3.27}$$

We can observe the qualitative behaviour of some of these flows by the figures provided on the following page.

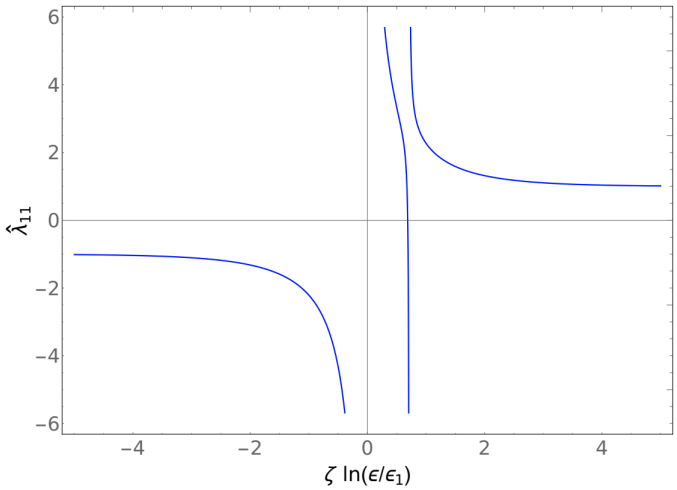

Figure 3.2: [9] The plot of λ_{11} vs $\zeta \ln(\epsilon/\epsilon_1)$ for $\zeta_1 = \zeta_2$, $y_1 = y_2 = +1$, $(\epsilon_2/\epsilon_1)^\zeta = 2$ and $(\epsilon_3/\epsilon_1)^\zeta = 0.02$. All the couplings flow to the UV fixed point in the $(\epsilon/\epsilon_i) \to 0$ limit and IR fixed point in the $\epsilon/\epsilon_i \to \infty$ limit. What is key to note is the implications of the horizontal asymptotes. In correspondence to M_{11}, one can only have $M_{11} = 0$ if $\lambda_{11} = \frac{1}{\zeta_1}$, which corresponds to the IR asymptote. Hence, by the running depicted here, this implies that the presence of the M_{11} brane coupling is obligatory.

One can see that the RG flows select out special scales that break the continuous scale invariance. In particular, it is generic for there to exist a scale that maps $\lambda_{11} \to \pm\infty$ and $\lambda_{12} \to \pm\infty$.

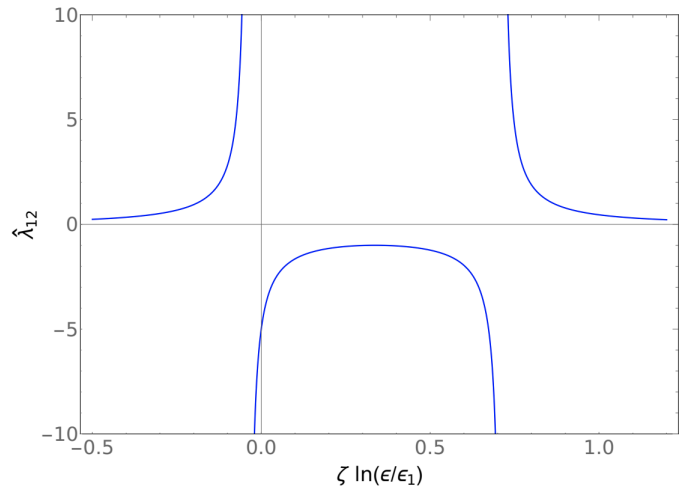

Figure 3.3: [9] Plot of λ_{12} vs $\zeta \ln(\epsilon/\epsilon_1)$ for $\zeta_1 = \zeta_2$, $y_1 = y_2 = y_3 = +1$, and $(\epsilon_2/\epsilon_1)^\zeta = 2$ and $(\epsilon_3/\epsilon_1)^\zeta = 0.02$. The mixing coupling $\hat{\lambda}_{12}$ flows to vanishing coupling in both the UV and IR. It's key to note that this vanishing coupling $\lambda_{12} = 0$ forms a horizontal asymptote, whose correspondence with M_{12} dictates that $M_{12} = 0$ if and only if $\lambda_{12} = 0$. The running therefore implies that such an interaction term on the brane is obligatory.

3.1.4 Scattering States

In this section, we flesh out the procedure for computing elastic and inelastic cross sections: the main observables of interest. We begin by substituting the low-r asymptotic forms for (3.17) into (3.20). There are a few technicalities that occur here, but once the dust has settled, we are able to isolate for a suitable choice of C-ratios (I chose C_{1-}/C_{1+} and C_{2-}/C_{1+}) as our elastic and inelastic cross sections will be directly cast in terms of these ratios. They are found to be

$$\frac{C_{1-}}{C_{1+}} \sim -(2ik_1\epsilon)^{\zeta_1}\Big[\frac{|M_{12}|^2 - \big[\frac{\pi\epsilon}{m_1}(1-\zeta_1)+M_{11}\big]\big[\frac{\pi\epsilon}{m_2}(1+\zeta_2)+M_{22}\big]}{|M_{12}|^2 - \big[\frac{\pi\epsilon}{m_1}(1+\zeta_1)+M_{11}\big]\big[\frac{\pi\epsilon}{m_2}(1+\zeta_2)+M_{22}\big]}\Big], \tag{3.28}$$

$$\frac{C_{2-}}{C_{1+}} \sim \sqrt{\frac{k_2}{k_1}}\,\frac{2\pi\epsilon\zeta_1(2ik_1\epsilon)^{\zeta_1/2}(2ik_2\epsilon)^{\zeta_2/2}M_{12}}{m_1\big[|M_{12}|^2 - \big[\frac{\pi\epsilon}{m_1}(1+\zeta_1)+M_{11}\big]\big[\frac{\pi\epsilon}{m_2}(1+\zeta_2)+M_{22}\big]\big]}. \tag{3.29}$$

One can consult Appendix F for further details on how these ratios were computed.

Elastic Scattering

We now turn to the case of elastic scattering. Without loss of generality, we can consider $1 \to 1$ or $2 \to 2$ scattering as both observable quantities can be permuted from one to the other through a simple change in the parameter index. We proceed by performing the regular argument for scattering, arguing that the large-r asymptotic form of the field to be comprised of an incident plane wave portion and an outgoing spherical wave [11] [See Appendix B]:

$$\psi_1(r) \sim \mathcal{N}\Big(e^{ik_1 z} + f_1(\theta)\frac{e^{ik_1 r}}{k_1 r}\Big) \text{ as } r \to \infty \tag{3.30}$$

where we once again assume scattering off a spherically symmetric potential so that the scattering amplitude $f_1(\theta,\phi) = f_1(\theta)$ is independent of the azimuthal angle ϕ (For the inverse-square system of interest, this argument checks out).

***Free-Wave* subspace: $\zeta = 1$**

We now consider the zero angular momentum subspace for which the inverse-square term isn't present: $g = 0$, $l = 0$, thereby setting $\zeta = 1$. The scattering amplitude is related to the phase shift $e^{2i\delta_l}$ in the usual manner [See Appendix B]. For notational convenience, we want to distinguish the scattering amplitude between the species and so we define f_{il} as the scattering amplitude for the i$^{\text{th}}$ species with angular momentum l.

Since we are interested in low-energy scattering, we need only look at s-wave scattering as it provides the dominant contribution to the cross section at these energies. Hence, we are interested in computing the partial cross section, σ_0. With the discussed notation in mind, we define $f_{1l} := \frac{1}{2ik_1}(e^{2i\gamma_l} - 1)$ and compute f_{10}:

$$\begin{aligned} f_{10} &= \frac{1}{ik_1}\Big(\frac{C_{1-}/C_{1+}}{2 - C_{1-}/C_{1+}}\Big) \\ &= -\epsilon\Big[\frac{T + \pi\epsilon(m_1M_{11} - m_2M_{22})}{T + \pi\epsilon tr(mM) + (2\pi\epsilon)^2 + 2ik_1\epsilon(T + \pi\epsilon[m_1M_{11} - m_2M_{22})]}\Big], \end{aligned} \tag{3.31}$$

where we have defined $T := \det(\mathbf{mM}) + \pi\epsilon\ \mathrm{tr}(\mathbf{mM})$. We note that the s-wave elastic cross section is related to this scattering amplitude by $\sigma_0^{(el)} = 4\pi|f_{10}|^2$ [See Appendix B]. For the observable of interest, we aim to compute the zero energy limit of the elastic cross section as this characterizes the scattering length. The result for $1 \to 1$ elastic scattering in the zero energy limit is depicted below by

$$\lim_{E\to 0} \sigma_0^{(el)} = \lim_{E\to 0} 4\pi|f_{10}|^2 = 4\pi\epsilon^2 \left| \frac{det(mM) + 2\pi\epsilon m_1 M_{11}}{T + \pi\epsilon \mathrm{tr(mM)} + (2\pi\epsilon)^2} \right|^2. \tag{3.32}$$

We can cast this with respect to the RG invariants of the problem [9]. As defined in §3.1.4, we represent $\sigma_s^{1\to 1}$ in terms of ϵ_1:

$$\lim_{E\to 0} \sigma_s^{1\to 1} = 4\pi\epsilon_1^2 \qquad (g = 0). \tag{3.33}$$

Hence, ϵ_1 serves as the parameter dictating the scattering length of $1 \to 1$ scattering. Similarly, by a permutation of the species index, we can obtain $2 \to 2$ scattering [9]:

$$\lim_{E\to 0} \sigma_s^{2\to 2} = 4\pi\epsilon_2^2 \qquad (g = 0). \tag{3.34}$$

where ϵ_2 characterizes the scattering length of the second species.

Inelastic Scattering

In this subsection, we devote our analysis towards the goal of encoding flavour changing processes. Such a phenomena is naturally encoded by inelastic cross sections. For our two-particle model, we want to generically compute $1 \to X$ inelastic scattering. We note that the process $1 \to 2$ is simply the inversion of $2 \to 1$ inelastic scattering, thereby allowing us to permute the index label to recover the other scattering process. Hence, without loss of generality we choose to compute $1 \to 2$ scattering. Following the usual procedure for doing so [11], we describe the large-r asymptotic form of our state vector to be comprised of an incident plane-wave and outgoing spherical wave[1] but with differing parameters:

$$\psi_1(r) \sim N_1 e^{-ik_1 z} \qquad \psi_2(r) \sim N_2 f_2(\theta,\phi)\frac{e^{ik_2 r}}{r} \tag{3.35}$$

This dictates to us that the large-r asymptotics of the second species is an outgoing spherical wave and that the incoming spherical wave component, $e^{-ik_2 r}/r$ must drop out. This places a requirement on the ratio C_{2-}/C_{2+} [See Appendix B] to be

$$\frac{C_{2-}}{C_{2+}} = 4^{\zeta_2}\frac{\Gamma\left[\zeta_2/2\right]}{\Gamma\left[-\zeta_2/2\right]}. \tag{3.36}$$

In computing this cross section, we find that the inelastic differential cross section is given by

$$\frac{d\sigma_{in}^{(1\to 2)}}{d\Omega} = \frac{k_2 m_1}{k_1 m_2}\frac{|N_2|^2 |f_2(\theta,\phi)|^2}{|N_1|^2}, \tag{3.37}$$

[1] ψ_1 and ψ_2 encodes the asymptotic incident and final states respectively.

Free-Wave subspace: $\zeta_1 = \zeta_2 = 1$

We now consider the $\zeta_1 = \zeta_2 = 1$ subspace for which we first note that $N_1 = N_2 = \frac{C_{1+}}{2\sqrt{\pi}}\left(\frac{C_{1-}}{C_{1+}} - 2\right)$ [See Appendix F]. We can therefore establish the s-wave inelastic differential cross section cast in terms of these C-ratios. This is seen below in (3.38).

$$\frac{d\sigma_0^{1\to 2}}{d\Omega} = \sqrt{\frac{m_1}{m_2}}\,\frac{\pi}{k_2^2}\left|\frac{C_{2-}/C_{1+}}{\frac{C_{1-}}{C_{1+}} - 2}\right|^2 \tag{3.38}$$

Our interest is in the low-energy asymptotic form of this cross section as to examine its behaviour in the low energy limit. In the previous section §3.1.3, the $M'_{ij}s$ are observed to renormalize so that they run with ϵ in a particular flow. We define a suitable choice of RG invariants, thereby being able to cast the low energy inelastic cross section in terms of ϵ_3 (See §3.1.4) by

$$\lim_{E\to 0}\sigma_0^{1\to 2} = 4\pi\frac{k_2}{k_1}\epsilon_3^2 \qquad (g = 0). \tag{3.39}$$

Since our fundamental objects are Schrodinger particles, we can observe that the ratio of momentas k_2/k_1 is a constant: $k_2/k_1 = \sqrt{m_2/m_1}$[2], thereby dictating non-zero absorption in the low-k limit. This flavour-violating cross section is non-zero only when the point-particle exhibits non-trivial flavour-violating properties. Such properties would be entirely encoded within ϵ_3. We note that this statement also means that flavour-violation would occur only if $h_{12} \neq 0$.[3]

3.2 Klein-Gordon Fields

Our efforts are now aimed at constructing an analogous system for which the fundamental objects of interest are Klein-Gordon fields. For this relativistic angle, we employ the Minkowski metric $\eta_{\mu\nu} = \text{diag}(-1,1,1,1)$. One of the primary utilities of §3.1 is that the Klein-Gordon field solutions and observables can be easily mapped onto from the parameters of the Schrodinger case[4].

To construct the action of this model, we define the bulk action, S_B to be the sum of two Klein-Gordon actions supplied with an inverse-square term

$$S_B^{(KG)} = \sum_{i=1}^{2}\int \mathrm{d}^4x\Big[-\frac{1}{2}\big(\partial_\mu\Phi_i\big)\big(\partial^\mu\Phi_i\big) - \frac{1}{2}m_i^2\Phi_i^2 + \frac{1}{2}\frac{g}{r^2}\Phi_i^2\Big], \tag{3.40}$$

where m_i denotes the mass of the i$^{\text{th}}$ species and Φ_i represents the KG field itself. We now construct the brane action in an analogous manner to the procedure of §2.5:

$$S_b^{(KG)} = -\sum_{i=1}^{2}\sum_{j=1}^{2}\int \mathrm{d}^4x\; h_{ij}\Phi_i\Phi_j\;\delta^3(x), \tag{3.41}$$

where h_{ij} denote the associated coupling constants. Together, these form the KG action $S_{KG} = S_B^{(KG)} + S_b^{(KG)}$.

[2] Due to the dispersion $k_i = \sqrt{2m_iE}$.

[3] One can observe this relation in (3.26).

[4] We'll observe how this is precisely the case, but part of the story is that they exhibit the same algebra.

The goal of this section is to demonstrate different qualitative behaviour than what was observed for the two species Schrodinger model for cross section - momenta dependence.

To begin, we compute the Klein-Gordon field equations for each species Φ_i, obtained by varying S_{KG}:

$$\big[-\partial_t^2+\nabla^2-m_i^2\big]\Phi_i+\frac{g}{r^2}\Phi_i=\sum_{j=1}^{2}h_{ij}\Phi_j\delta^3(x). \tag{3.42}$$

Standard separation techniques allows us to express the field solutions in the form $\Phi=e^{i\omega t}\chi(\mathbf{r})$. We therefore obtain

$$\big[\nabla^2-\kappa_i^2\big]\chi_i+\frac{g}{r^2}\chi_i=\sum_{j=1}^{2}h_{ij}\Phi_j\delta^3(x), \tag{3.43}$$

where we have defined $-\kappa_i^2=\omega^2-m_i^2$. ∇^2 denotes the Laplacian operator, defined just as in (2.3):

$$\nabla^2\chi=\frac{1}{r^2}\frac{\partial}{\partial r}\Big(r^2\frac{\partial\chi}{\partial r}\Big)+\frac{1}{r^2}\Delta_{S^2}\chi. \tag{3.44}$$

As motivated in §2.1, the angular momentum operator $\mathbf{L}^2$ is related to the spherical Laplacian via $\mathbf{L}^2=-\Delta_{S^2}$. By the spherical symmetry of the problem, we take χ to be in an eigenstate of $\mathbf{L}^2$ defining the eigenvalue relation: $\mathbf{L}^2\chi=l(l+1)\chi$. Hence, we have that $\chi=\phi(r)Y_l^m(\theta,\psi)$, taking ψ to be the azimuthal angle to avoid confusion. Hence, (3.43) induces a radial equation, given below by

$$r^2\frac{\partial^2\phi_i}{\partial r^2}+2r\frac{\partial\phi_i}{\partial r}+\big[g-l(l+1)-r^2\kappa_i^2\big]\phi_i=\sum_{j=1}^{2}h_{ij}\Phi_j\delta^3(x). \tag{3.45}$$

The generic solution to (3.45) is given by

$$\phi_i=C_{i-}\phi_{i-}+C_{i+}\phi_{i+}, \tag{3.46}$$

where $\{\phi_{i-},\phi_{i+}\}$ is the chosen basis for the linearly independent solutions, given by

$$\phi_{i\pm}(r)=(2\kappa_i r)^{\frac{1}{2}(-1\pm\zeta_i)}e^{-\kappa_i r}\mathscr{M}\Big[\frac{1}{2}\Big(1\pm\zeta_i\Big),1\pm\zeta_i;2\kappa_i r\Big], \tag{3.47}$$

where we have defined $\zeta_i:=\sqrt{(2l+1)^2-4g}$ and $\mathscr{M}$ to denote the confluent hypergeometrics. The asymptotics of (3.47) are precisely the same as earlier:

$$\phi_{i\pm}(r)\sim(2\kappa_i r)^{\frac{1}{2}(-1\pm\zeta_i)}\Big[1+\mathscr{O}(r^2)\Big]\text{ as }r\to 0 \tag{3.48}$$

with the main distinction to the Schrodinger case being κ_i defining a different dispersion relation to the energy of the particles via $-\kappa_i^2=E^2-m_i^2$.

3.2.1 Near Source Boundary Condition

Ultimately, we are interested in determining scattering cross sections for this system. Since they are cast in terms of the C-ratios, our priority is to determine what these are in terms of the parameters of the theory. To establish their value requires first developing the new near source boundary condition for the Klein-Gordon case. The procedure follows analogously to the Schrodinger field, with the mild modification being a factor of 2m. Hence, we integrate (3.45) over an infinitesimal ϵ-ball thereby generating the boundary condition:

$$4\pi\epsilon^2 \frac{\partial}{\partial r} |\phi\rangle \big|_{r=\epsilon} = \mathbf{h}_{KG} |\phi\rangle \big|_{r=\epsilon}, \tag{3.49}$$

where we have defined h_{KG} and $|\phi\rangle$ by

$$\mathbf{h}_{KG} = \begin{bmatrix} h_{11} & h_{12} \\ h_{21} & h_{22} \end{bmatrix}, \qquad |\phi\rangle = \begin{bmatrix} \phi_1 \\ \phi_2 \end{bmatrix}. \tag{3.50}$$

This is the underpinning condition that dictates what the quantities C_{i-}/C_{j+} must be. To establish this, we take the small-r asymptotic form of our radial profiles to be

$$\phi_{i\pm}(r) \sim (2\kappa_i r)^{\frac{1}{2}(-1\pm\zeta_i)} \ \text{ as } \ r \to 0. \tag{3.51}$$

We now want to make explicit use of all the results that were obtained in §3.1. To do this, we observe that we can recover the KG boundary condition from the Schrodinger case by a redefinition of the Schrodinger coupling constants M_{ij} via $M_{ij} \mapsto \frac{h_{ij}}{2m_i}$. In addition, since both fields are scalars and are described by the same bulk profiles[5] the algebra of §3.1.4 is easily transferred onto the Klein-Gordon case through a set of parameter re-definitions.

3.2.2 Scattering States

We now turn to the scattering states of the problem. As motivated in the prior paragraph, the scattering results of §3.1.4 can be precisely mapped onto the scattering observables for KG fields.

Elastic Scattering

We first consider the low energy $1 \to 1$ elastic scattering cross section in the case where no inverse-square is present *(g=0)*. We are interested in the qualitative behaviour that emerges at low k_1, exhibiting the same form as that of (3.32):

$$\sigma_{1\to1} \sim 4\pi\epsilon^2 \Big[\frac{|h_{12}|^2 - h_{11}\big(h_{22}+4\pi\epsilon\big)}{|h_{12}|^2 - \big(h_{11}+4\pi\epsilon\big)\big(h_{22}+4\pi\epsilon\big)} \Big]^2 \qquad \text{as } \ k_1 \to 0, \tag{3.52}$$

which can similarly be recasted in terms of an RG invariant

$$\lim_{E\to0} \sigma_s^{1\to1} = 4\pi\epsilon_1^2, \tag{3.53}$$

which depicts a constant value in the zero momentum limit, as expected.

[5] One can compare (3.17) and (3.47), noting that they differ up to a redefinition of parameters.

Inelastic Scattering

Our attention is once again focused onto the process of flavour changing phenomena, for which inelastic scattering would encode. Our cross sections can be found from the Schrodinger case through the parameter redefinition $M_{ij} \mapsto \frac{h_{ij}}{2m_i}$ and identifying $k_i = \sqrt{E^2 - m_i^2}$. In this case, we find that the inelastic $1 \to 2$ cross section at low energies is given by

$$\sigma_{1\to 2}^{(in)} \sim 16(2\pi\epsilon)^4 \frac{k_2}{k_1} \frac{|M_{12}|^2}{\left[|M_{12}|^2 - \big(M_{11} + 4\pi\epsilon\big)\big(M_{22} + 4\pi\epsilon\big)\right]^2} \qquad \text{as } k_1 \to 0. \tag{3.54}$$

In essence, we can observe that inelastic scattering for the Klein-Gordon species will replicate that of the Schrodinger case with the distinction between them being how the ratio k_2/k_1 depends on incident momenta. By (3.54), we can observe that

$$\sigma_{1\to 2}^{(in)} \propto \frac{k_2}{k_1} \qquad \text{at low energies.} \tag{3.55}$$

In the scenario that we have considered, no internal degrees of freedom are assigned to the point-particle at the origin. Its internal state is assumed to go unchanged via catalytic interactions, hence why we refer to it as a *catalyst*. All the energy-momentum transfer from the incident particle is therefore migrated to the new outgoing particle. Enforcing conservation of energy demands that we have $k_2 = \sqrt{k_1^2 + (m_1^2 - m_2^2)}$. The ratio k_2/k_1 is therefore not a constant as it was for Schrodinger particles, instead taking on different behaviour depending on the relationship between the parameters of the model. If we recast k_2 in terms of the masses m_1, m_2 and incoming particle momenta k_1, we can establish that

$$\frac{k_2}{k_1} = \frac{\sqrt{k_1^2 + (m_1^2 - m_2^2)}}{k_1} \qquad (m_1 > m_2). \tag{3.56}$$

We plot the $m_1 > m_2$ case in Fig 3.4, alongside a $1/k$-like function to demonstrate the low energy regime of overlap.

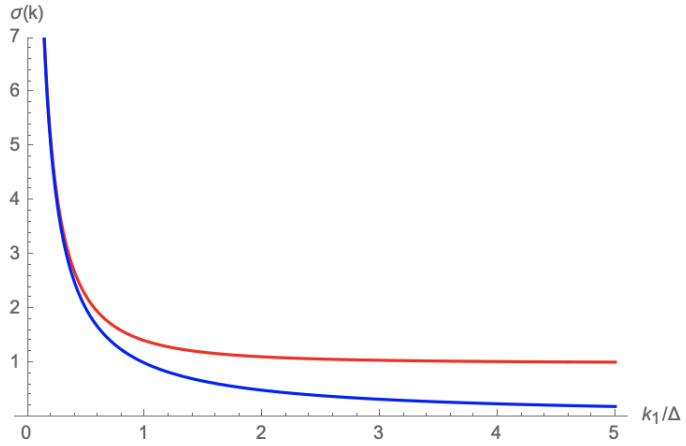

Figure 3.4: The figure demonstrates the asymptotic form of the low-momenta cross section in overlap with a $1/k$-like dependence. The graph is expressed in units of k_1/Δ where $\Delta := \sqrt{m_1^2 - m_2^2}$ and $m_1 > m_2$ [9]. The full function $\sqrt{1+\Delta^2/k_1^2}$ is plotted in red and Δ/k_1 in blue.

The $m_1 > m_2$ result is interesting as it demonstrates a $1/k_1$ enhancement for a flavour changing process between Klein-Gordon particles at low energies. Typically, one finds that the inelastic cross section becomes a constant at low energies. This was observed for the Schrodinger case in the prior section. However, we have found that this cross section predicts catalysis becoming enhanced at low energies.

However, if the incident particle mass is smaller than exiting, energy conservation dictates that there is a minimum allowable incident momentum that would grant such an interaction to have taken place. This minimum is $k_{min} = \sqrt{m_2^2 - m_1^2}$ and if $m_2 > m_1$, then this ratio can be defined by

$$\frac{k_2}{k_1} = \begin{cases} \frac{\sqrt{k_1^2-(m_2^2-m_1^2)}}{k_1} & \text{if } k_1 > \sqrt{m_2^2 - m_1^2} \\ 0 & \text{else} \end{cases} \qquad (m_2 > m_1) \tag{3.57}$$

The above relationship is plotted on the following page in Fig 3.5.

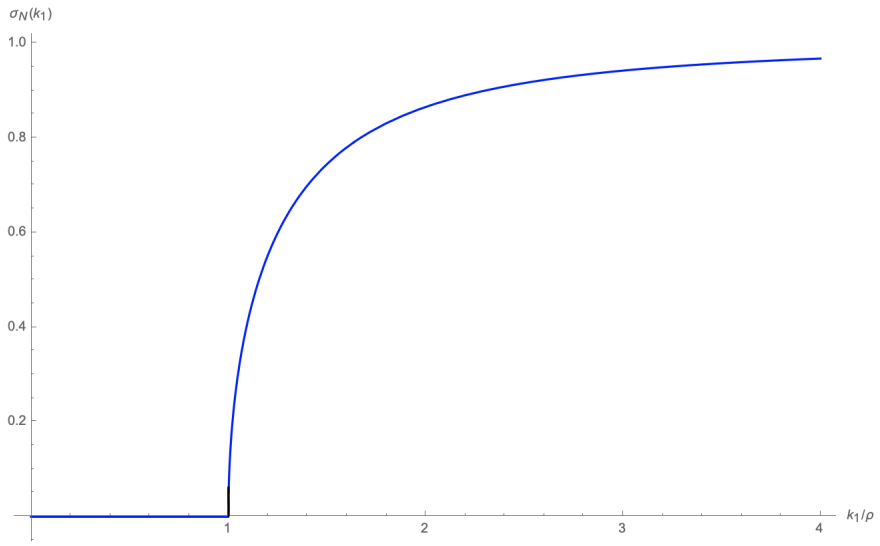

Figure 3.5: The normalized cross section at low energies vs incident momenta in units of k_1/ρ where $\rho := \sqrt{m_2^2 - m_1^2}$.

The last regime of interest is when the masses are the same, $m_1 = m_2$. In this case, we necessarily have that $k_2 = k_1$, thereby rendering the ratio to be a constant $k_2/k_1 = 1$. This would be the case that reproduces a constant cross section at low energies, analogous to the Schrodinger case.

CHAPTER 4

QUARTIC INTERACTIONS ON THE BRANE - NLO PPEFT

In §3, we considered the inverse-square problem supplied with a source action that was solely comprised of a quadratic term. One can take the viewpoint that this brane action was a *leading order* description of the PPEFT. In that spirit, one may consider the work of this chapter as a *next to leading order* formulation of the PPEFT for the same inverse-square bulk. In addition, we consider a non-self adjoint PPEFT so that we obtain a non-unitary boundary condition. This is established by allowing the brane couplings to be complex-valued.

As usual, we are motivated to build up a source action by demanding that it respects the symmetries of the bulk. With respect to the bulk of study, this brane can generically take the form

$$S_b = \int \mathrm{d}^4x \big[h_2|\Psi(x)|^2 + h_4|\Psi(x)|^4 + ..\big]\delta^3(x), \tag{4.1}$$

where the ellipsis represent all even higher orders of $|\Psi|$ and its derivative terms. This construction is chosen so as to respect the global U(1) symmetry $\Psi \to e^{i\theta}\Psi$ and rotational symmetry (by the action of the SO(3) group) of the bulk action. The collection of terms in (4.1) can effectively be viewed as a generalized multipole expansion of the source physics. Typically, one truncates this sum by only considering lower order terms. In the previous chapter, this was performed by examining a brane system solely comprised of the quadratic term. The field equations were therefore linear and manifested a delta-function potential.

The focus of this chapter is to therefore study the effect of keeping a quartic potential on the brane; a NLO description of the source physics. What emerges in this analysis is the requirement of using background field techniques, which is made clear by noting that the field equations manifest a cubic term contributed from the quartic interaction.

4.1 Quartic Contact Interaction

We first consider the case of when our source action solely contains a quartic term. One can observe that the field equations will necessarily be non-linear and therefore invoke background field methods to help linearize the problem[1].

We consider a Schrodinger field in the presence of a $1/r^2$ potential, $U(r) = -\frac{g}{r^2}$, where $g \in \mathbb{R}$ denotes the coupling strength. As usual, the action is partitioned into bulk and brane pieces, $S = S_B + S_b$ where we have the Schrodinger bulk action, S_B just as in §3:

$$S_B = \int \mathrm{d}^4x \left(\frac{i}{2}\left\{\Psi^*\dot{\Psi} - \Psi\dot{\Psi}^*\right\} - \frac{1}{2m}|\nabla\Psi|^2 + \frac{g|\Psi|^2}{r^2}\right). \tag{4.2}$$

On the brane, we consider a lone quartic interaction (i.e no quadratic term):

$$S_b = -\int \mathrm{d}\tau h_4|\Psi|^4 = -\int \mathrm{d}^4x\ h_4|\Psi|^4\ \delta^3(\mathbf{x}). \tag{4.3}$$

The field equations are obtained by finding the solutions that extremize the action. For the quartic interaction of interest, they are found to be

$$\frac{\delta S}{\delta \Psi^*} = i\partial_t\Psi + \frac{1}{2m}\nabla^2\Psi + g\frac{\Psi}{r^2} - 2h_4|\Psi|^2\Psi\delta^3(x) = 0. \tag{4.4}$$

Since linearization is the primary tool we aim to use to simplify the problem, we'll necessarily need to establish what the background field is.

4.1.1 The Background Field

In §2.2.4, we discussed the background field method as a way of linearizing non-linear differential equations. Since we have introduced a quartic interaction, our field equations will necessarily be non-linear. Foreseeing this problem, we want to first establish what the background field is so that we can expand about it when necessary. We first identify the Lagrangian, L for the actions listed above in (4.2), (4.3):

$$L = \int \mathrm{d}^3x \left(\frac{i}{2}\left\{\Psi^*\dot{\Psi} - \Psi\dot{\Psi}^*\right\} - \frac{1}{2m}|\nabla\Psi|^2 + g|\Psi|^2r^2 - h_4|\Psi|^4\delta^3(\mathbf{x})\right). \tag{4.5}$$

To establish the background field, we first construct the Hamiltonian functional, H obtained via a Legendre transformation of the above Lagrangian. The field solution that minimizes this Hamiltonian functional, subject to a suitable choice of boundary conditions will be identified as the background field. Our Hamiltonian functional is given by

$$H[\Psi] = \int \mathrm{d}^3x \left(\frac{1}{2m}|\nabla\Psi|^2 - g\frac{|\Psi|^2}{r^2} + h_4|\Psi|^4\delta^3(x)\right). \tag{4.6}$$

Since the objects of interest are Schrodinger fields, one feature to notice is the time-independence of the Hamiltonian. In addition, we say that the potential is attractive if $g > 0$ and repulsive if

[1] A reminder that linearization isn't necessary but a computational aid to help simplify the problem.

$g < 0$, though in this thesis, we are solely interested in the case of an attractive inverse-square potential. We can identify the potentials of our bulk and brane contributions by

$$V(\Psi) = V_B(\Psi) + V_b(\Psi)\delta^3(x), \tag{4.7}$$

where we have defined

$$V_B(\Psi) = -g\frac{|\Psi|^2}{r^2}, \qquad V_b(\Psi) = h_4|\Psi|^4. \tag{4.8}$$

When the inverse square component disappears, $g = 0$, the constant configurations are the fields that minimize the bulk Hamiltonian as we require $\nabla\Psi = 0$. This is explicitly seen by noting the positive-definiteness of the kinetic term. On the brane, if one takes h_4 to be positive then the choice $\Psi = 0$ is what minimizes the brane Hamiltonian, likewise following from a positive-definite argument.

If we now consider the bulk portion of the Hamiltonian, we have a tug of war between the kinetic and inverse-square term for establishing the background configuration that minimizes it. The analysis therefore requires extremization and use of boundary conditions to establish the existence of a possible non-zero background field.

We begin by taking the functional derivative of H with respect to Ψ^*:

$$\begin{aligned}\frac{\delta H}{\delta\Psi^*} &= -\frac{1}{2m}\nabla^2\Psi - g\frac{\Psi}{r^2} + 2h_4|\Psi|^2\Psi\delta^3(x)\\ &= -\frac{1}{2mr^2}\Big(\frac{\partial}{\partial r}\Big(r^2\frac{\partial\Psi}{\partial r}\Big) - \mathbf{L}^2\Psi\Big) - \frac{g}{r^2}\Psi + 2h_4|\Psi|^2\Psi\delta^3(x)\\ &= -\frac{1}{2mr^2}\frac{\partial}{\partial r}\Big(r^2\frac{\partial\Psi}{\partial r}\Big) - \frac{g}{r^2}\Psi + 2h_4|\Psi|^2\Psi\delta^3(x) = 0.\end{aligned} \tag{4.9}$$

It is convenient to adopt spherical coordinates and observe that the angular momentum component of the Laplacian is set to zero (between the second and third line of (4.9)). This is made clear by recognizing that any angular momentum will add energy to the system. We therefore choose the minimal eigenvalue of the $\mathbf{L}^2$ operator (i.e $l = 0$) as this is the angular state that the background configuration will occupy. Provided that $g \neq \frac{1}{8m}$, the solutions[2] to (4.9) are given by

$$\Psi_c(r) = \frac{r^{-1/2}}{\sqrt{4\pi}}\big(c_1 r^{\chi/2} + c_2 r^{-\chi/2}\big), \tag{4.10}$$

where we have defined $\chi := \sqrt{1-8mg}$ and note that the angular harmonic[3] Y_0^0 contributes the factor of $1/\sqrt{4\pi}$. The presence of χ in the EOM's for the background field signals a difference in behaviour that is dependent on the strength of the inverse-square coupling, g. Namely, there exists a critical value, $g_c = \frac{1}{8m}$ where the state would transition into imaginary χ. Since g controls the depth of the potential well, the classes $g < g_c$ and $g > g_c$ highlight a case analysis which will

[2]The listed solutions wouldn't be linearly independent if $g = 1/8m$ but will be considered in **Case 2:** $\chi = 0$.

[3]Recall that the full solution generically takes the form $\Psi_c = \phi_l(r)Y_l^m(\theta,\phi)$ where Y_l^m are the spherical harmonics. However, by the minimal energy argument, we necessarily require Y_0^0 in this particular instance.

now be examined.

Case 1: $\chi \in (0,1)$[4] **[$g < g_c$]**
We begin by evaluating the Hamiltonian at this family of configurations Ψ_c. We aim to ensure convergence as well as respect the PPEFT boundary condition. Since the manifold upon which our fields live extends to spatial infinity, we evaluate the Hamiltonian integral:

$$H_B[\Psi_c] = \frac{1}{\chi}\Big[\Big(\frac{1}{8m}(\chi-1)^2 - g\Big)r^{\chi}|c_1|^2 - \Big(\frac{1}{8m}(\chi+1)^2 - g\Big)r^{-\chi}|c_2|^2\Big]\Big|_{r=\epsilon}^{r=\infty} \tag{4.11}$$

Where we note that $g \neq 0$ so that $0 < \chi < 1$. To ensure convergence, we require that $c_1 = 0$ as r^{χ} diverges for large r. This condition therefore sets our background field to exhibit the following form:

$$\Psi_c(r) = \frac{1}{\sqrt{4\pi}}\frac{c_2}{r^{\frac{\chi+1}{2}}}. \tag{4.12}$$

The next step is to satisfy the PPEFT boundary condition. The procedure for doing so is the usual ϵ-ball integration that will provide us with the boundary condition at $r = \epsilon$. It is found to be

$$\frac{\partial \psi_c}{\partial r}\Big|_{r=\epsilon} = \frac{2mh_4}{(2\pi\epsilon)^2}|\psi_c|^2\psi_c\Big|_{r=\epsilon}. \tag{4.13}$$

We can now substitute (4.12) into this above condition and aim to find solutions for c_2. We observe that $c_2 = 0$ trivially satisfies this but would render our background field to be zero. Since this is not a case of interest, we instead suppose that $c_2 \neq 0$ and obtain a condition on c_2:

$$|c_2|^2 = -\frac{2(\chi+1)\pi^2\epsilon^{\chi+2}}{mh_4}. \tag{4.14}$$

For this condition to be satisfied, we would require that h_4 is real and negative. However, by design we want the background field to not only extremize the Hamiltonian but be a configuration that minimizes it. To ensure this, we look to the second variation of the Hamiltonian so as to guarantee a minimum. The sign of h_4 controls this as the restriction to $h_4 > 0$ provides the case in which extremization is a minimum [See Appendix C.2]. Hence, by construction our h_4 does not satisfy (4.14) and so we instead require $c_2 = 0$ to fulfill the boundary condition.

Therefore, we have found that the background field for this case is zero, $\Psi_c = 0$.

Case 2: $\chi = 0$ **[$g = g_c$]**
When this is the case, our prior solutions (4.10) are no longer linearly independent. Instead, the linearly independent solutions for this case are given by

$$\Psi_c(r) = \frac{r^{-1/2}}{\sqrt{4\pi}}\big(c_1 + c_2\log(r)\big). \tag{4.15}$$

[4]This notation represents the unit interval $(0,1) = \{x \in \mathbb{R} : 0 < x < 1\}$.

Echoing the prior case, we evaluate this family of configurations in the bulk Hamiltonian so as to demand convergence and satisfy the PPEFT boundary condition. Since $\chi = 0$ is the case when $g = \frac{1}{8m}$, we substitute these relations into the Hamiltonian functional and evaluate the integral

$$H_B[\Psi_c] = \frac{1}{2m}\int_\epsilon^\infty \mathrm{d}r \left(\frac{|c_2|^2(1-log(r)) - \mathrm{Re}[c_1^* c_2]}{r}\right) \tag{4.16}$$

$$= \frac{1}{2m}\Big[(|c_2|^2 - \mathrm{Re}[c_1^* c_2])log(r) - \frac{1}{2}|c_2|^2 log^2(r)\Big]\Big|_{r=\epsilon}^{r=\infty}. \tag{4.17}$$

By inspection, we can observe that the choice $c_2 = 0$ ensures convergence given that any non-zero choice leads to logarithmic divergences. The background field therefore reduces to:

$$\Psi_c(r) = \frac{c_1}{\sqrt{4\pi r}}. \tag{4.18}$$

We now employ the same boundary condition as found in (4.13). We can observe that $c_1 = 0$ trivially satisfies the boundary condition but would render our background to be zero, $\Psi_c = 0$. We therefore investigate the case when $c_1 \neq 0$, thereby giving rise to the requirement on c_1:

$$|c_1|^2 = -\frac{(\pi\epsilon)^2}{m h_4}. \tag{4.19}$$

Similar to Case 1, this condition is satisfied if h_4 is real and negative. However, the same argument of Case 1 is made, since by design we are interested in minimizing the Hamiltonian and have therefore set $h_4 > 0$. Hence, our h_4 does not satisfy the condition (4.19), therefore requiring the $c_1 = 0$ solution.

Therefore, this echoes Case 1, as we have established that the background field must be zero, $\Psi_c = 0$.

Case 3: $\chi := i\eta$ **[**$g > g_c$**]**

We now consider a sufficiently deep inverse-square potential to see whether a background field can exist. Hence, $8mg > 1$ and we define $\eta := \sqrt{8mg - 1}$. The family of background configurations are given below by

$$\Psi_c(r) = \frac{r^{-1/2}}{\sqrt{4\pi}}\big(c_1 r^{i\eta/2} + c_2 r^{-i\eta/2}\big). \tag{4.20}$$

We evaluate the bulk component of the Hamiltonian on these background configurations:

$$H_B[\Psi_c] = \int \left(\frac{1}{2m}|\nabla\Psi_c|^2 - g\frac{|\Psi_c|^2}{r^2}\right)\mathrm{d}^3x = -\frac{\eta}{4m}\int \frac{1}{r}\Big[c_1 c_2^* r^{i\eta}(\eta + i) + c_2 c_1^* r^{-i\eta}(\eta - i)\Big]dr \tag{4.21}$$

$$= -\frac{2\pi}{m}\Big[\mathrm{Im}\big[c_1 c_2^*(\eta+i)\big]\cos(\eta\,\log(r)) + \mathrm{Re}\big[c_1 c_2^*(\eta+i)\big]\sin(\eta\,\log(r))\Big]\Big|_{r=\epsilon}^{\infty} \tag{4.22}$$

Our aim is for the limit at infinity to attain a well-defined finite value. While we are guaranteed to have a bounded limit, seeing as $|\cos(\eta\,\log(r))| \leq 1$ (and like wise for sine), the limit oscillates

between -1 and 1, never reaching convergence at infinity. This is therefore undefined and so we would like to choose our c_1, c_2 so that it's well defined. Since no combination of coefficients for cosine and sine will give us a proper limit, we set both of their coefficients to zero, meaning that we want:

$$c_1 c_2^*(\eta+i) - c_2 c_1^*(\eta-i) = 0, \qquad c_1 c_2^*(\eta+i) + c_2 c_1^*(\eta-i) = 0. \tag{4.23}$$

This requires for at least one of the c_1, c_2 values to be set to zero. Hence, without loss of generality[5] we select $c_2 = 0$ which sets the large-r boundary term to go to zero. This reduces our background configuration to exhibit the form

$$\Psi_c(r) = \frac{c_1 r^{i\eta/2}}{\sqrt{4\pi r}}. \tag{4.24}$$

We now aim to satisfy the PPEFT boundary condition of (4.13). We once again observe that $c_1 = 0$ trivially satisfies (4.13) but would render our background field to be zero. We suppose that $c_1 \neq 0$, thereby establishing the condition

$$|c_1|^2 = \frac{(\frac{i\eta}{2} - 2)\pi^2\epsilon^3}{m h_4} = \frac{\pi^2\epsilon^3}{m|h_4|^2}\big[-2h_R + \eta h_I + i(2h_I + \eta h_R)\big], \tag{4.25}$$

where we have defined $h_4 := h_R + i h_I$.[6] If h_4 is real, it can be seen that it cannot satisfy the above condition. For this reason, we consider the case of complex h_4. In addition to $h_4 \in \mathbb{C}$, we would require the real and imaginary components to be related to one another via $2h_I + \eta h_R = 0$[7], thereby generating

$$|c_1|^2 = -\frac{\pi^2\epsilon^3}{m|h_4|^2}\big[4 + \eta^2\big]h_R. \tag{4.26}$$

Since we are only interested in the $h_R > 0$ case that would describe a minimization problem, then our h_R would not satisfy this condition. This demonstrates that $c_1 = 0$ is the required condition, in turn establishing our background field to be zero, $\Psi_c = 0$.

These cases have exhausted all potential scenarios for the quartic contact interaction in a bulk inverse-square action and so we therefore turn to an improved model that includes the quadratic piece.

4.2 Quadratic and Quartic Contact Interactions - The Double Well Potential

Since a quartic interaction alone gives rise to a trivial background field, the linearization procedure for finding the fluctuations reproduces the well studied inverse-square potential with

[5] We argue that this choice shouldn't matter as it would differ Ψ_c by at most a phase factor, $\epsilon^{-i\eta}$ which should not be observable due to the $U(1)$ symmetry.

[6] Where $h_R := \mathrm{Re}[h_4]$ and $h_I := \mathrm{Im}[h_4]$.

[7] So as to make the imaginary component of (4.25) disappear.

no brane terms. This is rather uninteresting and so we reattempt the problem by including a quadratic term on the brane. The goal is to establish a non-zero background field so that expansion about it and linearization in the fluctuations ensures a non-trivial system[8]. For this reason, we construct the quadratic-quartic brane action by

$$S_b = -\int \mathrm{d}t\ \mathrm{d}^3x\big(-h_2|\Psi(x,t)|^2 + h_4|\Psi(x,t)|^4\big)\delta^3(x), \tag{4.27}$$

where $\mathrm{Re}[h_2] > 0$ and $\mathrm{Re}[h_4] > 0$. In addition, we identify the brane potential by

$$V_b(\Psi) = -h_2|\Psi|^2 + h_4|\Psi|^4. \tag{4.28}$$

If we are interested in real couplings, the graph of $V_b[\Psi]$ for the choice $h_2 = 2$, $h_4 = 5$ is plotted below:

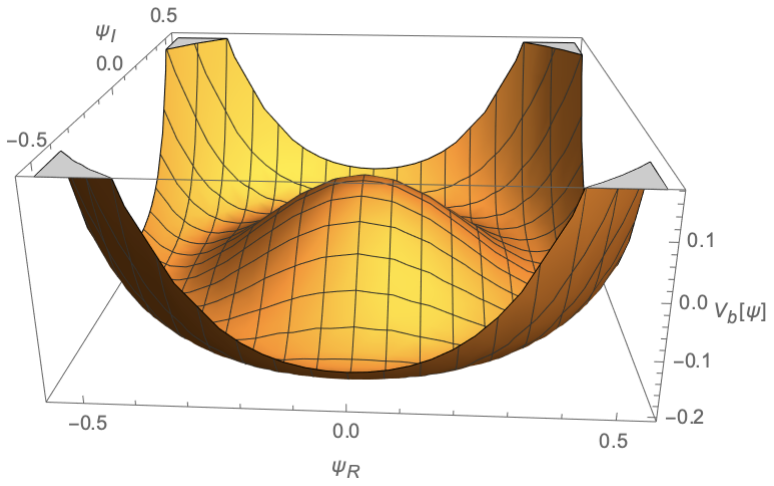

Figure 4.1: The Double-Well Potential of the Brane Action for the choice $h_2 = 2$, $h_4 = 5$.

This sign difference construction is motivated by the observation that the background field on the brane[9] would produce a negative energy value for H_b. Just as before, we define the full action of our model to be $S = S_B + S_b$ with the bulk, S_B being the usual inverse-square:

$$S_B = \int d^4x \left(\frac{i}{2}\left\{\Psi^*\dot{\Psi} - \Psi\dot{\Psi}^*\right\} - \frac{1}{2m}|\nabla\Psi|^2 + \frac{g|\Psi|^2}{r^2}\right). \tag{4.30}$$

[8] In the sense that the point-particle action still contributes to the field equations.

[9] We note that there exists a solution Ψ_c^b satisfying $\frac{\partial V_b}{\partial \Psi}\Big|_{\Psi=\Psi_c^b} = 0$ such that $V_b[\Psi_c^b] < 0$. Explicitly, Ψ_c^b satisfies

$$|\Psi_c^b|^2\Big|_{r=\epsilon} = \frac{h_2}{2h_4} \tag{4.29}$$

4.2.1 The Background Field

In this section, we will demonstrate the existence of a non-zero background field. We will demonstrate this for the three cases of interest that were explored in §4.1.1.

To begin, we Legendre transform our action to obtain the full Hamiltonian for this system by

$$H[\Psi] = \int \mathrm{d}^3x \left[\frac{1}{2m}|\nabla\Psi|^2 - g\frac{|\Psi|^2}{r^2} + \big(-h_2|\Psi|^2 + h_4|\Psi|^4\big)\delta^3(x)\right]. \tag{4.31}$$

The configurations that extremize this Hamiltonian are those that satisfy the following:

$$0 = \frac{\delta H}{\delta\Psi^*} = -\frac{1}{2m}\nabla^2\Psi - g\frac{\Psi}{r^2} + \big(2h_4|\Psi|^2\Psi - h_2\Psi\big)\delta^3(x). \tag{4.32}$$

Echoing §4.1.1, the angular momentum eigenvalue is minimized (i.e $l = 0$) as it solely contributes positive energy to the Hamiltonian. We once again define $\chi := \sqrt{1-8mg}$ and denote the solutions satisfying (4.32) by Ψ_c. In the case that $\chi \neq 0$, the linearly independent solutions determine Ψ_c to take the form

$$\Psi_c(r) = \frac{r^{-1/2}}{\sqrt{4\pi}}\big(c_1 r^{\chi/2} + c_2 r^{-\chi/2}\big), \tag{4.33}$$

where $c_1, c_2 \in \mathbb{C}$ are the associated integration constants. We'll once again aim to establish the background field for each case, just as was performed in §4.1.1. We note that the *convergence at infinity* argument follows precisely as it did in §4.1.1 as the bulk Hamiltonian is the same. Hence, in the cases that follow, it won't be explicitly demonstrated for the second time. We will instead emphasize the new PPEFT boundary condition and its analysis.

Case 1: $\chi \in (0,1)$ **[**$g < g_c$**]**
The convergence at spatial infinity argument follows precisely as it did in §4.1.1 Case 1. This sets $c_1 = 0$, therefore setting the background field configurations to

$$\Psi_c(r) = \frac{c_2}{\sqrt{4\pi r^{\chi+1}}}. \tag{4.34}$$

The modification to the story comes from the PPEFT boundary condition on the ϵ-scale. We once again integrate over an ϵ-ball centred at the origin so as to give rise to the following boundary condition:

$$\frac{2\pi\epsilon^2}{m}\frac{\partial\Psi_c}{\partial r}\Big|_{r=\epsilon} = \big[2h_4|\Psi_c|^2 - h_2\big]\Psi_c\Big|_{r=\epsilon}. \tag{4.35}$$

We note that $c_2 = 0$ trivially satisfies this condition but would render our background field to be zero. We suppose that $c_2 \neq 0$, thereby requiring for it to satisfy

$$|c_2|^2 = \frac{\epsilon^{\chi+1}}{2mh_4}\big[mh_2 - 2\pi\epsilon(\chi+1)\big]. \tag{4.36}$$

Subcase 1: $h_2, h_4 \in \mathbb{R}$

We first consider the case where h_2, h_4 are taken to be real. In this instance, we have considered $h_2 > 0$ and $h_4 > 0$. From the above relation (4.36), one requires $mh_2 - 2\pi\epsilon(\chi+1)$ to be positive. Provided that $h_2 > \frac{2\pi\epsilon(\chi+1)}{m}$, this ensures that we have a non-zero background field, a result that will turn out to be correct down the road. Therefore, the background field satisfies

$$|\Psi_c(\epsilon)|^2 = \frac{mh_2 - 2\pi\epsilon(\chi+1)}{2mh_4}. \tag{4.37}$$

Subcase 2: $h_2, h_4 \in \mathbb{C}$

We now consider the case where $h_2, h_4 \in \mathbb{C}$ and express h_2 and h_4 in their real and imaginary components[10]. In turn, the condition on c_2 (4.36) becomes

$$|c_2|^2 = \frac{\epsilon^{\chi+1}}{2m|h_4|^2}\Big[m\big(h_2^R h_4^R + h_2^I h_4^I\big) - 2\pi\epsilon(\chi+1)h_4^R + i\big(m\big(h_2^I h_4^R - h_2^R h_4^I\big) + 2\pi\epsilon(\chi+1)h_4^I\big)\Big]. \tag{4.38}$$

For consistency, this enforces two constraints on h_2, h_4:

1. **(Complex Tuning Condition)** If $c_2 \neq 0$, we require the imaginary component of (4.38) to vanish[11]. This would set a tuning condition on h_2, h_4:

   $$m\big(h_2^I h_4^R - h_2^R h_4^I\big) + 2\pi\epsilon(\chi+1)h_4^I = 0. \tag{4.40}$$

   We emphasize that this forms a marginal slice from the (h_2, h_4) parameter space and if h_2, h_4 are not related in this precise way, then the only consistent solution is to set $c_2 = 0$. This would set the background field to zero.

2. Since $|c_2|^2$ is strictly positive, if the complex tuning condition is satisfied where $h_4^I, h_2^I \neq 0$, then we require h_2^I, h_4^I to be of the same parity. That is, we need $h_2^I > 0$ and $h_4^I > 0$; or $h_2^I < 0$ and $h_4^I < 0$.

Therefore, provided that h_2, h_4 satisfy these relations, we have a non-zero solution for c_2 satisfying (4.38). However, as discussed, this tuning comprises a tiny subset of the full parameter space. If $h_2, h_4 \in \mathbb{C}$ are not tuned in the precise way described by Equation (4.40), then the background field must be zero. In the analysis that follows, we will present both ends of this argument. We will provide a heading titled '*Complex Tuning*' when considering the case that they are tuned in this precise way. The more general case (where complex tuning does not hold) yields the linearized field equations reducing to the same ones found by considering a brane action with a non-self adjoint quadratic term [A case that was studied in [13]]. The running of h_4 does not enter into

[10] We define $h_2^R := \mathrm{Re}[h_2]$, $h_2^I := \mathrm{Im}[h_2]$, $h_4^R := \mathrm{Re}[h_4]$ and $h_4^I := \mathrm{Im}[h_4]$.

[11] If our system exhibits the property that $h_4^I \neq 0$ and $\chi \in \mathbb{R}$ then we have

$$|c_2|^2 = \frac{h_2^I \epsilon^{\chi+1}}{2h_4^I}. \tag{4.39}$$

the eventual analysis as it precisely drops out once linearization is applied. If one were interested in seeing how h_4 were to run, this could be informed by considering different observables than the $\Psi + P \to \Psi + P$ type interactions considered here (where P denotes the point-particle source).

To ensure that the *complex tuning* would indeed give us the background field, we evaluate the Hamiltonian functional for the non-trivial Ψ_c. It is computed to be

$$H[\Psi_c] = -\frac{1}{4m^2 h_4}\left[mh_2 - \pi\epsilon(\chi+1)\right]^2 \tag{4.41}$$

Hence, this result indeed establishes that this configuration is the true background given that we have obtained a negative energy solution.

Case 2: $\chi = 0$ **[**$g = g_c$**]**
For this case, we note that our linearly independent solutions are once again described by (4.15). Applying the *convergence at spatial infinity* argument, as observed in §4.1.1 Case 2, the background field becomes

$$\Psi_c(r) = \frac{c_1}{\sqrt{4\pi r}}. \tag{4.42}$$

Using the PPEFT boundary condition of (4.35), we observe that $c_1 = 0$ trivially satisfies this but would make our background field zero. We instead suppose that $c_1 \neq 0$ and determine the requirement on c_1.

Subcase 1: $h_2, h_4 \in \mathbb{R}$
If $h_2, h_4 \in \mathbb{R}$, then one obtains

$$|c_1|^2 = \frac{\epsilon}{2mh_4}(mh_2 - 2\pi\epsilon), \tag{4.43}$$

requiring that $h_2 > \frac{2\pi\epsilon}{m}$ to be consistent with $|c_1|^2$ being positive-definite.

Subcase 2: $h_2, h_4 \in \mathbb{C}$
If $h_2, h_4 \in \mathbb{C}$, then one finds a similar expression as was seen in Case 1. If $c_1 \neq 0$, then one has

$$|c_1|^2 = \frac{\epsilon}{2m|h_4|^2}\left[h_4^R(mh_2^R - 2\pi\epsilon) + mh_4^I h_2^I + i\left[m(h_2^I h_4^R - h_4^I h_2^R) + 2\pi\epsilon h_4^I\right]\right], \tag{4.44}$$

We note that the same two constraints seen in Case 1, Subcase 2 are required for a consistent non-zero solution for c_1. Hence, in general, if h_2, h_4 do not satisfy the complex tuning condition when they are complex, then this would render the background field to be zero. For the imaginary component to disappear, we require h_2, h_4 to satisfy the tuning condition

$$m(h_2^I h_4^R - h_4^I h_2^R) + 2\pi\epsilon h_4^I = 0. \tag{4.45}$$

If this holds, the Hamiltonian evaluates to

$$\begin{aligned} H[\Psi_c] &= \left[h_4|\Psi_c|^2 - h_2\right]|\Psi_c|^2\big|_{r=\epsilon} \\ &= -\frac{1}{2m}\left[mh_2 + \pi\epsilon\right]|\Psi_c|^2\big|_{r=\epsilon} \end{aligned} \tag{4.46}$$

The above result (4.46) confirms that this is indeed a non-zero background field that minimizes the Hamiltonian.

Case 3: $\chi := i\eta$ **[**$g > g_c$**]**
Just as in §4.1.1, we define $\eta := \sqrt{8mg-1}$ where $\eta \in \mathbb{R}$. Following the same procedure of §4.1.1 Case 3, we want a well defined convergent value for the Hamiltonian functional, requiring us to make a choice in setting c_1 or c_2 to zero in (4.20). Without loss of generality, we set $c_1 = 0$ thereby obtaining

$$\Psi_c(r) = \frac{c_2 r^{i\eta/2}}{\sqrt{4\pi r}}. \tag{4.47}$$

Substituting this relation into the boundary condition (4.35), we observe that $c_2 = 0$ trivially satisfies it but would render our background field to be zero. Supposing that $c_2 \neq 0$, we obtain a condition on c_2:

$$|c_2|^2 = \frac{\epsilon}{2mh_4}\Big[mh_2 - 2\pi\epsilon(i\eta+1)\Big] \tag{4.48}$$

In this instance, we observe that $h_2, h_4 \in \mathbb{R}$ would not satisfy the above equation as $|c_2|^2$ would be complex valued. Let $h_2, h_4 \in \mathbb{C}$, then expanding into real and imaginary components, we obtain:

$$|c_2|^2 = \frac{\epsilon}{2m|h_4|^2}\Big\{h_4^R(mh_2^R - \pi\epsilon) + h_4^I(mh_2^I - 2\eta\pi\epsilon) + i\Big[h_4^R(mh_2^I - 2\eta\pi\epsilon) - h_4^I(mh_2^R - \pi\epsilon)\Big]\Big\}. \tag{4.49}$$

We want to make the right hand side real and positive definite. We can observe that one set of solutions is if we have the simultaneous equalities of $h_2^R = \frac{\pi\epsilon}{m}$ and $h_2^I = \frac{2\eta\pi\epsilon}{m}$. However, this would turn $c_2 = 0$ which is not a case of interest. Instead, if we demand that

$$h_4^R(mh_2^I - 2\eta\pi\epsilon) - h_4^I(mh_2^R - \pi\epsilon) = 0 \tag{4.50}$$

such that $h_2^R \neq \frac{\pi\epsilon}{m}$ and $h_2^I \neq \frac{2\eta\pi\epsilon}{m}$, then the imaginary component vanishes and we obtain

$$|c_2|^2 = \frac{\epsilon}{2mh_4^I}\big(mh_2^I - 2\eta\pi\epsilon\big). \tag{4.51}$$

In this case, the Hamiltonian evaluates to

$$\begin{aligned} H[\Psi_c] &= \left[h_4|\Psi_c|^2 - h_2\right]|\Psi_c|^2\big|_{r=\epsilon} \\ &= -\frac{1}{2m}\left[mh_2 + 2\pi\epsilon(i\eta+1)\right]|\Psi_c|^2\big|_{r=\epsilon}. \end{aligned} \tag{4.52}$$

The above result, (4.52) confirms that this is indeed a non-zero background field that minimizes the Hamiltonian.

In addition, the $U(1)$ symmetry of the model allows us to choose c_2 up to a phase. For convenience, we choose the following:

$$c_2 = \epsilon^{i\eta/2}\sqrt{\frac{\epsilon}{2mh_4}\Big[mh_2 - 2\pi\epsilon(i\eta+1)\Big]} \tag{4.53}$$

Observe that this turns the background field into a purely real function at $r=\epsilon$ as we have the property that $\Psi_c^2\big|_{r=\epsilon} = |\Psi_c|^2\big|_{r=\epsilon}$.

Summary: The above three cases can be compactly summarized by the following statement: If $h_2, h_4 \in \mathbb{R}$ and $g \in [0, 1/8m]$; or $h_2, h_4 \in \mathbb{C}$, $g \in \mathbb{R}^+$ and the *complex tuning* condition is satisfied, then the background configuration satisfies

$$|\Psi_c|^2\big|_{r=\epsilon} = \frac{1}{2mh_4}[mh_2 - 2\pi\epsilon(\chi+1)], \qquad \text{where} \qquad \chi := \sqrt{1-8mg}. \tag{4.54}$$

However, if $h_2, h_4 \in \mathbb{C}$ and the *complex tuning* condition is not satisfied, then

$$\Psi_c = 0. \tag{4.55}$$

4.2.2 Field Equations

The field equations encode all the information we will inquire about the system. Since we have established the existence of non-zero background fields in the prior sections, the main quantum dynamics can now be fleshed out. This algorithm is performed by expanding the field variable about the background field ψ_c, resolve the field equations via extremizing the action and linearize.

We therefore begin by writing down $\Psi = \psi_c + \Phi$ where Φ are second quantized spin-0 Schrodinger fields. The new bulk action is therefore described below by

$$\begin{aligned} S_B = \int d^4x \Big(\frac{i}{2}\Big\{\psi_c^*\partial_t\psi_c - \psi\partial_t\psi_c^*\Big\} + \frac{1}{2m}\psi_c^*\nabla^2\psi_c + \frac{g}{r^2}|\psi_c|^2\Big) \\ + \Big(i\psi_c^*\partial_t\Phi + \frac{1}{2m}\psi_c^*\nabla^2\Phi + \frac{g}{r^2}\psi_c^*\Phi\Big) + \Big(-i\psi_c\partial_t\Phi^* + \frac{1}{2m}\psi_c\nabla^2\Phi^* + \frac{g}{r^2}\psi_c\Phi^*\Big) \\ + \Big(\frac{i}{2}\Big\{\Phi^*\partial_t\Phi - \Phi\partial_t\Phi^*\Big\} + \frac{1}{2m}\Phi^*\nabla^2\Phi + \frac{g}{r^2}|\Phi|^2\Big). \end{aligned} \tag{4.56}$$

In an effort to make these computations more visually digestible, the point-particle actions for the quadratic and quartic pieces will be denoted by S_b^2 and S_b^4 respectively. The quadratic brane action is given by

$$S_b^2 = \int d^4x\; h_2\big(|\psi_c|^2 + |\Phi|^2 + \psi_c^*\Phi + \psi_c\Phi^*\big)\delta^3(x), \tag{4.57}$$

whereas the quartic brane action is given by

$$\begin{aligned} S_b^4 = -\int d^4x\; h_4\Big(|\psi_c|^4 + |\Phi|^4 + (\psi_c^*)^2\Phi^2 + \psi_c^2(\Phi^*)^2 + 4|\psi_c|^2|\Phi|^2 \\ + 2|\psi_c|^2\psi_c^*\Phi + 2|\psi_c|^2\psi_c\Phi^* + 2\psi_c^*|\Phi|^2\Phi + 2\psi_c|\Phi|^2\Phi^*\Big)\delta^3(x). \end{aligned} \tag{4.58}$$

The next turn of the crank will now be performed. We aim to extremize the action as this is what will provide us with the equations of motion. Just as above, we'll perform this computation in parts and then bring it home at the very end. The variation of the bulk action is found to be

$$\frac{\delta S_B}{\delta \Phi^*} = \Big[i\partial_t \Phi - \Big(-\frac{1}{2m}\nabla^2 \Phi - \frac{g}{r^2}\Phi \Big) \Big] + \Big[i\partial_t \psi_c - \Big(-\frac{1}{2m}\nabla^2 \psi_c - \frac{g}{r^2}\psi_c \Big) \Big], \tag{4.59}$$

Variation of the point-particle quadratic action is given by

$$\frac{\delta S_b^2}{\delta \Phi^*} = (h_2 \Phi + h_2 \psi_c)\delta^3(x), \tag{4.60}$$

and variation of the quartic action:

$$\frac{\delta S_b^4}{\delta \Phi^*} = -2h_4\big(|\Phi|^2 \Phi + \psi_c^2 \Phi^* + 2|\psi_c|^2 \Phi + |\psi_c|^2 \psi_c + \psi_c \Phi^2 + 2\psi_c |\Phi|^2 \big)\delta^3(x). \tag{4.61}$$

The variation of the total action, S is what we set to zero and so the relevant equation of motion is given by

$$0 = \frac{\delta S}{\delta \Phi^*} = \frac{\delta S_B}{\delta \Phi^*} + \frac{\delta S_b^2}{\delta \Phi^*} + \frac{\delta S_b^4}{\delta \Phi^*}. \tag{4.62}$$

To avoid clutter, (4.62) is left stated as is but we'll perform a few arguments as to have (4.63) emerge. One feature to notice is the presence of the background field in both the bulk and brane contributions of (4.59)-(4.61). We recall that ψ_c satisfies (4.32) and is also time-independent. Applying this fact eliminates some of the lingering background field pieces contained in (4.62).

The next step is addressing the non-linearity of S_b^4's contribution as we have terms that are quadratic and cubic in the Φ fields. To that end, we now apply the final tool of our field equation arsenal: linearize Φ by eliminating terms that go as $\mathcal{O}(\Phi^2)$. This finally yields the equation of motion for this system, given below by

$$0 = \Big[i\partial_t \Phi - \Big(-\frac{1}{2m}\nabla^2 \Phi - \frac{g}{r^2}\Phi \Big) \Big] + \big[h_2 \Phi - 2h_4\big(\psi_c^2 \Phi^* + 2|\psi_c|^2 \Phi \big) \big]\delta^3(x). \tag{4.63}$$

The way to go about interpreting this result is to find the general solutions to the bulk piece, expressed as $\Phi = e^{-iE_l t}\phi_l(r) Y_l^m(\theta,\phi)$[12] and then use the delta-function contribution to establish the boundary condition. The bulk piece of the radial equation is just as it was in §2.1, with the novel property of there now being a brane contribution. Expressing (4.63) in coordinate form gives us

$$\frac{1}{2mr^2}\Big(\frac{\partial}{\partial r}\Big(r^2 \frac{\partial \Phi}{\partial r} \Big) \Big) - \frac{l(l+1)}{2mr^2}\Phi + g\frac{\Phi}{r^2} + i\partial_t \Phi = \Big[2h_4\big(\psi_c^2 \Phi^* + 2|\psi_c|^2 \Phi \big) - h_2 \Phi \Big]\delta^3(x), \tag{4.64}$$

where we have taken $\mathbf{L}^2 Y_l^m = l(l+1)Y_l^m$. The argument follows analogously just as in §2.1 for $d = 3$. We define $-\kappa^2 := 2mE$ and provided that $\zeta \neq 0$, the solutions to the bulk are given by the following linearly independent functions:

$$\phi_\pm(r) = (2\kappa r)^{\frac{1}{2}(-1\pm\zeta)} e^{-\kappa r}\mathcal{M}\Big[\frac{1}{2}\Big(1 \pm \zeta \Big), 1 \pm \zeta; 2\kappa r \Big] \tag{4.65}$$

[12]Where we have again denoted Y_l^m as the spherical harmonics in three dimensions.

where we have defined $\zeta := \sqrt{(2l+1)^2 - 8mg}$ and $\mathscr{M}$ denoting the confluent hypergeometrics. The radial solutions are given by

$$\phi_l(r) = C_-\phi_-(r) + C_+\phi_+(r) \tag{4.66}$$

where $C_-, C_+ \in \mathbb{C}$ will serve primary importance in establishing observables of interest.

4.2.3 Near Source Boundary Condition and Probability Conservation

We are interested in precisely what boundary condition emerges for the fields near the source. This argument now follows just as it did in §3. We begin by writing down a superposition of states:

$$\Phi = \sum_{l',m'} e^{-iE_{l'}t}\phi_{l'}(r)Y_{l'}^{m'}(\theta,\phi). \tag{4.67}$$

We then want to perform an integration over an ϵ-ball and exploit orthogonality in the spherical harmonics to make this more viable. Hence, just as we have already encountered, we multiply both sides by Y_l^m and proceed to integrate [Refer back to §2.2.3 for the detailed computation]:

$$\int_{B_\epsilon(0)} \mathrm{d}^3x\ \frac{1}{2mr^2}\frac{\partial}{\partial r}\Big(r^2\frac{\partial}{\partial r}\Big(\sum_{l',m'}\phi_{l'}(r)Y_{l'}^{m'}Y_l^m\Big)\Big) = \frac{\epsilon^2}{2m}\frac{\partial\phi_l}{\partial r}\Big|_{r=\epsilon}, \tag{4.68}$$

where $B_\epsilon(0)$ denotes the 3-ball of radius ϵ centred at the origin. We next compute the $\delta^3(x)$ contribution as well:

$$\int \mathrm{d}^3x\Big[2h_4\big(\psi_c^2\Phi^* + 2|\psi_c|^2\Phi\big) - h_2\Phi\Big]\delta^3(\mathbf{x}) = \frac{1}{4\pi}\Big[2h_4\big[\psi_c^2(\epsilon)\phi_l^*(\epsilon) + 2|\psi_c(\epsilon)|^2\phi_l(\epsilon)\big] - h_2\phi_l(\epsilon)\Big]. \tag{4.69}$$

Hence, the linearized PPEFT boundary condition that emerges is given by:

$$\frac{4\pi\epsilon^2}{2m}\frac{\partial\phi_l}{\partial r}\Big|_{r=\epsilon} = \Big[2h_4\big(\psi_c^2\phi_l^* + 2|\psi_c|^2\phi_l\big) - h_2\phi_l\Big]\Big|_{r=\epsilon}. \tag{4.70}$$

One can observe that substituting ϕ_l into (4.70) will encode information about the ratio C_-/C_+, thereby allowing us to inquire about probability amplitudes in scattering scenarios.

One can therefore see that if $h_2, h_4 \in \mathbb{C}$ and the *complex tuning condition* is not satisfied, then $\psi_c = 0$, thereby recovering the boundary condition

$$\frac{4\pi\epsilon^2}{2m}\frac{\partial\phi_l}{\partial r}\Big|_{r=\epsilon} = -h_2\phi_l\big|_{r=\epsilon} \tag{4.71}$$

Probability Conservation

In this section, our aim is to compute the probability flux and see under what conditions does the point-particle serve as a sink/source of probability. There are some subtleties that arise in this analysis, and so we lay out the assumptions experienced thus far clearly. The punchline is that

the *total* probability current (defined shortly) is conserved under the condition that the brane couplings h_2, h_4 are real. Our system satisfies the following continuity equation

$$\frac{\partial \rho}{\partial t} = \nabla \cdot \mathbf{J}, \tag{4.72}$$

where $\rho = \Psi^* \Psi$ and $\mathbf{J} = \frac{1}{2mi}(\Psi^* \nabla \Psi - \Psi \nabla \Psi^*)$. The first subtlety now enters our discussion. The quantity Ψ is the full function associated with both the background field and quantum fluctuation components. In essence

$$\Psi = \psi_c + \Phi, \tag{4.73}$$

where ψ_c denotes the background field and $\Phi = e^{-iE_l t}\phi_l(r)Y_{lm}(\theta,\phi)$. Therefore, one can write $\mathbf{J} = \mathbf{J}_0 + \mathbf{J}_1 + \mathbf{J}_2$, where $\mathbf{J}_i$ denotes the current terms where ϕ appears i times. Hence, $\mathbf{J}_0$ is the current associated with the background field, $\mathbf{J}_1$ are the mixing terms and $\mathbf{J}_2$ is the current associated with the fluctuations. Their explicit expressions are given by

$$\mathbf{J}_0 = \frac{1}{2mi}\left(\psi_c^* \nabla \psi_c - \psi_c \nabla \psi_c^*\right) = 0, \tag{4.74}$$

$$\mathbf{J}_1 = \frac{1}{2mi}\left[(\phi^* - \phi)\nabla \psi_c + \psi_c(\nabla \phi - \nabla \phi^*)\right], \tag{4.75}$$

$$\mathbf{J}_2 = \frac{1}{2mi}\left(\phi^* \nabla \phi - \phi \nabla \phi^*\right), \tag{4.76}$$

where for convenience, we take $\psi_c \in \mathbb{R}$ just as was performed in the thesis. Therefore, the important quantities are $\mathbf{J}_1$ and $\mathbf{J}_2$. We denote the probability flux through a spherical surface of radius $r = \epsilon$ by $\mathscr{P}$. It is defined as follows[13]:

$$\mathscr{P} = \int_{B_\epsilon(0)} \mathrm{d}^2 x \; \mathbf{J} \cdot \hat{\mathbf{n}} = 4\pi\epsilon^2 j = 4\pi\epsilon^2(j_q + j_c), \tag{4.77}$$

where $\hat{\mathbf{n}}$ is the unit-outward normal vector of the sphere and j denotes the radial component of the total current $\mathbf{J}$ with j_1, j_2 being the corresponding radial portions of $\mathbf{J}_1$ and $\mathbf{J}_2$ respectively. Their expressions are explicitly given by

$$j_1 = \frac{1}{2mi}\left[(\phi^* - \phi)\frac{\partial \psi_c}{\partial r} + \psi_c\left(\frac{\partial \phi}{\partial r} - \frac{\partial \phi^*}{\partial r}\right)\right]\Big|_{r=\epsilon}, \tag{4.78}$$

$$j_2 = \frac{1}{2mi}\left[\phi^* \frac{\partial \phi}{\partial r} - \phi \frac{\partial \phi^*}{\partial r}\right]\Big|_{r=\epsilon}. \tag{4.79}$$

We now present the relevant boundary conditions near the origin, as was discovered earlier for our fluctuations. The full-boundary condition for the radial fluctuations ϕ were given by

$$\frac{4\pi\epsilon^2}{2m}\frac{\partial \phi}{\partial r}\Big|_{r=\epsilon} = \underbrace{2h_4\psi_c^2(\phi^* + 2\phi) - h_2\phi}_{\text{linear}} + \underbrace{2h_4\left[\psi_c\phi^2 + 2\psi_c|\phi|^2 + |\phi|^2\phi\right]}_{\text{non-linear}}\Big|_{r=\epsilon}, \tag{4.80}$$

where through linearization, we discounted the terms labelled *non-linear* and only kept the *linear* terms. Discounting the non-linear terms immediately would lead to a naive issue of

[13] We denote the set of all points on the sphere of radius $r = \epsilon$, centred at the origin by $B_\epsilon(0) = \{x \in \mathbb{R}^3 : |x| = \epsilon\}$.

the probability current *appearing* to not be conserved even for $h_2, h_4 \in \mathbb{R}$. We emphasize that computing the probability flux correctly requires the full boundary condition containing both *linear* and *non-linear* components. The reason this occurs is because terms appearing at quadratic order in ϕ from j_1 precisely cancel out the quadratic terms appearing in j_2. For completeness, we recall that the background field's boundary condition at $r = \epsilon$ was given by

$$\frac{4\pi\epsilon^2}{2m}\frac{\partial\psi_c}{\partial r}\Big|_{r=\epsilon} = \left[2h_4\psi_c^2 - h_2\right]\psi_c\Big|_{r=\epsilon}. \tag{4.81}$$

With all the ingredients laid out, we can now compute the probability flux through a surface at radius $r = \epsilon$. It is given by

$$\mathscr{P} = \frac{1}{i}\Big[(h_4-h_4^*)\Big[2\psi_c^3(\phi+2\phi^*)+2\psi_c^2(\phi^2+(\phi^*)^2)+8\psi_c^2|\phi|^2+4\psi_c|\phi|^2(\phi+\phi^*)+2|\phi|^4\Big]-(h_2-h_2^*)(|\phi|^2+\phi^*\psi_c)\Big]\Big|_{r=\epsilon}. \tag{4.82}$$

Hence, one has a sanity check that if the couplings are real: $h_2 = h_2^*$ and $h_4 = h_4^*$, then the source does indeed conserve probability as we find that $\mathscr{P} = 0$. It's interesting to note that the probability current associated with just the fluctuations ϕ does not appear to conserve probability when $h_2, h_4 \in \mathbb{R}$. One finds that

$$\mathscr{P}_2 = \int_{B_\epsilon(0)} \mathrm{d}^2x\, \mathbf{J}_2\cdot\hat{\mathbf{n}} = \frac{1}{i}\Big[\underbrace{2\psi_c^2 h_4((\phi^*)^2-\phi^2)}_{\text{linear}}+\underbrace{2\psi_c h_4|\phi|^2(\phi^*-\phi)}_{\text{non-linear}}\Big]\Big|_{r=\epsilon} = 2i\psi_c h_4(\phi-\phi^*)\left[\psi_c(\phi^*+\phi)+|\phi|^2\right]\Big|_{r=\epsilon}, \tag{4.83}$$

where the *linear* label corresponds to the terms that arise when just the linearized boundary condition is applied and *non-linear* being the additional terms arising from the full boundary condition. The important point is that this precisely cancels out with the current $\mathbf{J}_1$ associated with mixing terms. Hence, $\mathscr{P}_2 = -\mathscr{P}_1$ so one indeed finds a total conservation of probability $\mathscr{P} = \mathscr{P}_1 + \mathscr{P}_2 = 0$.

Though a different system, such behaviour also arises in studies of Bose-Einstein condensates when one writes out the full wave-function in terms of the *condensate* and *excitations*. The procedure is similarly motivated in that the focal equation, often referred to as the Gross-Pitaevskii Equation is a non-linear Schrodinger equation. The wave-function expression would take the form $\Psi = \Psi_0 + \delta\Psi$ with Ψ_0 denoting the condensate and $\delta\Psi$ the quantum excitations. Analogous to what was done here, it is the full current associated with Ψ that satisfies the continuity equation and conserves probability [16].

4.2.4 Renormalization

In this section, we aim to establish the *running* of the quadratic coupling h_2 in the case where it is real as well as complex. One observation to note is that the linearization procedure allows h_4 to precisely drop out of the problem[14], a feature that will be demonstrated shortly. The PPEFT

[14] We therefore do not concern ourselves with its running.

boundary condition of (4.70) encodes C_-/C_+ in terms of the parameters of our theory and therefore has a direct influence on scattering observables. Given a state of interest, ϕ_l we will now aim to establish what this C_-/C_+ ratio should be. This journey begins by considering the small-r asymptotics of the bulk solutions and shaving off higher-order terms. We recall that the low-r asymptotic form of $\phi_\pm$ is given by

$$\phi_\pm(r) \sim (2\kappa r)^{\frac{1}{2}(-1\pm\zeta)}\left[1+\mathcal{O}(r^2)\right] \text{ as } r\to 0. \tag{4.84}$$

Since we'll primarily be interested in scattering scenarios, we define $k := -i\kappa = \sqrt{2mE}$ and write the low-r asymptotic bulk solutions:

$$\phi(r) \sim (2ik\epsilon)^{-1/2}\left[C_+(2ik\epsilon)^{\zeta/2} + C_-(2ik\epsilon)^{-\zeta/2}\right] \text{ as } r\to 0. \tag{4.85}$$

In §4.2.1, we determined the background field in several cases that depended on the strength of the inverse square coupling. For our interest, we only concern ourselves with the case where $g < g_c = 1/8m$. This determines that $\zeta, \chi \in \mathbb{R}$. For convenience, we define $x := 2k\epsilon$. We substitute our radial field solutions (4.85) and background field configuration (left as ψ_c since it can either be zero or non-trivial) into (4.70) and aim to isolate for the ratio C_-/C_+. One simplification that we use is the U(1) symmetry of the action, thereby setting $C_- \in \mathbb{R}$ and leaving $C_+ \in \mathbb{C}$ [15]. The PPEFT boundary condition therefore gives us the following relation:

$$\begin{aligned}\frac{\pi\epsilon}{m}\left[(\zeta-1)x^\zeta - (\zeta+1)\Big(\frac{C_-}{C_+}e^{-i\pi\zeta/2}\Big)\right] &= 2h_4\psi_c^2\left[ie^{-i\pi\zeta/2}\Big(x^\zeta + \Big(\frac{C_-}{C_+}e^{-i\pi\zeta/2}\Big)^*\Big) + 2\Big(x^\zeta + \frac{C_-}{C_+}e^{-i\pi\zeta/2}\Big)\right] \\ &\quad - h_2\Big(x^\zeta + \frac{C_-}{C_+}e^{-i\pi\zeta/2}\Big).\end{aligned} \tag{4.86}$$

Case 1: Trivial Background Field: $h_2, h_4 \in \mathbb{C}$ without Complex Tuning

When $h_2, h_4 \in \mathbb{C}$ and the complex tuning condition does not hold, then we obtain $\psi_c = 0$. In this case, the boundary condition reduces to

$$\frac{\pi\epsilon}{m}\left[(\zeta-1)x^\zeta - (\zeta+1)\Big(\frac{C_-}{C_+}e^{-i\pi\zeta/2}\Big)\right] = -h_2\Big(x^\zeta + \frac{C_-}{C_+}e^{-i\pi\zeta/2}\Big). \tag{4.87}$$

This is a case that was explored in [13]. Our results were rederived and verified with this paper. Isolating for C_-/C_+, we find that

$$\frac{C_-}{C_+} = e^{i\pi\zeta/2}x^\zeta\frac{\hat{\lambda}-\zeta}{\hat{\lambda}+\zeta}, \tag{4.88}$$

where we have defined $\hat{\lambda} = -\frac{mh_2}{\pi\epsilon} + 1$. Since observables such as cross sections should not depend on any arbitrary scales that were introduced in our system, we introduce a renormalization argument. The ϵ parameter is a calculational tool that should be eliminated from (4.88) so as to have final predictions of the theory cast in terms of RG invariant quantities. This fact dictates

[15] This is essentially fixing a particular phase of the field solutions.

to us that h_2 necessarily runs in ϵ to precisely cancel out the apparent ϵ-dependence present in (4.88). We note that through a convenient redefinition, we are looking for a running in $\hat{\lambda}$. Differentiating C_-/C_+ with respect to ϵ and arguing its $\epsilon-$independence, one can arrive at the following Beta equation for $\hat{\lambda}$

$$\epsilon\frac{d\hat{\lambda}}{d\epsilon} = \frac{1}{2}(\zeta^2 - \hat{\lambda}^2), \tag{4.89}$$

whose solution, set by the initial condition $\hat{\lambda}(\epsilon_0) := \hat{\lambda}_0$ is given by

$$\hat{\lambda}(\epsilon) = \zeta\frac{(\hat{\lambda}_0+\zeta)(\epsilon/\epsilon_0)^\zeta + (\hat{\lambda}_0-\zeta)}{(\hat{\lambda}_0+\zeta)(\epsilon/\epsilon_0)^\zeta - (\hat{\lambda}_0-\zeta)}. \tag{4.90}$$

Since $\hat{\lambda}$ is a complex function, we can express this in its real and imaginary components $\hat{\lambda}_R$, $\hat{\lambda}_I$ by

$$\hat{\lambda}_R(\epsilon) = \frac{|\hat{\lambda}_0+\zeta|^2(\epsilon/\epsilon_0)^{2\zeta} - |\hat{\lambda}_0-\zeta|^2}{|\hat{\lambda}_0+\zeta|^2(\epsilon/\epsilon_0)^{2\zeta} + |\hat{\lambda}_0-\zeta|^2 - 2(\epsilon/\epsilon_0)^\zeta(|\hat{\lambda}_0|^2-\zeta^2)}, \tag{4.91}$$

$$\hat{\lambda}_I(\epsilon) = \frac{4\zeta^2\hat{\lambda}_0^I(\epsilon/\epsilon_0)^\zeta}{|\hat{\lambda}_0+\zeta|^2(\epsilon/\epsilon_0)^{2\zeta} + |\hat{\lambda}_0-\zeta|^2 - 2(\epsilon/\epsilon_0)^\zeta(|\hat{\lambda}_0|^2-\zeta^2)}, \tag{4.92}$$

where we have denoted $\hat{\lambda}_0 := \hat{\lambda}_0^R + i\hat{\lambda}_0^I$. We note that these beta equations only hold for $h_2, h_4 \in \mathbb{C}$ when they do not satisfy the complex tuning condition. These arose from a trivial background field which does not depict what occurs when h_2, h_4 are real.

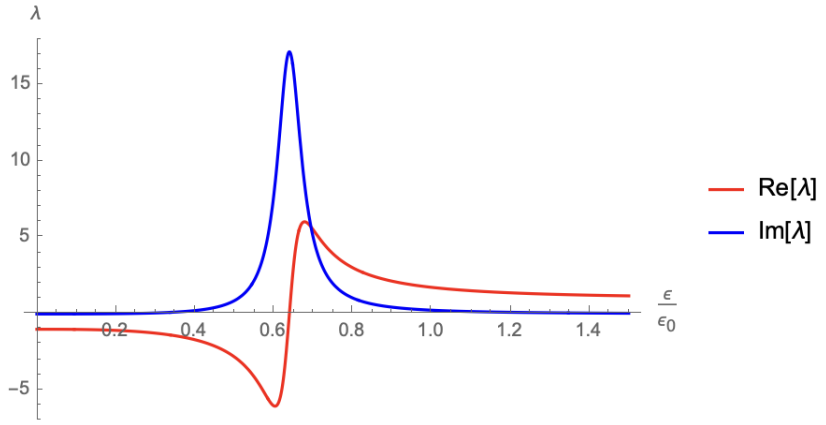

Figure 4.2: Typical RG flow of λ for the chosen values of $mg = 0.1$, $l = 1$, $\lambda_0^R = 5$ and $\lambda_0^I = 0.5$. It's key that each RG flow selects out a special scale ϵ_* where Re $\lambda = 0$. This breaks the continuous scale invariance. In the case that Im$[\lambda] = 0$, one can recover the regular single-particle RG flow.

RG Invariants

The RG flow in Figure 4.2 depicts a typical flow for $\hat{\lambda}$. It is therefore useful to use a (ϵ_*, y_*) parameterization of the RG flow. We note that for every possible flow, one can always find a scale where Re $\lambda = 0$. We therefore use this to define our RG invariants as follows:

$$\hat{\lambda}(\epsilon_*) := 0 + iy_*. \tag{4.93}$$

One can therefore write out C_-/C_+ in terms of these RG invariant quantities. It can be expressed as

$$\frac{C_-}{C_+} = (2k\epsilon_*)^\zeta e^{i\pi\zeta/2} T_*, \text{ where } T_* := \frac{\zeta - iy_*}{\zeta + iy_*}. \tag{4.94}$$

For the cases that we consider, we only treat ζ to be a real quantity, hence T_* is a pure phase. In the unitary limit where $y_* \to 0$ or $y_* \to \pm\infty$, we recover $T_* = 1$ or $T_* = -1$.

Case 2: Non-Trivial Background Field: $h_2, h_4 \in \mathbb{R}$; or $h_2, h_4 \in \mathbb{C}$ with Complex Tuning

We now consider the case where we have a non-trivial background field. This can occur in two ways: $h_2, h_4 \in \mathbb{R}$; or $h_2, h_4 \in \mathbb{C}$ and the *complex tuning* condition is satisfied. In either case, ψ_c exhibits the same form with the distinction simply being whether h_2, h_4 are complex valued. We'll work with the complex case as it is more general and the analysis holds equally well had we simply assumed $h_2 \in \mathbb{R}$ (One can simply dial down the imaginary component of h_2 to zero to recover this case). We recall that the PPEFT boundary condition for a non-trivial background field ψ_c ends up being

$$\begin{aligned}\frac{\pi\epsilon}{m}\Big[(\zeta-1)x^\zeta - (\zeta+1)\Big(\frac{C_-}{C_+}e^{-i\pi\zeta/2}\Big)\Big] &= 2h_4\psi_c^2\Big[ie^{-i\pi\zeta/2}\Big(x^\zeta + \Big(\frac{C_-}{C_+}e^{-i\pi\zeta/2}\Big)^*\Big) + 2\Big(x^\zeta + \frac{C_-}{C_+}e^{-i\pi\zeta/2}\Big)\Big] \\ &\quad - h_2\Big(x^\zeta + \frac{C_-}{C_+}e^{-i\pi\zeta/2}\Big).\end{aligned} \tag{4.95}$$

Since this equation is expressed in terms of both C_-/C_+ and its conjugate $(C_-/C_+)^*$, we can determine C_-/C_+ by conjugating the above equation and then solving for C_-/C_+ by treating it as a system of two linear equations. One can also observe that the quantity $h_4\psi_c^2$ is h_4-independent, as the h_4 cancels out with the h_4 coming from the background field. For additional convenience, we use a redefinition of our coupling, defined as $\lambda := \frac{m}{\pi\epsilon}\big[h_2 - \frac{2\pi\epsilon}{m}(\chi+1)\big]$ and denoting its real and imaginary components by $\lambda_R := \mathrm{Re}(\lambda)$, $\lambda_I := \mathrm{Im}(\lambda)$. Once the dust settles, we find that

$$\frac{C_-}{C_+} = e^{i\pi\zeta/2}x^\zeta \frac{(2\chi+1)^2 - \zeta^2 + 2\lambda_R(\zeta\sin(\pi\zeta/2) - (2\chi+1)) - 2\zeta\lambda_I\cos(\pi\zeta/2) + 2i\zeta\big[\cos(\pi\zeta/2)\lambda_R + (1+\sin(\pi\zeta/2))\lambda_I\big]}{(2\chi+1-\zeta)(2\lambda_R - (2\chi+1-\zeta))}. \tag{4.96}$$

We argue that observables such as cross sections should not depend on any arbitrary scales that were introduced in our system. The ϵ parameter is a calculational tool that should be eliminated from (4.96) so as to have final predictions of the theory cast in terms of RG invariant quantities. This fact dictates to us that h_2 necessarily runs in ϵ to precisely cancel out the apparent ϵ-dependence present in (4.96). Determining this running is the goal of this section.

To determine the running amounts to the statement that only h_2 holds any ϵ dependence. Since ζ and χ have a g-dependence, this statement is arguing that all the running lies in the brane couplings themselves and none carried for those in the bulk, such as g.

To establish this, we differentiate (4.96), making the argument $\frac{d}{d\epsilon}\big(C_-/C_+\big) = 0$ and carry through isolating for $\frac{d\lambda}{d\epsilon}$. This gives rise to a set of beta equations for λ, given below in its real

component running

$$\epsilon\frac{d\lambda_R}{d\epsilon} = -\Big(\lambda_R - \frac{2\chi+1-\zeta}{2}\Big)\Big(\lambda_R - \frac{2\chi+1+\zeta}{2}\Big) \tag{4.97}$$

and imaginary component running:

$$\epsilon\frac{d\lambda_I}{d\epsilon} = -\Big(\lambda_R - \frac{2\chi+1-\zeta}{2}\Big)\Big(\lambda_I + \frac{\cos(\pi\zeta/2)(2\chi+1+\zeta)}{2(1+\sin(\pi\zeta/2))}\Big) \tag{4.98}$$

Defining $\lambda(\epsilon_0) := \lambda_0^R + i\lambda_0^I$ as a generic initial condition, the solutions to the system of equations (4.97), (4.98) are given below by

$$\lambda_R(\epsilon) = -\frac{1}{2}\Big[\frac{(2\lambda_0^R-(2\chi+1+\zeta))(2\chi+1-\zeta)-(\epsilon/\epsilon_0)^\zeta(2\lambda_0^R-(2\chi+1-\zeta))(2\chi+1+\zeta)}{2\zeta-(2\lambda_0^R-(2\chi+1-\zeta))(1-(\epsilon/\epsilon_0)^\zeta)}\Big] \tag{4.99}$$

and

$$\lambda_I(\epsilon) = \frac{1}{2}\Big[\frac{4\lambda_0^I\zeta(1+\sin(\pi\zeta/2))+(2\chi+1-\zeta)\cos(\pi\zeta/2)(2\lambda_0^R-(2\chi+1-\zeta))(1-(\epsilon/\epsilon_0)^\zeta)}{\big[2\zeta-(2\lambda_0^R-(2\chi+1-\zeta))(1-(\epsilon/\epsilon_0)^\zeta)\big](1+\sin(\pi\zeta/2))}\Big]. \tag{4.100}$$

We note that each of these solutions can be classed into two categories, completely dependent on the initial conditions λ_0^R and λ_0^I. These can be observed in the Figure 4.3 on the following page, where we have chosen the values $mg = 0.1$, $l = 1$ thereby setting $\chi = \sqrt{0.2}$ and $\zeta = \sqrt{8.2}$. In essence, the *topology* of the graphs is generic in that all flows belonging to one of the classes will exhibit the same asymptotic properties.

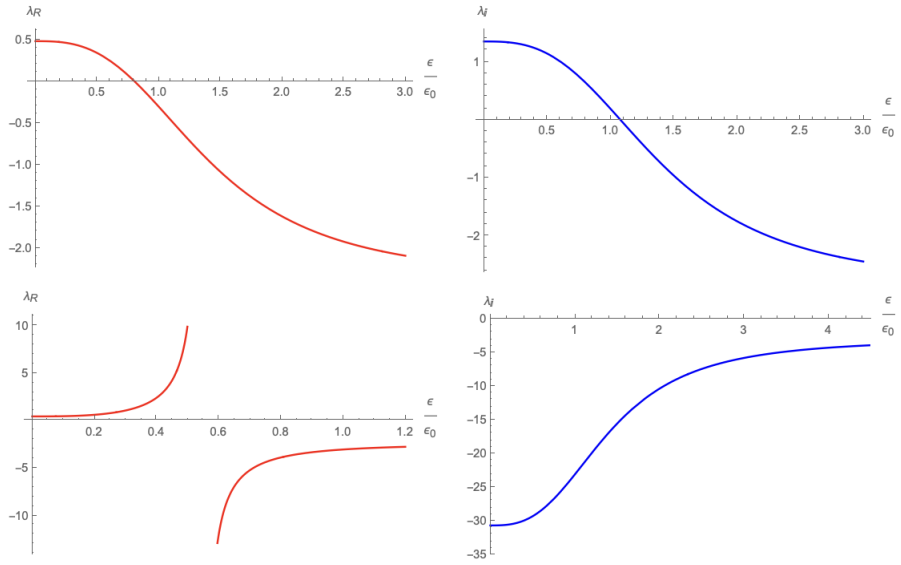

Figure 4.3: The two classes of flows for the real and imaginary components of $\hat{h}_2$. The top left profile occurs when λ_0^R lies in between the two fixed points and the bottom left profile when it's outside. We have chosen the values $mg = 0.1$ and $l = 1$ so that $\chi = \sqrt{0.2}$ and $\zeta = \sqrt{8.2}$. In correspondence to h_2, there does not exist any scale where $h_2 = 0$. As similarly argued earlier, this running suggest that the presence of the brane couplings is obligatory.

RG Invariants

Ultimately, we would like to cast our observables in terms of RG invariant variables. We can establish a suitable choice of RG invariants by analyzing the running behaviour of our coupling λ. We define an RG invariant scale, ϵ_* with respect to the running of λ_R. The two fixed points of (4.97) play a role in partitioning the family of runnings into two classes. Each of these possess qualitative behaviour that is universal to each class. For the complex h_2 case, we naturally include a second RG invariant that we will denote by y_*.

Subcase 2.1: $h_2 \in \mathbb{C} \leftrightarrow \lambda \in \mathbb{C}$

1. If $\lambda_0^R < 2\chi + 1 - \zeta$ or $\lambda_0^R > 2\chi + 1 + \zeta$, one can observe from Fig 4.3 that there always exists a scale that crosses the imaginary axis. We therefore define the RG invariant scale ϵ_* satisfying:

$$\lambda(\epsilon_*) := 0 + i y_*, \tag{4.101}$$

where we have introduced a second RG invariant parameter, y_*[16]. In essence, for $\lambda_R = 0$ to be satisfied, we required there to be some ϵ where

$$(\epsilon/\epsilon_0)^{\zeta} = \frac{[2\lambda_0^R - (2\chi + 1 + \zeta)][2\chi + 1 - \zeta]}{[2\lambda_0^R - (2\chi + 1 - \zeta)][2\chi + 1 + \zeta]} \tag{4.103}$$

[16]For the class of flows that don't begin between the fixed points, another canonical choice for RG invariants are

Since our primary concern is in s-wave scattering (i.e $l = 0 \to \chi = \zeta$), then λ_0^R controls whether or not such a solution exist. One can see that we require λ_0^R to simultaneously lie outside of the fixed points region, therefore restricted to flows that contain a divergence.

2. If however, λ_0^R lies in between the two fixed points: $2\chi+1-\zeta < \lambda_0^R < 2\chi+1+\zeta$, we instead define:

$$\lambda(\epsilon_*) := \frac{2\chi+1}{2} + iy_* \tag{4.104}$$

In this case, this coupling strength is chosen as there always exists a scale that yields a coupling at the average of the two fixed points. This is seen explicitly by isolating for ϵ when $\hat{h}_2^R = 3(\chi+1)+\zeta$:

$$\left(\frac{\epsilon}{\epsilon_0}\right)^\zeta = -\frac{3\chi+\zeta+2-h_0^R}{3\chi+\zeta+4-h_0^R}. \tag{4.105}$$

Solutions for positive ϵ exist if $3\chi+\zeta+2 < h_0^R < 3\chi+\zeta+4$, as desired.

We represent this definition for ϵ_* more compactly by the following statement:

$$\lambda(\epsilon_*) = \frac{2\chi+1}{4}\big[1-R_*\big] + iy_*, \tag{4.106}$$

where we have defined $R_* = \text{sgn}(\big|\lambda - \frac{2\chi+1}{2}\big| - \frac{\zeta}{2})$.

Subcase 2.2: $h_2 \in \mathbb{R}$ **[**$h_2^I = 0$**]**
From comparisons among equations (4.97)-(4.98) one can see that we require λ to lie at the larger fixed point of the beta function:

$$\lambda_{R;fix} = \frac{2\chi+1-\zeta}{2} \tag{4.107}$$

This condition is required as it is the only choice for λ that satisfies both equations. Transferring into the original coupling gives us

$$h_2^R = \frac{\pi\epsilon}{m}\big(3\chi+\zeta+4\big). \tag{4.108}$$

Let's reexamine the original condition for $|c_2|^2$ in the background field where we required $mh_2 - 2\pi\epsilon(\chi+1) > 0$ for there to be a non-trivial background. A natural question arises in the running of h_2 and whether this inequality is satisfied for arbitrary ϵ. We note that $|c_2|^2 \propto \lambda_R$, hence when $\zeta = \chi$, one recovers $2\chi+1-\zeta = \chi+1 > 0$, verifying that our background field approach works out.

---

the ϵ scales where $\lambda_R \to \pm\infty$. This is seen by the fact that when ϵ satisfies:

$$\left(\frac{\epsilon}{\epsilon_0}\right)^\zeta = \frac{2\lambda_0^R - (2\chi+1+\zeta)}{2\lambda_0^R - (2\chi+1-\zeta)} \tag{4.102}$$

Then $\lambda_R \to \pm\infty$. Solutions for a positive ϵ exist if $\lambda_0^R < 2\chi+1-\zeta$ or $2\chi+1+\zeta < \lambda_0^R$.

4.2.5 Bound States

Bound states are characterized as the normalizable negative energy solutions to the field equations.

Normalizability at infinity is imposed by demanding that $C_-\Phi_- + C_+\Phi_+$ decays sufficiently quickly to zero. Using the fields radial functions (4.65), we establish the large-r asymptotic forms to be

$$\phi_-(r) \sim \frac{1}{2}\Big[\frac{\Gamma(1-\zeta)}{\Gamma(\frac{1}{2}(1-\zeta))}\Big(\frac{e^{\kappa r}}{\kappa r}\Big) + \frac{\Gamma(1-\zeta)}{\Gamma(\frac{1}{2}(1-\zeta))}e^{-\frac{i\pi}{2}(1-\zeta)}\Big(\frac{e^{-\kappa r}}{\kappa r}\Big)\Big], \tag{4.109}$$

and

$$\phi_+(r) \sim \frac{1}{2}\Big[\frac{\Gamma(1+\zeta)}{\Gamma(\frac{1}{2}(1+\zeta))}\Big(\frac{e^{\kappa r}}{\kappa r}\Big) + \frac{\Gamma(1+\zeta)}{\Gamma(\frac{1}{2}(1+\zeta))}e^{-\frac{i\pi}{2}(1+\zeta)}\Big(\frac{e^{-\kappa r}}{\kappa r}\Big)\Big]. \tag{4.110}$$

This fixes the C_-/C_+ ratio so that any divergences from the growing exponentials $e^{\kappa r}$ are eliminated. This ratio is found to be

$$\frac{C_-}{C_+} = 4^{\zeta}\frac{\Gamma[\zeta/2]}{\Gamma[-\zeta/2]}. \tag{4.111}$$

Case: $\chi \in \mathbb{R}$

We now aim to consider the bound state spectrum when $\chi \in \mathbb{R}$. We define $x := 2\kappa\epsilon$ and $-\kappa^2 = 2mE$. Using the boundary condition in (4.70), we can substitute our low-r asymptotic field solution, obtaining

$$\begin{aligned}(\zeta-1)x^{\zeta} - (\zeta+1)\Big(\frac{C_-}{C_+}\Big) = (x^*)^{\zeta}\big[\hat{h}_2 - (\chi+1)\big]\Big(\frac{x^*}{x}\Big)^{-\frac{1+\zeta}{2}} + x^{\zeta}\big[\hat{h}_2 - 2(\chi+1)\big] \\ + \Big(\frac{C_-}{C_+}\Big)\Big[\big[\hat{h}_2 - (\chi+1)\big]\Big(\frac{x^*}{x}\Big)^{-\frac{1+\zeta}{2}} + \big[\hat{h}_2 - 2(\chi+1)\big]\Big].\end{aligned} \tag{4.112}$$

The most general case to consider is when we have complex energy eigenvalues[17]. However, it was found that establishing bound state energies was difficult in this instance, due to the degree of the polynomials that were emerging for the phase and magnitude of x. Instead, we consider the case of real κ, such that the energy E is real and negative. This turns x into a real parameter, allowing us to establish that

$$x = 4\Big[\frac{\Gamma[\zeta/2]}{\Gamma[-\zeta/2]}\frac{\zeta+1+2(\lambda-(\chi+1))}{\zeta-1-2(\lambda-(\chi+1))}\Big]^{1/\zeta}. \tag{4.113}$$

For there to be stable bound state solutions, one prerequisite is that $\lambda \in \mathbb{R}$.

We first consider $\zeta \neq 1$. By the running in §4.2.4, λ must lie at the fixed point $\lambda = (2\chi + 1 - \zeta)/2$. Substituting this into the above expression gets us

$$x = 0 \leftrightarrow E = 0. \tag{4.114}$$

[17] This would allow us to describe decaying solutions since the field solutions would go as $\phi \sim e^{-iEt}e^{-\frac{\Gamma}{2}t}$.

Something to note is that the running of h_2 should presumably be the same irregardless of whether we had considered scattering or bound states and so apply the same running behaviour that was found earlier. In addition, the running behaviour found in the renormalization section has a potential issue with a divergence in the scattering C_-/C_+ ratio occurring at this fixed point. However, this is something we need not worry about for bound states.

We now consider the $\zeta = 1$ case. This ensures that λ runs in the manner described by the beta equations with $\lambda_I = 0$. For this particular case, we define $\lambda(\epsilon_*) = 1$ for trajectories satisfying $sgn\left(|\lambda - \frac{3}{2}| - \frac{1}{2}\right) = -1$ which establishes that $E = 0$. However, we define $\lambda(\epsilon_*) \to +\infty$ for trajectories satisfying $sgn\left(|\lambda - \frac{3}{2}| - \frac{1}{2}\right) = +1$. In this case, one obtains the bound state energy

$$E = -\frac{1}{2m\epsilon_*^2}, \tag{4.115}$$

which is in agreement with what was found in other papers, where a delta-function potential was present [3].

4.2.6 Scattering Cross Sections

In this section, we aim to compute scattering observables such as scattering lengths and cross sections. Our aim is to examine the qualitative behaviour of cross sections in various momenta-regimes of interest. Our focus will be in elastic and inelastic cross sections but we first turn to scattering length computations for several cases.

Scattering Length

The scattering length, a_s is canonically defined through the low energy limit of the s-wave elastic cross section. In particular, it's given below by

$$\frac{1}{a_s} := -\lim_{k\to 0} k\ \cot(\delta_0(k)). \tag{4.116}$$

Since phase shifts, $e^{2i\delta}$ were the main quantities that were computed throughout the thesis, it's useful to cast the scattering length in terms of the phase shift:

$$\frac{1}{a_s} = i\lim_{k\to 0} k\frac{e^{2i\delta_0(k)}+1}{e^{2i\delta_0(k)}-1}. \tag{4.117}$$

Since we are interested in s-wave scattering, $l = 0$, we define $\zeta_0 := \zeta_{l=0} = \sqrt{1-8mg}$.

Case 1: $\zeta_0 = 1$
In this instance, we are considering the *free-wave subspace* for which the inverse-square coupling disappears, $g = 0$.

Subcase 1: Trivial Background Field

In this case, we consider $h_2, h_4 \in \mathbb{C}$ such that the *complex tuning* condition is not satisfied. We find that

$$\frac{C_-}{C_+}\Big|_{\zeta_0=1} = 2ik\epsilon_* \frac{\zeta - iy_*}{\zeta + iy_*}. \tag{4.118}$$

Evaluating the limit of (4.117) with (4.118) gets us

$$a_s = \epsilon_* \frac{\zeta - iy_*}{\zeta + iy_*}. \tag{4.119}$$

Hence, $a_s = \pm\epsilon_*$ in the unitary limit, corresponding to whether $y_* \to 0$ or $y_* \to \pm\infty$.

Subcase 2: Non-Trivial Background Field

We now consider the case where the background field is non-trivial. In particular, we take the case of $h_2, h_4 \in \mathbb{C}$ such that they satisfy the *complex tuning* condition. This allows us to simultaneously address both the real and complex case. Casting (4.96) in terms of the corresponding RG invariants, we obtain

$$\frac{C_-}{C_+}\Big|_{\zeta_0=1} = 2ik\epsilon_* \frac{8 - 3(1-R_*) + 4iy_*}{3(1-R_*) - 4}. \tag{4.120}$$

Evaluating the limit of (4.117) with (4.120) furnishes the following scattering length:

$$a_s = -\epsilon_* \frac{3(1-R_*) - 8 - 4iy_*}{3(1-R_*) - 4}, \tag{4.121}$$

where we recall that $R_* = sgn\big(|\lambda - \frac{3}{2}| - \frac{1}{2}\big)$.

Case 2: $0 < \zeta_0 < 1$ **(i.e** $\zeta_0 = \chi = \sqrt{1 - 8mg}$**)**

This analysis can be performed for both types of field configurations. This is the case where $g < g_c$, thereby rendering $0 < \zeta_0 < 1$. The quantity $\frac{e^{2i\delta_0}+1}{e^{2i\delta_0}-1}$ is computed to be

$$\frac{e^{2i\delta_0}+1}{e^{2i\delta_0}-1} = \frac{C_0 ie^{-i\pi\chi/2}(1 - ie^{-i\pi\chi/2}) - \mathscr{A}(ie^{-i\pi\chi/2}+1)}{C_0 ie^{-i\pi\chi/2}(1 + ie^{-i\pi\chi/2}) - \mathscr{A}(ie^{-i\pi\chi/2}-1)}, \tag{4.122}$$

where we have defined $C_0 := \frac{C_-}{C_+}\big|_{l=0}$ and $\mathscr{A} := 4^\chi \frac{\Gamma[\chi/2]}{\Gamma[-\chi/2]}$. We observe that $C_0 \propto k^\chi$ and that $ie^{-i\pi\zeta_0/2} \neq 1 \ \forall\ \zeta_0 \in [0,1)$. With all these quantities established we find that

$$\frac{1}{a_s} = i \lim_{k\to 0} k \frac{e^{2i\delta_0(k)}+1}{e^{2i\delta_0(k)}-1} = 0, \tag{4.123}$$

establishing that the scattering length, $a_s \to \infty$.

Case 3: $\zeta_0 := i\eta$

We now consider the case where $g > g_c$, turning ζ into an imaginary value. We define $\zeta := i\eta$ where $\eta = \sqrt{8mg-1}$. We once again compute

$$\frac{e^{2i\delta_0}+1}{e^{2i\delta_0}-1} = \frac{C_0\left[1+ie^{\pi\eta/2}\right]ie^{\pi\eta/2} + \mathscr{A}\left[1-ie^{\pi\eta/2}\right]}{C_0\left[1+ie^{\pi\eta/2}\right]ie^{\pi\eta/2} - \mathscr{A}\left[1-ie^{\pi\eta/2}\right]}, \tag{4.124}$$

where we have analogously defined $\mathscr{A} = 4^{i\eta}\frac{\Gamma[i\eta/2]}{\Gamma[-i\eta/2]}$. In this case, we have $C_0 \propto k^{i\eta} = \cos\big(\eta[\log(k)]\big) + i\sin\big(\eta[\log(k)]\big)$. While both $\cos\big(\eta[\log(k)]\big)$ and $\sin\big(\eta[\log(k)]\big)$ do not have a well defined value in the zero k limit, they are bounded. Hence, easy application of the squeeze theorem demonstrates that

$$\lim_{k\to 0} k\,\cos\big(\eta[\log(k)]\big) = \lim_{k\to 0} k\,\sin\big(\eta[\log(k)]\big) = 0 \tag{4.125}$$

We therefore continue to likewise have the property that

$$\frac{1}{a_s} = 0, \tag{4.126}$$

establishing that the scattering length, $a_s \to \infty$.

Elastic Cross Sections

We now turn to the main observables of interest. We are tracking scattering between a Schrodinger particle interacting with the point-particle source. In terms of the phase shift and momenta, the partial elastic cross sections are defined by [See Appendix B]

$$\sigma_l^{(el)} = \frac{\pi}{k^2}(2l+1)|e^{2i\delta_l}-1|^2. \tag{4.127}$$

We consider real ζ values and only consider the low energy limit of $|e^{2i\delta_l}-1|^2$. We note that our analysis for both trivial and non-trivial backgrounds turns out to yield the same low-energy behaviour. Their distinction simply lies in the finer details that emerge, such as the different sets of parameters / factors.

Case 1: Trivial Background Field

In this section, we consider the case where $h_2, h_4 \in \mathbb{C}$, and the *complex tuning* condition does not hold. With reference to Appendix B, we can expand the quantity $|1-e^{2i\delta_l}|^2$ to the lowest orders in C_-/C_+. Keeping the first three terms gets us

$$|1-e^{2i\delta_l}|^2 \sim 2\Big[(1-(-1)^l\sin(\pi\zeta/2)) - x^\zeta\frac{(-1)^l}{\mathscr{A}}\left[(1-2(-1)^l\sin(\pi\zeta/2))\mathrm{Im}(T_*) - \mathrm{Im}(e^{-i\pi\zeta}T_*)\right] + x^{2\zeta}\frac{(1-\cos(\pi\zeta))}{\mathscr{A}^2}\Big], \tag{4.128}$$

where $x = 2k\epsilon_*, \mathscr{A} = 4^\zeta\frac{\Gamma[\zeta/2]}{\Gamma[-\zeta/2]}$ and $T_* = \frac{1-iy_*}{1+iy_*}$. In essence, the low energy behaviour when $\zeta \neq 1$ is dominated by the first term shown in $|1-e^{2i\delta_l}|^2$:

$$\sigma_l^{(el)} \sim \frac{2\pi}{k^2}\left[1-(-1)^l\sin(\pi\zeta/2)\right] \text{ as } k\to 0 \tag{4.129}$$

Subcase: $\zeta_0 = 1$

When we consider the disappearance of the inverse-square potential, one recovers $\zeta = 1$ for the s-wave case. This sets the first two terms appearing in $|1-e^{2i\delta_l}|^2$ to zero with the third term being the first non-zero term. In this instance, we find the elastic cross section to behave as one would expect:

$$\sigma_0^{(el)} = 4\pi\epsilon_*^2 + \mathcal{O}(k), \tag{4.130}$$

therefore recovering a constant value in the zero-k limit.

Case 2: Non-Trivial Background Field: $h_2, h_4 \in \mathbb{R}$**; or** $h_2, h_4 \in \mathbb{C}$ **with Complex Tuning**

In this portion of our analysis, we consider the case where $h_2, h_4 \in \mathbb{R}$ or $h_2, h_4 \in \mathbb{C}$ with the *complex tuning* condition satisfied. We find that Taylor expanding $|1-e^{2i\delta_l}|^2$ about C_-/C_+ (since $C_-/C_+ \propto k^\zeta$) up to the first three terms gets us

(4.131)

$$|1-e^{2i\delta_l}|^2 \sim 2\Big[(1-(-1)^l\sin(\pi\zeta/2)) - x^\zeta\frac{(-1)^l}{\mathscr{A}}\big[(1-2(-1)^l\sin(\pi\zeta/2))\mathrm{Im}(\alpha) - \mathrm{Im}(e^{-i\pi\zeta}\alpha)\big] + x^{2\zeta}\frac{(1-\cos(\pi\zeta))}{\mathscr{A}^2}|\alpha|^2\Big]$$

where we have defined $x := 2k\epsilon_*$, $\mathscr{A} = 4^\zeta\frac{\Gamma[\zeta/2]}{\Gamma[-\zeta/2]}$ and α by

$$\mathrm{Re}(\alpha) = \frac{2((2\chi+1)^2-\zeta^2) + (2\chi+1)(1-R_*)(\zeta\sin(\pi\zeta/2) - (2\chi+1)) - 4\zeta y_*\cos(\pi\zeta/2)}{2(2\chi+1-\zeta)[(2\chi+1)(1-R_*) - 2(2\chi+1-\zeta)]}, \tag{4.132}$$

$$\mathrm{Im}(\alpha) = \zeta\frac{(2\chi+1)(1-R_*)\cos(\pi\zeta/2) + 4y_*(1+\sin(\pi\zeta/2))}{2(2\chi+1-\zeta)[(2\chi+1)(1-R_*) - 2(2\chi+1-\zeta)]}, \tag{4.133}$$

where we remind ourselves that $R_* := \mathrm{sgn}\big(|\lambda - (2\chi+1)/2| - \zeta/2\big)$ classifies a particular flow. In essence, the low energy behaviour when $\zeta \neq 1$ is dominated by the first term shown in $|1-e^{2i\delta_l}|^2$:

$$\sigma_l^{(el)} \sim \frac{2\pi}{k^2}\big[1-(-1)^l\sin(\pi\zeta/2)\big] \text{ as } k \to 0 \tag{4.134}$$

Subcase: $\zeta_0 = 1$

When we consider the disappearance of the inverse-square potential, one recovers $\zeta = \chi = 1$ for the s-wave case. This sets the first two terms appearing in $|1-e^{2i\delta_l}|^2$ to zero with the third term being the first non-zero term. In this instance, we find the elastic cross section to behave as one would expect:

$$\sigma_0^{(el)} = 4\pi\epsilon_*^2|\alpha|^2 + \mathcal{O}(k), \tag{4.135}$$

therefore recovering a constant value in the zero-k limit.

Inelastic Cross Sections

We now turn to the inelastic cross section that determines absorptive / emissive interactions [For a brief overview on the observable, see Appendix B]. In terms of the phase shift and momenta, the partial inelastic cross sections are defined by

$$\sigma_l^{(in)} = \frac{\pi}{k^2}(2l+1)\big[1-|e^{2i\delta_l}|^2\big]. \tag{4.136}$$

Case 1: Trivial Background Field

In this case, we consider $h_2, h_4 \in \mathbb{C}$, where the *complex tuning* condition is not satisfied. We are interested in the low energy asymptotics, hence the low-energy behaviour of $1-|e^{2i\delta_l}|^2$ is found to be

$$1-|e^{2i\delta_l}|^2 \sim \frac{x^\zeta \zeta\Gamma[-\zeta/2]}{4^{\zeta-1}\Gamma[\zeta/2]}\frac{\sin(\pi\zeta/2)2\zeta y_*}{\zeta^2+y_*^2} \text{ as } k\to 0, \tag{4.137}$$

where $x = 2k\epsilon_*$. One can therefore compute the inelastic cross section at low energies to be

$$\sigma_l^{(in)} \sim 8\pi\epsilon_*^2 \frac{x^{\zeta-2}\zeta\Gamma[-\zeta/2]}{4^{\zeta-1}\Gamma[\zeta/2]}\frac{\sin(\pi\zeta/2)2\zeta y_*}{\zeta^2+y_*^2} \text{ as } k\to 0. \tag{4.138}$$

The total cross section is a summation over each partial cross section for angular momentum modes l. At low energies, this forms a hierarchy where higher angular momentum modes are further suppressed due to the powers of x. It is the s-wave contribution that helps determine its asymptotic behaviour at low energies. From the result found, one can see that

$$\sigma_0^{(in)} \propto \frac{1}{k^{2-\chi}} \qquad \text{at low energies} \tag{4.139}$$

where $1 < 2-\chi < 2$, thereby demonstrating strong enhancement for the zero-angular momentum modes.

Subcase: $\zeta_0 = 1$

We now consider the *free-wave subspace* for which the inverse-square potential disappears ($g = 0$). The s-wave partial inelastic cross section is described by setting $l = 0$. From (4.139), setting $\zeta = 1$, we find that

$$\sigma_s^{(in)} \sim -\frac{16\pi\epsilon_* y_*}{k(1+y_*^2)} \text{ as } k\to 0 \tag{4.140}$$

Hence, one can observe that we have obtained $\sigma_s^{(in)} \propto 1/k$ behaviour at low energies.

Case 2: Non-Trivial Background Field

We first consider the general case where $h_2 \in \mathbb{C}$ is complex valued. We will cast the *phase shift component* of the cross section in terms of RG invariant parameters, analogous to (4.131):

$$1-|e^{2i\delta_l}|^2 \sim \frac{2x^\zeta \sin(\pi\zeta/2)\Gamma[-\zeta/2]}{4^\zeta\Gamma[\zeta/2]}\frac{\zeta(2\chi+1)(1-R_*)\cos(\pi\zeta/2)-4\zeta y_*(1+\sin(\pi\zeta/2))}{(2\chi+1-\zeta)[(2\chi+1)(1-R_*)-2(2\chi+1-\zeta)]} \text{ as } k\to 0 \tag{4.141}$$

where we have defined $x := 2k\epsilon_*$. We are typically interested in the asymptotic behaviour, observing whether some cases may yield divergences at low energies. The low energy limit of the partial cross sections were found to be

(4.142)
$$\sigma_l^{(in)} \sim 8\pi\epsilon_*^2 \frac{x^{\zeta-2}\sin(\pi\zeta/2)\Gamma[-\zeta/2]}{4^\zeta\Gamma[\zeta/2]} \frac{\zeta(2\chi+1)(1-R_*)\cos(\pi\zeta/2) - 4\zeta y_*(1+\sin(\pi\zeta/2))}{(2\chi+1-\zeta)[(2\chi+1)(1-R_*)-2(2\chi+1-\zeta)]} \qquad \text{as } k \to 0.$$

The partial cross sections generically depict a hierarchy of contributions, with higher angular momentum modes being further suppressed by the powers of x. Hence, it is the *s-wave* that has the largest contribution to the total cross section at low energies. We can observe that

(4.143)
$$\sigma_0^{(in)} \propto \frac{1}{k^{2-\chi}} \qquad \text{at low energies}$$

where $1 < 2-\chi < 2$, thereby demonstrating strong enhancement for the zero-angular momentum modes.

Subcase: $\zeta_0 = 1$

We consider the *free-wave subspace* for which the inverse-square potential disappears, $g = 0$. The s-wave partial inelastic cross section is described by setting $l = 0$. We're interested in computing the low energy cross section; the regime in which $k \to 0$. From (4.142), we find

(4.144)
$$\sigma_s^{(in)} \sim \frac{8\pi\epsilon_* y_*}{k[3(1-R_*)-4]},$$

where we remind ourselves that $R := \text{sign}\big(|\lambda - 3/2| - 1/2\big)$. Hence, one can observe that we have obtained $\sigma_s^{(in)} \propto 1/k$ behaviour at low energies.

On the other hand, had $h_2 \in \mathbb{R}$, then we do not recover this $1/k$ behaviour at low energies. Instead we find that

(4.145)
$$\sigma_s^{(in)}(k = 0; h_2 \in \mathbb{R}) = 0.$$

We therefore find that a non-unitary boundary condition is necessary to predict a *low-k* enhancement in the inelastic cross section for our single-species model.

CHAPTER 5

CONCLUSION AND FUTURE WORK

In this thesis, we focused on non-relativistic scalar fields that are subject to an inverse-square potential and their interaction with a point-particle at the origin. In §3, we take a LO description of the PPEFT for a two-species model and a NLO description of a single-particle non-self-adjoint PPEFT in §4. In chapter 3, our aim was to encode a flavour violating process. It was observed that the point-particle was able to induce a catalytic process with cross sections having dependence $k_{\text{out}}/k_{\text{in}}$ of outgoing and incoming momenta for both Schrodinger and Klein-Gordon particles at low energies. While the Schrodinger case generates a constant value at low energies, it was observed that should the incident particle mass be greater than the exiting ($m_1 > m_2$), that we are able to obtain a $1/k_{\text{in}}$ enhancement for the Klein-Gordon inelastic cross section. In general, flavour violation could encode processes such as Baryon number violation and therefore serves for great theoretical interest. In particular, it is believed that magnetic monopoles can serve as catalysts for baryon violation [1][7], a domain of research that is currently being further explored.

The majority of the author's work in this thesis lies in Chapter 4, in which we similarly consider Schrodinger fields subject to an inverse-square potential in the bulk but take a NLO description of the point-particle action. For the PPEFT considered here, one finds that the field equations are non-linear and an attempt is therefore made to linearize them in accordance with a background field expansion. Consequently, we follow the same algorithm for arriving at a boundary condition near the origin just as was performed in §3. Linearizing only helps us if the background field turns out to be non-zero and so our goal was to establish whether this is the case. We first consider the case where the quadratic term is not present ($h_2 = 0$) but the quartic term is. For this scenario, we find that the background field is indeed zero, so we halt any further inquiry for this case. On a comparative note, the research performed in [3, 4, 13] had manifestly

linear field equations and so did not require any linearization techniques. For completeness, we note that the background field for this single quadratic case is zero. We then moved into considering a more general case I had termed the *double well* where both quadratic and quartic PPEFT terms are present. For this case, we found a non-zero background field for the different cases generated by whether the inverse-square coupling, g satisfies $g > g_c, g < g_c, g = g_c$, where $g_c = 1/8m$. Once we vary the action with respect to the Schrodinger fluctuations, linearize and substitute the background field, we observe that the quartic coupling, h_4 completely drops out of the field equations. This can help cement the notion why going to first order (i.e only the quadratic term) can be sufficient for most cases. However, expanding and linearizing about a non-zero background field does change things in a way that is *non-trivial*. It was observed that h_2 continues to require renormalization but runs in a manner that slightly differs than that of what was found among other papers (such as [3, 13]). The first finding was that our definition of λ mapped onto the definition of $\hat{\lambda}$ in [3, 13] runs in a different manner. One instance of this was that λ_R had to lie precisely at the fixed point if it is real whereas it was observed to run in a very similar manner to λ_R when λ is taken to be complex. When we considered the case for the brane coupling, h_2 to be complex-valued, we obtained a modification to the running differing than what was found in [13]. Qualitatively, the flow topology is analogous but the fixed points are shifted by the presence of the χ variable contributed from the background field. In the case where $\chi \in \mathbb{R}$, the bound states of this model were found to exhibit stability if and only if $\hat{h}_2 \in \mathbb{R}$ but would have to be zero-energy eigenstates. In the $\zeta = 1$ limit, one finds a non-zero energy eigenstate. The decay rates of these states are another future avenue that can be explored; in addition, examining whether we continue to find a tower of bound states when ζ is imaginary (A feature that was observed in [13], among other papers). It was also observed that when considering the probability flux at the source, it was demonstrated to generically not be conserved. It was shown that conservation occurs if the complex phase, $e^{i\theta}$ of the field is an integral multiple of $\pi/2$ (i.e. $\theta = n\pi/2$ for some $n \in \mathbb{N}$) as this would make it either purely real or imaginary [See (**??**)]. For scattering cross sections, we observed that a $1/k$ inelastic behaviour continues to be demonstrated at low energies for the special case of $\zeta = 1$ but requires a non-self-adjoint boundary action since the brane couplings would have to be complex. If $h_2 \in \mathbb{R}$, then $\sigma_0^{(in)} \to 0$. More generally, it was seen that we establish $\sigma_0^{(in)} \propto 1/k^{2-\chi}$ behaviour at low energies when $0 < \chi < 1$, which is a more enhanced interaction than the previously encountered $1/k$, but requiring a non-self adjoint PPEFT. While the model of §4 was not mapped onto a precise experimental scenario, we wish to comment on where this work may be applied. Since the primary object that we worked with are Schrodinger scalar fields, one foreseeable application may lie in condensed matter systems, particularly involving bosonic states such as Bose-Einstein Condensates.

APPENDIX A

ANGULAR HARMONICS

We note that our solutions are given by $Y_{lm}(\theta,\phi) = C_l P_l^m(cos\theta)e^{im\phi}$ where P_l^m are the associated Legendre polynomials. They are defined below by (A.1).

$$P_l^m(x) = \frac{(-1)^m}{2^l l!}(1-x^2)^{m/2}\frac{d^{l+m}}{dx^{l+m}}(x^2-1)^l \tag{A.1}$$

We emphasize some key properties of the functions comprising the spherical harmonics:

$$\int_0^{2\pi} e^{i(m+m')\phi}d\phi = 2\pi\ \delta_{m,-m'} \tag{A.2}$$

$$\int_{-1}^{1} P_l^m(x)P_{l'}^{m'}(x)dx = \frac{2}{2l+1}\frac{(l+m)!}{(l-m)!}\ \delta_{ll'} \tag{A.3}$$

In $d = 3$, we have that $d\Omega = sin\theta\ d\theta d\phi$ and the angular solutions therefore satisfy (A.4).

$$\int\int Y_{lm}(\theta,\phi)Y^*_{l'm'}(\theta,\phi)\ d\Omega = \frac{4\pi}{2l+1}\delta_{ll'}\delta_{mm'} \tag{A.4}$$

If we seek to normalize the spherical harmonics so that we have

$$\int \mathrm{d}\Omega\ \left|Y_{lm}(\theta,\phi)\right|^2 = 1 \tag{A.5}$$

Then we require that the constant C_l satisfies $C_l = \sqrt{\frac{2l+1}{4\pi}}$. Hence, we have

$$Y_{lm}(\theta,\phi) = \sqrt{\frac{2l+1}{4\pi}}P_l^m(cos\theta)e^{im\phi} \tag{A.6}$$

APPENDIX B

SCATTERING SETUP

Scattering scenarios comprise a natural avenue in which we can probe the physics of different particles interacting with one another. This appendix aims to provide details on the story and mathematics behind non-relativistic scattering used in the main sections of this thesis. For further details on the topic, see *Landau and Lifshitz: Non-Relativistc Theory* [11] and *Landau and Lifshitz: Relativistic Theory* [10].

B.1 Plane Wave Expansion

When computing cross sections, the setup generically takes the form of an incident plane wave scattering off of a potential. An incident plane wave means that our incident asymptotic wave function is described by $\psi_{in} \approx e^{ikz}$ where $z = rcos\theta$ in spherical coordinates. If we recall the azimuthal angular momentum operator $L_z = L_3 = -i\frac{\partial}{\partial\phi}$, one can easily see that $L_z e^{ikz} = 0$. Hence, the quantum number m in this instance is $m = 0$. We note that this represents the projection of the angular momentum onto the z-axis. Since, angular momentum is conserved, we necessarily have $m_{out} = 0$ as well (here m_{out} describes the azimuthal quantum number of the outgoing wave). This setup serves to reduce the parameters of the scattering scenario, making computation much more viable.

We can decompose our plane wave with respect to Bessel functions and Legendre polynomials. This expansion is seen by the following series

$$e^{ikz} = \sum_{l=0}^{\infty}(2l+1)i^l j_l(kr)P_l(cos\theta) \rightarrow \sum_{l=0}^{\infty}(2l+1)i^l\Big(\frac{e^{i(kr-l\pi/2)} - e^{-i(kr-l\pi/2)}}{2ikr}\Big)P_l(cos\theta) \text{ as } r\rightarrow\infty \tag{B.1}$$

Then we substitute the relation $Y_{l0} = \sqrt{(2l+1)/4\pi}\ P_l^0$.

$$e^{ikz} \sim \sum_{l=0}^{\infty} \Big[\frac{i^{l-1}\sqrt{\pi(2l+1)}}{k} \Big(\frac{e^{i(kr-l\pi/2)}}{r} - \frac{e^{-i(kr-l\pi/2)}}{r} \Big) Y_{l0} \Big] \tag{B.2}$$

B.2 Elastic Scattering

Hence, the setup is the following asymptotic form of the wave-function:

$$\psi(r) \sim \mathcal{N}\Big(e^{ikz} + f(\theta)\frac{e^{ikr}}{r} \Big) \tag{B.3}$$

Hence, we have that

$$\Psi_{\infty}^{Sch}(r) - \mathcal{N} e^{ikz} = \mathcal{N} f(\theta)\frac{e^{ikr}}{r} \tag{B.4}$$

Where we have

$$\Psi_{\infty}^{Sch}(r,\theta) = \sum_l \Big(A_l \frac{e^{i(kr-l\pi/2)}}{r} + B_l \frac{e^{-i(kr-l\pi/2)}}{r} \Big) Y_{l0} \tag{B.5}$$

$$\Psi_{\infty}^{Sch}(r) - \mathcal{N} e^{ikz} = \sum_l \Big[\Big(A_l - \mathcal{N}\frac{i^{l-1}\sqrt{\pi(2l+1)}}{k} \Big) \frac{e^{i(kr-l\pi/2)}}{r} \tag{B.6}$$

$$+ \Big(B_l + \mathcal{N}\frac{i^{l-1}\sqrt{\pi(2l+1)}}{k} \Big) \frac{e^{-i(kr-l\pi/2)}}{r} \Big] Y_{l0} \tag{B.7}$$

Since there can be no incoming spherical wave in the scattering solutions, we can *read off* the condition imposed on B_l:

$$B_l = -\mathcal{N} i^{l-1}\frac{\sqrt{\pi(2l+1)}}{k} \qquad \forall\ l \in \mathbb{N} \tag{B.8}$$

We can also identify the scattering amplitude, as it would be given by the following:

$$f(\theta) = \frac{1}{\mathcal{N}} \sum_{l=0}^{\infty} \Big(A_l - \mathcal{N}\frac{i^{l-1}\sqrt{\pi(2l+1)}}{k} \Big) e^{-il\pi/2} Y_{l0} \tag{B.9}$$

$$= \sum_l \frac{1}{2ik} \Big(-\frac{A_l}{B_l} - 1 \Big) (2l+1) P_l(cos\theta) \tag{B.10}$$

$$= \frac{1}{2ik} \sum_{l=0}^{\infty} (2l+1)(e^{2i\delta_l} - 1) P_l(cos\theta) \tag{B.11}$$

$$= \sum_{l=0}^{\infty} (2l+1) f_l P_l(cos\theta) \qquad \text{where } f_l := \frac{1}{2ik}(e^{2i\delta_l} - 1) \tag{B.12}$$

Where we have defined the phase $e^{2i\delta_l} := -\frac{A_l}{B_l}$. We also note that the elastic differential cross section is given by the following:

$$\frac{d\sigma_{el}}{d\Omega} = |f(\theta)|^2 \tag{B.13}$$

Hence, using the obtained formula and applying orthogonality of Legendre polynomials we obtain:

$$\sigma_{el} = \int |f(\theta)|^2 d\Omega \tag{B.14}$$

$$= \frac{\pi}{k^2}\sum_{l=0}^{\infty}(2l+1)|e^{2i\delta_l}-1|^2 := \sum_{l=0}^{\infty}\sigma_l^{(el)} \tag{B.15}$$

B.3 Inelastic Scattering [Spinless]

There are several ways to obtain this but we will approach this by way of the optical theorem, defining inelastic scattering as the *leftover* piece from the total cross section. That is, $\sigma_l^{(tot)} := \sigma_l^{(el)} + \sigma_l^{(in)}$. Note that $\sigma^{(tot)} = \sum_l \sigma_l^{(tot)} = \sum_l \sigma_l^{(el)} + \sigma_l^{(in)} = \sigma^{(el)} + \sigma^{(in)}$. The total partial cross sections are given by the following:

$$\sigma_l^{(tot)} = \frac{4\pi(2l+1)}{k}\mathrm{Im}(f_l) = \frac{\pi(2l+1)}{k^2}\big(2 - e^{2i\delta_l} - (e^{2i\delta_l})^*\big), \tag{B.16}$$

where we have denoted the imaginary component of f_l by $\mathrm{Im}(f_l)$. We are therefore able to obtain the partial inelastic cross sections:

$$\sigma_l^{(in)} = \frac{\pi}{k^2}(2l+1)(1-|e^{2i\delta_l}|^2) \tag{B.17}$$

$$\sigma^{(in)} = \frac{\pi}{k^2}\sum_{l=0}^{\infty}(2l+1)(1-|e^{2i\delta_l}|^2) \tag{B.18}$$

B.4 Scattering Phase Shift for Inverse-Square

The general radial solutions are given by the hypergeometrics:

$$\psi_{\pm}(r) = (2ikr)^{\frac{1}{2}(-1\pm\zeta)}e^{-ikr}\mathscr{M}\Big[\frac{1}{2}\Big(1\pm\zeta\Big), 1\pm\zeta; 2ikr\Big] \tag{B.19}$$

Where we have defined $\zeta := \sqrt{1-4[2mg-(l(l+1)]} = \sqrt{(2l+1)^2-4\xi}$ with $\xi := 2mg$. For sufficiently large-r, we obtain the following asymptotics:

$$\psi_+(r) \sim \frac{1}{2i}\Big[\frac{\Gamma(1+\zeta)}{\Gamma(\frac{1}{2}(1+\zeta))}\Big(\frac{e^{ikr}}{kr}\Big) + \frac{\Gamma(1+\zeta)}{\Gamma(\frac{1}{2}(1+\zeta))}e^{-\frac{i\pi}{2}(1+\zeta)}\Big(\frac{e^{-ikr}}{kr}\Big)\Big] \tag{B.20}$$

$$\psi_-(r) \sim \frac{1}{2i}\Big[\frac{\Gamma(1-\zeta)}{\Gamma(\frac{1}{2}(1-\zeta))}\Big(\frac{e^{ikr}}{kr}\Big) + \frac{\Gamma(1-\zeta)}{\Gamma(\frac{1}{2}(1-\zeta))}e^{-\frac{i\pi}{2}(1-\zeta)}\Big(\frac{e^{-ikr}}{kr}\Big)\Big] \tag{B.21}$$

We can then establish that from taking $\psi(r) = C_+\psi_+ + C_-\psi_-$

$$A_l = \frac{1}{2ik}\Big(\Gamma\big[1+\frac{1}{2}\zeta\big]2^{\zeta}C_+ + \Gamma\big[1-\frac{1}{2}\zeta\big]2^{-\zeta}C_-\Big)\frac{e^{i\pi l/2}}{\sqrt{\pi}} \tag{B.22}$$

$$B_l = \frac{1}{2ik}\Big(\Gamma\big[1+\frac{1}{2}\zeta\big]2^{\zeta}C_+ + \Gamma\big[1-\frac{1}{2}\zeta\big]2^{-\zeta}e^{-i\pi\zeta}C_-\Big)\frac{e^{i(1+\zeta-l)\pi/2}}{\sqrt{\pi}} \tag{B.23}$$

$$e^{2i\delta_l} = -\frac{A_l}{B_l} = i(-1)^l e^{-i\pi\zeta/2}\frac{\Gamma\big[1+\frac{1}{2}\zeta\big]4^{\zeta} + \Gamma\big[1-\frac{1}{2}\zeta\big]\Big(\frac{C_-}{C_+}\Big)}{\Gamma\big[1+\frac{1}{2}\zeta\big]4^{\zeta} + \Gamma\big[1-\frac{1}{2}\zeta\big]\Big(\frac{C_-}{C_+}\Big)e^{-i\pi\zeta}} \tag{B.24}$$

If we take $\zeta = 1$ (l=g=0), then we have

$$e^{2i\delta_0} = \frac{2+\frac{C_-}{C_+}}{2-\frac{C_-}{C_+}} \tag{B.25}$$

We note the following:

$$f(z) = \frac{2+z}{2-z} = 1 + \sum_{n=1}^{\infty}\frac{z^n}{2^{n-1}} \text{ on } |z|<2 \tag{B.26}$$

Hence, we can approximate:

$$e^{2i\delta_0} \approx 1 + \frac{C_-}{C_+} + \frac{1}{2}\Big(\frac{C_-}{C_+}\Big)^2 + \mathcal{O}\Big[\Big(\frac{C_-}{C_+}\Big)^3\Big] \tag{B.27}$$

APPENDIX C

MISCELLANEOUS COMPUTATIONS

C.1 The Rate of Potential Integral Convergence

Th. C.1. Suppose that in d+1-spacetime, we take our radial wave function integrals to satisfy the following:

$$\lim_{\epsilon\to 0}\int_0^\epsilon \mathrm{d}r\ \psi(r) = 0 \tag{C.1}$$

If $V(r)\sim 1/r^n$ as $r\to 0$ where $n\leq d-1$ then $\lim_{\epsilon\to 0}\int_0^\epsilon \mathrm{d}r\ r^{d-1}V(r)\psi(r)=0$

Proof. Our interest is in the small r-limit, and for this we can consider the asymptotic forms of our functions. We naturally assume that the radial wave-functions should vanish in the limiting integral which sets a condition for the asymptotic form of our potential. We are interested in bounding the integral:

$$\left|\int_0^\epsilon \mathrm{d}r\ r^{d-1}V(r)\psi(r)\right| \leq \int_0^\epsilon \mathrm{d}r\left|\ r^{d-1}V(r)\psi(r)\right| \leq \int_0^\epsilon \mathrm{d}r\ \left|\psi(r)\right| \tag{C.2}$$

This is accomplished by supposing that $V(r)\sim r^{-n}$ as $r\to 0$ where $n\leq d-1$. We then have $r^{d-1}V(r)\sim r^{d-1-n}$ where $d-1-n\geq 0$. By this, we choose $\epsilon<1$ and thereby have the terms suppressing the integral, satisfying $r^{d-1}V(r)\psi(r)\leq\psi(r)$ on the domain $[0,\epsilon]$. Therefore, the integral vanishes and we are done. ■

If one is interested in the rate at which such an integral vanishes, we can consider the following: Given some function $\psi:\mathbb{R}\to\mathbb{R}$, we define an integral representation for another function $W:\mathbb{R}\to\mathbb{R}$ below by (C.3).

$$W(\epsilon) = \int_0^\epsilon \mathrm{d}r\ r^{d-1}V(r)\psi(r) \tag{C.3}$$

We're interested in the rate at which this integral approaches $\epsilon = 0$. To that end, we compute

$$\frac{dW}{d\epsilon}\Big|_{\epsilon=0} = \epsilon^{d-1} V(\epsilon)\psi(\epsilon)\big|_{\epsilon=0} \geq \mathcal{O}\big[\psi(\epsilon)\big]\big|_{\epsilon=0} \tag{C.4}$$

If the potential, V isn't sufficiently singular then we can have the rate of convergence for the integral disappear sufficiently quickly, that being on the order of the field itself. In essence, the last inequality requires that $V(r) \geq \mathcal{O}\big[1/r^{d-1}\big]$.

C.2 Second Variation of the Quartic System

It helps to show case the second variation explicitly, as to make the minimization problem explicit. We'll do this by way of the quartic potential. Given the Energy functional of (C.5), we say that if $h_4 > 0$ then extremization leads to minimization whereas $h_4 < 0$ leads to maximization.

$$H_B[\Psi] = \int d^3x \Big(\frac{1}{2m}|\nabla\Psi|^2 - g\frac{|\Psi|^2}{r^2}\Big) \qquad H_b[\Psi] = h_4 \int d^3x |\Psi|^4 \delta^3(x) \tag{C.5}$$

Proof. The increment is defined as $\Delta H[\psi_c, \eta] = H[\psi_c + \eta] - H[\psi_c]$. We note that:

$$\begin{aligned} H_B[\psi_c + \eta] = \int d^3x \Big[&\Big(\frac{1}{2m}|\nabla\Psi_c|^2 - g\frac{|\Psi_c|^2}{r^2}\Big) + \Big(\frac{1}{2m}\nabla\Psi^* \cdot \nabla\eta - g\frac{\Psi_c^*\eta}{r^2}\Big) \\ &+ \Big(\frac{1}{2m}\nabla\Psi \cdot \nabla\eta^* - g\frac{\Psi_c\eta^*}{r^2}\Big) + \Big(\frac{1}{2m}|\nabla\eta|^2 - g\frac{|\eta|^2}{r^2}\Big)\Big] \end{aligned} \tag{C.6}$$

$$\begin{aligned} H_b[\psi_c + \eta] = h_4 \int d^3x \ \Big(&|\psi_c|^4 + |\eta|^4 + (\psi_c^*)^2\eta^2 + \psi_c^2(\eta^*)^2 + 4|\psi_c|^2|\eta|^2 \\ &+ 2|\psi_c|^2\psi_c^*\eta + 2|\psi_c|^2\psi_c\eta^* + 2\psi_c^*|\eta|^2\eta + 2\psi_c|\eta|^2\eta^*\Big)\delta^3(x) \end{aligned} \tag{C.7}$$

We can perform integration by parts on the two middle bulk portions to retrieve the following increment:

(C.8)
$$\Delta H = \int d^3x \Big[\Big(-\frac{1}{2m}\nabla^2\psi_c - g\frac{\psi_c}{r^2} + 2h_4|\psi_c|^2\psi_c\delta^3(x)\Big)\eta^* + \Big(-\frac{1}{2m}\nabla^2\psi_c^* - g\frac{\psi_c^*}{r^2} + 2h_4|\psi_c|^2\psi_c^*\delta^3(x)\Big)\eta\Big]$$

(C.9)
$$+ \int d^3x \ \Big[\frac{1}{2m}|\nabla\eta|^2 - g\frac{|\eta|^2}{r^2} + h_4\big[(\psi_c^*)^2\eta^2 + \psi_c^2(\eta^*)^2 + 4|\psi_c|^2|\eta|^2\big]\delta^3(x)\Big] + \mathcal{O}(||\eta||^3)$$

(C.10)
$$= h_4 \int d^3x \big[(\psi_c^*)^2\eta^2 + \psi_c^2(\eta^*)^2 + 4|\psi_c|^2|\eta|^2\big]\delta^3(x) + \mathcal{O}(||\eta||^3) := \delta^2 H[\psi_c, \eta] + \mathcal{O}(||\eta||^3)$$

The second equality is established from the fact that ψ_c satisfies the field equations. Hence, the second variation, $\delta^2 H$ is easily identified here and is a quadratic functional.

$$\delta^2 H = \int d^3x \ \Big[\frac{1}{2m}|\nabla\eta|^2 - g\frac{|\eta|^2}{r^2} + h_4\big[(\psi_c^*)^2\eta^2 + \psi_c^2(\eta^*)^2 + 4|\psi_c|^2|\eta|^2\big]\delta^3(x)\Big] \tag{C.11}$$

$$\geq h_4 \int d^3x\big[(\psi_c^*)^2\eta^2 + \psi_c^2(\eta^*)^2 + 4|\psi_c|^2|\eta|^2\big]\delta^3(x) \tag{C.12}$$

$$= h_4 \int d^3x \ \big[4\big(\mathrm{Re}[\psi_c\eta^*]\big)^2 + 2|\psi_c|^2|\eta|^2\big]\delta^3(x) \geq 0 \ \text{[if } h_4 > 0\text{]} \tag{C.13}$$

Here we have also used the fact that

$$H[\eta] = \int d^3x \ \Big[\frac{1}{2m}|\nabla\eta|^2 - g\frac{|\eta|^2}{r^2}\Big] \geq 0 \quad \forall\eta \tag{C.14}$$

The positive-definiteness is best visible in the final form. Hence, sign(h_4) controls whether or not we indeed have a minimization problem via extremization. Hence, we conclude that if $h_4 > 0$, then

$$\delta^2 H[\psi_c, \eta] \geq 0 \quad \forall\eta \tag{C.15}$$

■

C.3 Quartic Renormalization

We identify the running of the parameters in our theory being completely housed within the quadratic couplings h_2. The renormalization argument therefore argues the following:

$$\frac{d}{d\epsilon}\Big(\frac{C_-}{C_+}\Big) = \frac{d\zeta}{d\epsilon} = \frac{d\chi}{d\epsilon} = \frac{dk}{d\epsilon} = 0 \tag{C.16}$$

Hence, we differentiate both sides of (4.96) and aim to establish the running. For compactness, we employ one more redefinition of h_2 via $\bar{h}_2^R := \hat{h}_2^R - (\chi + 1)$ and $z := \chi + \zeta$. To make computation more viable, we separate the differential equation into real and imaginary components which determines a system of two equations given by (C.17), (C.18).

$$0 = \zeta\Big[2\big[(z+1)\bar{h}_2^R - \hat{h}_2^I\big] - z(z+2)\Big](z+2-2\bar{h}_2^R) + 2\epsilon\Big[\frac{d\bar{h}_2^R}{d\epsilon}(z+2-2\hat{h}_2^I) - \frac{d\hat{h}_2^I}{d\epsilon}(z+2-2\bar{h}_2^R)\Big] \tag{C.17}$$

$$0 = \zeta(z+2-2\bar{h}_2^R)(\bar{h}_2^R + \hat{h}_2^I) + \epsilon\Big[\frac{d\bar{h}_2^R}{d\epsilon}(z+2+2\hat{h}_2^I) + \frac{d\hat{h}_2^I}{d\epsilon}(z+2-2\bar{h}_2^R)\Big] \tag{C.18}$$

APPENDIX D

CALCULUS OF VARIATIONS

Consider a functional $J : \mathbb{L}^p \to \mathbb{R}$, which maps from the space of $\mathbb{L}^p$ functions to the scalars, $\mathbb{R}$ (Typically we're interested in $\mathbb{L}^p$ spaces as the functions converge accordingly). A standard example is for a single variable and function:

$$J[y] = \int_a^b f(x, y)\, dx \tag{D.1}$$

The definitions and theorems contained within this appendix and more can be found in [8].

Def D.1: Increment
We define the *increment*, $\Delta J[h]$ as follows:

$$\Delta J[h] = J[y + h] - J[y] \tag{D.2}$$

Def D.2: Norm [Linear Algebra]
A linear space / vector space $\mathscr{R}$ is said to be *normed*, if each element $x \in \mathscr{R}$ is assigned a nonnegative number $||x||$, called the *norm* of x, such that

1. $||x|| = 0$ if and only if x = 0;
2. $||\alpha x|| = |\alpha|||x||$;
3. $||x + y|| \leq ||x|| + ||y||$.

Def D.3: Continuous Functional
Let $\mathscr{R}$ be a function space. The functional $J[y]$ is said to be continuous at the point $\hat{y} \in \mathscr{R}$ if for any $\epsilon > 0$, there is a $\delta > 0$ such that

$$|J[y] - J[\hat{y}]| < \epsilon \tag{D.3}$$

provided that $||y - \hat{y}|| < \delta$.

Def D.4: Linear Functional

Given a normed linear space $\mathscr{R}$, let each element $h \in \mathscr{R}$ be assigned a number $\psi[h]$, i.e., let $\psi[h]$ be a functional defined on $\mathscr{R}$. Then $\psi[h]$ is said to be a (continuous) linear functional if

1. $\psi[\alpha h] = \alpha\psi[h]$ for any $h \in \mathscr{R}$ and any $\alpha \in \mathbb{R}$;
2. $\psi[h_1 + h_2] = \psi[h_1] + \psi[h_2]$ for any $h_1, h_2 \in \mathscr{R}$.
3. $\psi[h]$ is continuous (for all $h \in \mathscr{R}$).

Def D.5: Variation / Differentiable Functional

Suppose that the increment satisfies $\Delta J[h] = \psi[h] + \epsilon||h||$ where $\psi[h]$ is a linear functional and $\epsilon \to 0$ as $||h|| \to 0$. If this holds, then we say that $\Delta J[h]$ is differentiable and $\psi[h]$ (the principal linear part) is called the *variation* (or differential) and is denoted by $\delta J[h]$.

For a functional of n functions up to first derivatives $J[y_1, ..., y_n] = \int_a^b F[x, y_1, .., y_n, y_1', .., y_n']dx$ we compute first variation

$$\delta J = \int_a^b \sum_{i=1}^{n} \left(F_{y_i} h_i + F_{y_i'} h_i' \right) dx \tag{D.4}$$

If we consider a functional of one function, up to its nth derivative, $J[y] = \int_a^b F(x, y, y', ..., y^{(n)})dx$ then we can compute:

$$\delta J[y] = \int_a^b \left[F_y - \frac{d}{dx} F_{y'} + \frac{d^2}{dx^2} F_{y''} - .. + (-1)^n \frac{d^n}{dx^n} F_{y^{(n)}} \right] h(x)dx \tag{D.5}$$

Obtained by having applied the boundary conditions

$$h(a) = h'(a) = ... = h^{(n-1)}(a) = 0 \tag{D.6}$$

$$h(b) = h'(b) = ... = h^{(n-1)}(b) = 0 \tag{D.7}$$

and integrating by parts.

Note: We're interested in fixing a y function and to then consider the shift by h, and so although y is dropped from the notation, the variations / increment should really be considered as dependent upon y and h.

Theorem D.1: Extremums

A necessary condition for a differentiable functional $J[y]$ to have an extremum at $y = \hat{y}$ is that the variation vanish for $y = \hat{y}$, i.e. that $\delta J[\hat{y}, h] = 0$ for $y = \hat{y}$ and all admissible h.

Def D.6: Bilinear and Quadratic Functional

A functional $B[x,y]$ depending on two elements x and y, belonging to some normed linear space $\mathscr{R}$, is said to be *bilinear* if it is a linear functional of y for any fixed x and a linear functional of x for any fixed y. Thus,

$$B[x+y,z] = B[x,z] + B[y,z], \tag{D.8}$$

$$B[\alpha x, y] = \alpha B[x,y], \tag{D.9}$$

and

$$B[x, y+z] = B[x,y] + B[x,z], \tag{D.10}$$

$$B[x, \alpha y] = \alpha B[x,y] \tag{D.11}$$

for any $x, y, z \in \mathscr{R}$ and $\alpha \in \mathbb{R}$.

If we set y = x in a bilinear functional, we obtain a *quadratic functional*. Hence, a quadratic functional would take the form $A[x] = B[x,x]$.

Def D.7: Twice Differentiable / Second Variation

We say that a functional $J[y]$ is *twice differentiable* if its increment can be written in the form:

$$\Delta J[h] = \psi_1[h] + \psi_2[h] + \epsilon ||h||^2 \tag{D.12}$$

Where $\psi_1[h]$ is a linear functional (the first variation), $\psi_2[h]$ is a quadratic functional, and $\epsilon \to 0$ as $||h|| \to 0$. The quadratic functional $\psi_2[h]$ is called the *second variation* (or *second differential*) of the functional J[y], and is denoted by $\delta^2 J[h]$.

Theorem D.2: Minimum Condition

A necessary condition for the functional $J[y]$ to have a minimum for $y = \hat{y}$ is that

$$\delta^2 J[y] \geq 0 \tag{D.13}$$

for $y = \hat{y}$ and all admissible h. For a maximum, the sign $\geq$ is replaced by $\leq$.

Def D.8: Strongly Positive

We say that a quadratic functional $\psi_2[h]$ defined on some normed linear space $\mathscr{R}$ is *strongly positive* if there exists a constant $k > 0$ such that

$$\psi_2[h] \geq k||h||^2 \tag{D.14}$$

for all h.

Theorem D.3: Sufficient Minimum Condition for Vanishing Variation
A sufficient condition for a functional $J[y]$ to have a minimum for $y = \hat{y}$, given that the first variation $\delta J[h]$ vanishes for $y = \hat{y}$, is that its second variation $\delta^2 J[h]$ be strongly positive for $y = \hat{y}$.

Note that a functional of n functions $J[y_1,..,y_n] = \int F(x, y_1, ..y_n, y_1', ..y_n')\ dx$ would have the following second variation:

$$\delta^2 J[h] = \frac{1}{2}\int_a^b \Big(\sum_{i,k=1}^{n} F_{y_i,y_k} h_i h_k + 2\sum_{i,k=1}^{n} F_{y_i,y_k'} h_i h_k' + \sum_{i,k=1}^{n} F_{y_i',y_k'} h_i' h_k' \Big) dx \tag{D.15}$$

Employing the usual notation of $F_{y_i,y_k} := \frac{\partial^2 F}{\partial y_i \partial y_k}$.

Proposition D.1
Suppose that we have n functionals $\{H_i[\phi], i \in \mathbb{Z}_n\}$. Let $\mathscr{H}$ be a Hilbert space defined as $\mathscr{H} = \{\psi \in \mathscr{L}^2 : -\infty < H_i[\psi] < \infty\}$. For each H_i suppose that there exists a unique $\psi_c \in \mathscr{H}$ satisfying $H_i[\psi_c] \leq H_i[\phi]\ \forall \phi \in \mathscr{H}$ (i.e minimizes the functionals). If we define $H = \sum_{i=1}^{n} H_i$, then ψ_c minimizes H.

Proof. This follows quite immediately from the inequalities defined on each functional. Notice that we necessarily have

$$\sum_{i=1}^{n} H_i[\psi_c] \leq \sum_{i=1}^{n} H_i[\phi]\ \forall \phi \in \mathscr{H} \tag{D.16}$$

$$\rightarrow H[\psi_c] \leq H[\phi]\ \forall \phi \in \mathscr{H} \tag{D.17}$$

■

Conjecture: Suppose that we have an action $S = S_B + S_b$ so that we write the Hamiltonian functional $H = H_B + H_b$ obtained via a Legendre transformation. Suppose that a background field that minimizes the bulk Hamiltonian exists on H_B such that $H_B(0) = 0$ and $\frac{\delta H_B}{\delta \psi}\Big|_{\psi=0} = 0$. Suppose that on the brane, there exists some field $\psi_c^b \neq 0$ such that $H_b(\psi_c^b) < 0$ and $\frac{\delta H_b}{\delta \psi}\Big|_{\psi=\psi_c^b} = 0$. Then, there exists a background field $\Psi_c \neq 0$ for the entire system that satisfies $H(\Psi_c) < 0$ and $\frac{\delta H}{\delta \psi}\Big|_{\psi=\Psi_c} = 0$.

APPENDIX E

GENERALIZED BRANE ACTION

In this appendix, we generalize the non-derivative brane action towards coupling interactions that go up to some order $2k$. We first observe what background field should emerge for the inverse-square system and the boundary condition of the quantum fluctuations after linearization of the field equations.

We consider the inverse square system, depicted by the bulk action, S_B.

$$S_B = \int d^4x \left(\frac{i}{2} \left\{ \Psi^* \partial_t \Psi - \Psi \partial_t \Psi^* \right\} - \left[\frac{1}{2m} |\nabla \Psi|^2 + \Psi^* \hat{V}(r) \Psi \right] \right) \tag{E.1}$$

We now consider a generalized brane action up to $2k$ order in the field couplings with no derivative terms, S_b.

$$S_b = \int d^4x \sum_{n=1}^{k} h_{2n} |\Psi|^{2n} \delta^3(x) \tag{E.2}$$

The variation of the point-particle action is therefore given below:

$$\frac{\delta S_b}{\delta \Psi^*} = \sum_{n=1}^{k} n h_{2n} |\Psi|^{2(n-1)} \Psi \delta^3(x) \tag{E.3}$$

Establishing background field for the inverse square bulk gets us $\Psi_c = \frac{c_2}{r^{(\chi+1)/2}}$. The boundary condition that emerges requires that c_2 satisfy the following:

$$\sum_{n=1}^{k-1} (n+1) \hat{h}_{2(n+1)} \frac{|c_2|^{2n}}{\epsilon^{n(\chi+1)}} + [\hat{h}_2 + (\chi+1)] = 0 \tag{E.4}$$

Hence, we essentially have a polynomial of degree $2(k-1)$ which can be trivially mapped to one of degree $k-1$ through the redefinition $|c_2|^2 \mapsto \mathbf{c}_2$. The more generalized boundary condition is

obtained via:

$$\frac{\partial \psi_c}{\partial r}\Big|_{r=\epsilon} = -\frac{m}{2\pi\epsilon^2}\sum_{n=1}^{k} n\ h_{2n}|\psi_c|^{2(n-1)}\psi_c\Big|_{r=\epsilon} \tag{E.5}$$

Where we have assumed that the potential contribution to the epsilon-ball integration goes to zero

$$\lim_{\epsilon\to 0}\int_{D^3(0,\epsilon)} \mathrm{d}^3x\ \hat{V}(r)\Psi \to 0 \qquad \text{sufficiently quickly,} \tag{E.6}$$

where $\hat{h}_i = \frac{2mh_i}{\pi\epsilon}$. We'll now expand about the background configuration. This gets us

$$\frac{\delta S_b}{\delta \eta^*} = \sum_{n=1}^{k} n\ h_{2n}(\psi_c^* + \eta^*)^{n-1}(\psi_c + \eta)^n \delta^3(x) \tag{E.7}$$

$$= \sum_{n=1}^{k} n\ h_{2n}\Big[\sum_{j=0}^{n-1}\sum_{l=0}^{n}\binom{n-1}{j}\binom{n}{l}(\psi_c^*)^{n-1-j}(\eta^*)^j\psi_c^{n-l}\eta^l\Big]\delta^3(x) \tag{E.8}$$

$$\approx \sum_{n=1}^{k} n h_{2n}\Big[|\psi_c|^{2(n-1)}\psi_c + n|\psi_c|^{n-1}\eta + (n-1)|\psi_c|^{2(n-2)}\psi_c^2\eta^*\Big]\delta^3(x) \tag{E.9}$$

The final line is obtained via linearization. Within the summand indices of the second line, we are essentially keeping terms that satisfy $j + l \leq 1$ which are precisely the three pairs $(j,l) \in \{(0,0),(0,1),(1,0)\}$.

$$\frac{\delta S}{\delta \eta^*} = -\Big[-\frac{1}{2m}\nabla^2\psi_c + \hat{V}(r)\psi_c - \sum_{n=1}^{k} n\ h_{2n}|\psi_c|^{2(n-1)}\psi_c\ \delta^3(x)\Big] \tag{E.10}$$

$$+ i\partial_t\eta - \Big[-\frac{1}{2m}\nabla^2\eta + \hat{V}(r)\eta\Big] + \sum_{j=1}^{k} h_{2j}\Big[j^2|\psi_c|^{2(j-1)}\eta + j(j-1)|\psi_c|^{2(j-2)}\psi_c^2\eta^*\Big]\delta^3(x) \tag{E.11}$$

$$= i\partial_t\eta - \Big[-\frac{1}{2m}\nabla^2\eta + \hat{V}(r)\eta\Big] + \sum_{j=1}^{k} h_{2j}\Big[j^2|\psi_c|^{2(j-1)}\eta + j(j-1)|\psi_c|^{2(j-2)}\psi_c^2\eta^*\Big]\delta^3(x) = 0 \tag{E.12}$$

The boundary condition that follows is given by:

$$\lim_{\epsilon\to 0} 2\pi\epsilon^2\frac{\partial\eta}{\partial r}\Big|_{r=\epsilon} = -\lim_{\epsilon\to 0}\ m\sum_{j=1}^{k} h_{2j}\Big[j^2|\psi_c|^{2(j-1)}\eta + j(j-1)|\psi_c|^{2(j-2)}\psi_c^2\eta^*\Big]\Big|_{r=\epsilon} \tag{E.13}$$

APPENDIX F

MULTIPLE SPECIES CATALYSIS RATIOS

In this appendix, we go over the leading order and next to leader order computations for the C-ratios which determine $1 \to 1$ and $1 \to 2$ type cross sections.

F.1 Computations

We denote $\psi_i = C_{i+}\psi_{i+} + C_{i-}\psi_{i-}$ just as before. We abbreviate the notation so that $\psi_i' := \frac{\partial \psi_i}{\partial r}$ and $\bar{\psi}_i' := \frac{2\pi\epsilon^2}{m_i}\psi_i'$. We also temporarily define $D_i := C_{i-}/C_{1+}$ and impose the relation $C_{2+} = R_2 C_{2-}$.

$$\bar{\psi}_{1+}' + D_1\bar{\psi}_{1-}' = M_{11}\big(\psi_{1+} + D_1\psi_{1-}\big) + M_{12}D_2\big(R_2\psi_{2-} + \psi_{2-}\big) \tag{F.1}$$

$$D_2\big(R_2\bar{\psi}_{2+}' + \bar{\psi}_{2-}'\big) = M_{21}\big(\psi_{1+} + D_1\psi_{1-}\big) + M_{22}D_2\big(R_2\psi_{2+} + \psi_{2-}\big) \tag{F.2}$$

Going back to the original C-ratios, we are therefore able to obtain the following relations:

$$\frac{C_{2-}}{C_{1+}} = \frac{\psi_{1+}}{\psi_{2-}} \frac{M_{21}\big(\frac{\bar{\psi}_{1+}'}{\psi_{1+}} - \frac{\bar{\psi}_{1-}'}{\psi_{1-}}\big)}{\big[R_2\frac{\psi_{2+}}{\psi_{2-}} + 1\big]\Big[|M_{12}|^2 - \big(\frac{\bar{\psi}_{1-}'}{\psi_{1-}} - M_{11}\big)Z\Big]} \tag{F.3}$$

$$\frac{C_{1-}}{C_{1+}} = -\frac{\psi_{1+}}{\psi_{1-}} \frac{\Big[|M_{12}|^2 - \Big(\frac{\bar{\psi}_{1+}'}{\psi_{1+}} - M_{11}\Big)Z\Big]}{\Big[|M_{12}|^2 - \Big(\frac{\bar{\psi}_{1-}'}{\psi_{1-}} - M_{11}\Big)Z\Big]} \tag{F.4}$$

Where we have

$$Z = \frac{R_2\bar{\psi}_{2+}' + \bar{\psi}_{2-}'}{R_2\psi_{2+} + \psi_{2-}} - M_{22} \tag{F.5}$$

Leading Order in $k\epsilon$

Let $x_i := 2ik_i\epsilon$. We then note that the small $k\epsilon$ asymptotics of our radial wave functions are given as follows:

$$\psi_1(x_1) \sim C_{1+}x_1^{-\frac{(1-\zeta)}{2}} + C_{1-}x_1^{-\frac{(1+\zeta)}{2}} \tag{F.6}$$

$$\frac{\partial\psi_1(x_1)}{\partial r} \sim \frac{ik_1}{x_1^{3/2}}\big(C_{1+}(\zeta-1)x_1^{\zeta/2} - C_{1-}(\zeta+1)x_1^{-\zeta/2}\big) \tag{F.7}$$

$$\psi_2(x_2) \sim C_{2-}x_2^{-\frac{(1+\zeta)}{2}} \tag{F.8}$$

$$\frac{\partial\psi_2(x_2)}{\partial r} \sim -ik_2C_{2-}(\zeta+1)x_2^{-3/2-\zeta/2} \tag{F.9}$$

We are therefore able to compute the following:

$$\frac{\bar{\psi}'_{i\pm}}{\psi_{i\pm}} = \frac{2\pi\epsilon^2}{m_i}\frac{\psi'_{i\pm}}{\psi_{i\pm}} \sim -\frac{\pi\epsilon}{m_i}(1\mp\zeta) \tag{F.10}$$

$$\frac{\psi_{1+}}{\psi_{1-}} \sim (2ik_1\epsilon)^{\zeta} \tag{F.11}$$

$$\frac{\psi_{2+}}{\psi_{2-}} \sim 0 \tag{F.12}$$

$$Z \sim \frac{\bar{\psi}'_{2-}}{\psi_{2-}} - M_{22} = -\Big[\frac{\pi\epsilon}{m_2}(1+\zeta) + M_{22}\Big] \tag{F.13}$$

We therefore establish:

$$|M_{12}|^2 - \Big(\frac{\bar{\psi}'_{1\pm}}{\psi_{1\pm}} - M_{11}\Big)Z \sim -\Big[\frac{T + \pi\epsilon\zeta(m_1M_{11} \mp m_2M_{22}) + (\pi\epsilon)^2(1+\zeta(1\mp1)\mp\zeta^2)}{m_1m_2}\Big] \tag{F.14}$$

Where we have defined $T := \det(\mathrm{mM}) + \pi\epsilon\,\mathrm{tr}(\mathrm{mM})$.

$$\frac{C_{2-}}{C_{1+}} \sim -\sqrt{\frac{k_2}{k_1}}\frac{2\pi\epsilon\zeta(2ik_1\epsilon)^{\zeta/2}(2ik_2\epsilon)^{\zeta/2}m_2M_{21}}{T + \pi\epsilon\zeta(m_1M_{11} + m_2M_{22}) + (\pi\epsilon)^2(1+\zeta)^2} \tag{F.15}$$

$$\frac{C_{1-}}{C_{1+}} \sim -(2ik_1\epsilon)^{\zeta}\Big(\frac{T + \pi\epsilon\zeta(m_1M_{11} - m_2M_{22}) + (\pi\epsilon)^2(1-\zeta^2)}{T + \pi\epsilon\zeta(m_1M_{11} + m_2M_{22}) + (\pi\epsilon)^2(1+\zeta)^2}\Big) \tag{F.16}$$

Sub-leading order in $k\epsilon$

We recall that:

$$\psi_\pm = (2ik\epsilon)^{\frac{1}{2}(-1\pm\zeta)}e^{-ik\epsilon}\mathscr{M}\big[\frac{1}{2}(1\pm\zeta), 1\pm\zeta; 2ik\epsilon\big] \tag{F.17}$$

we therefore obtain the small $k\epsilon$ asympototics as:

$$\psi_{\pm} \sim (2ik\epsilon)^{\frac{1}{2}(-1\pm\zeta)}\big[1-ik\epsilon+\mathcal{O}((k\epsilon)^2)\big]\big[1+ik\epsilon+\mathcal{O}((k\epsilon)^2)\big] \tag{F.18}$$

$$\sim (2ik\epsilon)^{\frac{1}{2}(-1\pm\zeta)}\big[1+\mathcal{O}((k\epsilon)^2)\big] \tag{F.19}$$

The adjustments to the second particle's wave function are therefore given by keeping the (+) mode, once again defining the relation $C_{2+} = R_2 C_{2-}$.

$$\psi_2 \sim x_2^{-1/2} C_{2-}\big(R_2 x_2^{\zeta/2} + x_2^{-\zeta/2}\big) \tag{F.20}$$

$$\frac{\partial\psi_2}{\partial r} \sim \frac{ik_2}{x_2^{3/2}} C_{2-}\big(R_2(\zeta-1)x_2^{\zeta/2} - (\zeta+1)x_2^{-\zeta/2}\big) \tag{F.21}$$

$$\psi'_{i\pm} \sim \pm\frac{ik_i}{x_i^{3/2}}(\zeta\mp 1)x_i^{\pm\zeta/2} \tag{F.22}$$

$$\frac{\bar{\psi}'_{i\pm}}{\psi_{i\pm}} = \frac{2\pi\epsilon^2}{m_i}\frac{\psi'_{i\pm}}{\psi_{i\pm}} \sim -\frac{\pi\epsilon}{m_i}(1\mp\zeta) \tag{F.23}$$

$$\frac{\psi_{i+}}{\psi_{i-}} \sim (2ik_i\epsilon)^{\zeta} \tag{F.24}$$

$$\frac{\bar{\psi}'_{i+}}{\bar{\psi}'_{i-}} = \frac{\psi'_{i+}}{\psi'_{i-}} = \frac{1-\zeta}{1+\zeta}x_i^{\zeta} \tag{F.25}$$

We also make an expansion about small $\psi_{2+}/\psi_{2-} = x_2^{\zeta}$ as to obtain the following approximation for Z:

$$Z \approx \frac{\bar{\psi}'_{2-}}{\psi_{2-}}\Big(\frac{1+R_2\frac{\bar{\psi}'_{2+}}{\bar{\psi}'_{2-}}}{1+R_2\frac{\psi_{2+}}{\psi_{2-}}}\Big) - M_{22} \approx \frac{\bar{\psi}'_{2-}}{\psi_{2-}}\big[1+R_2\Big(\frac{\bar{\psi}'_{2+}}{\bar{\psi}'_{2-}} - \frac{\psi_{2+}}{\psi_{2-}}\Big)\big] - M_{22} \tag{F.26}$$

$$= -\big[\frac{\pi\epsilon}{m_2}(1+\zeta)\big]\Big[1-\frac{2\zeta R_2(2ik_2\epsilon)^{\zeta}}{1+\zeta}\Big] - M_{22} \tag{F.27}$$

$$\frac{C_{1-}}{C_{1+}} = -(2ik_1\epsilon)^{\zeta}\frac{\Big[|M_{12}|^2 - \Big(\frac{\pi\epsilon}{m_1}(1-\zeta)+M_{11}\Big)\Big(\frac{\pi\epsilon}{m_2}(1+\zeta)\big[1-\frac{2\zeta R_2(2ik_2\epsilon)^{\zeta}}{1+\zeta}\big]+M_{22}\Big)\Big]}{\Big[|M_{12}|^2 - \Big(\frac{\pi\epsilon}{m_1}(1+\zeta)+M_{11}\Big)\Big(\frac{\pi\epsilon}{m_2}(1+\zeta)\big[1-\frac{2\zeta R_2(2ik_2\epsilon)^{\zeta}}{1+\zeta}\big]+M_{22}\Big)\Big]} \tag{F.28}$$

$$\frac{C_{1-}}{C_{1+}} = -(2ik_1\epsilon)^{\zeta}\frac{\Big(\mathcal{N} + \big[\frac{\pi\epsilon}{m_1}(1-\zeta)+M_{11}\big]\big[\frac{2\pi\epsilon}{m_2}\zeta R_2(2ik_2\epsilon)^{\zeta}\big]\Big)}{\Big(\mathcal{D} + \big[\frac{\pi\epsilon}{m_1}(1+\zeta)+M_{11}\big]\big[\frac{2\pi\epsilon}{m_2}\zeta R_2(2ik_2\epsilon)^{\zeta}\big]\Big)} \tag{F.29}$$

Where we have defined

$$\mathscr{N} = |M_{12}|^2 - \Big(\frac{\pi\epsilon}{m_1}(1-\zeta) + M_{11}\Big)\Big(\frac{\pi\epsilon}{m_2}(1+\zeta) + M_{22}\Big) \tag{F.30}$$

$$\mathscr{D} = |M_{12}|^2 - \Big(\frac{\pi\epsilon}{m_1}(1+\zeta) + M_{11}\Big)\Big(\frac{\pi\epsilon}{m_2}(1+\zeta) + M_{22}\Big) \tag{F.31}$$

We can use a small $k\epsilon$ expansion to yield the following relations:

$$\frac{C_{1-}}{C_{1+}} \approx -(2ik_1\epsilon)^\zeta \frac{\mathscr{N}}{\mathscr{D}}\Big[1 + \Big(\frac{\frac{\pi\epsilon}{m_1}(1-\zeta) + M_{11}}{\mathscr{N}} - \frac{\frac{\pi\epsilon}{m_1}(1+\zeta) + M_{11}}{\mathscr{D}}\Big)\frac{2\pi\epsilon\zeta}{m_2}R_2(2ik_2\epsilon)^\zeta\Big] \tag{F.32}$$

$$\frac{C_{1-}}{C_{1+}} \approx -(2ik_1\epsilon)^\zeta \frac{\mathscr{N}}{\mathscr{D}}\Big[1 - \frac{(2\pi\epsilon\zeta)^2}{m_1 m_2}\frac{|M_{12}|^2 R_2(2ik_2\epsilon)^\zeta}{\mathscr{N}\mathscr{D}}\Big] \tag{F.33}$$

BIBLIOGRAPHY

[1] I. Afflecka and J. Sagi.
Monopole-catalysed baryon decay: A boundary conformal field theory approach.
Nucl. Phys. B, 417:374–402, 1994.
doi:10.1016/0550-3213(94)90478-2.

[2] C.P. Burgess.
Introduction to effective field theory.
Ann. Rev. Nucl. Part. Sci, 57:329–362, 2007.
doi:hep-th/0701053.

[3] C.P. Burgess, P. Hayman, M. Williams, and L. Zalavari.
Point-particle effective field theory i: Classical renormalization and the inverse-square potential.
JHEP, 04(106), 2017.

[4] C.P. Burgess, P. Hayman, M. Williams, and L. Zalavari.
Point-particle effective field theory ii: Relativistic effects and coulomb/inverse-square competition.
JHEP, 04(106), 2017.

[5] C.P. Burgess, P. Hayman, M. Williams, and L. Zalavari.
Point-particle effective field theory iii:relativistic fermions and the dirac equation.
JHEP, 04(106), 2017.

[6] C.P. Burgess, D. Hoover, C. de Rham, and G. Tasinato.
Effective field theories and matching for codimension-2 branes.
JHEP, 03:124, 2009.
doi:10.1088/1126-6708/2009/03/124.

[7] Curtis G. Callan.
Monopole catalysis of baryon decay.
Nuclear Physics B, 212:391–400, 1983.
doi:10.1016/0550-3213(83)90677-6.

[8] I.M. Gelfand and S.V. Fomin.
Calculus of Variations.
Prentice-Hall, Inc, 1963.

[9] P. Hayman and C.P Burgess.
Point-particle catalysis.
2019.
doi:https://arxiv.org/abs/1905.00103.

[10] L.D Landau and E.M Lifshitz.
Relativistic Quantum Theory.
Pergamon press, 1971.

[11] L.D Landau and E.M Lifshitz.
Quantum Mechanics: Non-relativistic Theory.
Pergamon press, 1976.

[12] M.E. Peskin and D.V. Schroeder.
An Introduction to Quantum Field Theory.
Perseus Books Publishing, 1995.

[13] R. Plestid, C.P. Burgess, and D.H.J O'Dell.
Fall to the centre in atom traps and point-particle eft for absorptive systems.
arXiv, 2018.
doi:https://arxiv.org/abs/1804.10324.

[14] Joseph Polchinski.
String Theory.
Cambridge University Press, 2005.

[15] Iain Stewart.
Effective field theory: Lecture notes, EFT Course 8.851 2014; Massachusetts Institute of Technology.

[16] Shunji Tsuchiya and Yoji Ohashi.
Anomalous enhancement of quasiparticle current near a potential barrier in a bose-einstein condensate.
Phys. Rev. A, 78:013628, Jul 2008.
doi:10.1103/PhysRevA.78.013628.